AFWAL-TR-87-3091

HEAT TRANSFER RATES ON AN ANALYTIC FOREBODY
IN THE AFWAL MACH 3 HIGH REYNOLDS NUMBER WIND TUNNEL

AD–A199 523

Comparison of Test Results with Predictions from STAPAT
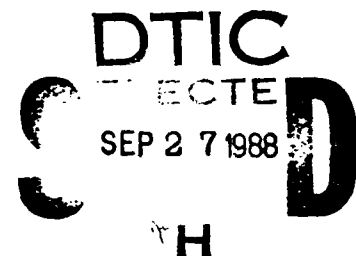(A Specific Thermal Analyzer Program for Aircraft Transparencies)

Charles A. Babish III   and   James R. Hayes
Aircrew Protection Branch   High Speed Aero Performance Branch
Vehicle Subsystems Division   Aeromechanics Division

April 1988

Final Report for the Period October 1984 - September 1986

DTIC
ELECTE
SEP 2 7 1988
H

88 9 27 113

REPORT DOCUMENTATION PAGE				Form Approved OMB No. 0704-0188

1a. REPORT SECURITY CLASSIFICATION UNCLASSIFIED	1b. RESTRICTIVE MARKINGS N/A

2a. SECURITY CLASSIFICATION AUTHORITY N/A	3. DISTRIBUTION/AVAILABILITY OF REPORT Approved for public release; distribution is unlimited.
2b DECLASSIFICATION/DOWNGRADING SCHEDULE N/A	

4. PERFORMING ORGANIZATION REPORT NUMBER(S) AFWAL-TR-87-3091	5. MONITORING ORGANIZATION REPORT NUMBER(S)

6a. NAME OF PERFORMING ORGANIZATION Flight Dynamics Laboratory AFWAL AFSC	6b. OFFICE SYMBOL (If applicable) AFWAL/FIER	7a. NAME OF MONITORING ORGANIZATION

6c. ADDRESS (City, State, and ZIP Code) Wright-Patterson AFB, Ohio 45433-6553	7b. ADDRESS (City, State, and ZIP Code)

8a. NAME OF FUNDING/SPONSORING ORGANIZATION	8b. OFFICE SYMBOL (If applicable)	9 PROCUREMENT INSTRUMENT IDENTIFICATION NUMBER

8c. ADDRESS (City, State, and ZIP Code)	10. SOURCE OF FUNDING NUMBERS			
	PROGRAM ELEMENT NO	PROJECT NO	TASK NO	WORK UNIT ACCESSION NO
	62201F	2402	03	50

11 TITLE (Include Security Classification)
Heat Transfer Rates on an Analytic Forebody in the AFWAL Mach 3 High Reynolds Number Wind Tunnel - Comparison of Test Results with Predictions from STAPAT

12 PERSONAL AUTHOR(S)
Babish, Charles A. III and Hayes, James R.

13a. TYPE OF REPORT Final	13b TIME COVERED FROM 84 Oct TO 86 Sep	14. DATE OF REPORT (Year, Month, Day) 1988, Apr 22	15 PAGE COUNT 123

16. SUPPLEMENTARY NOTATION

17. COSATI CODES			18. SUBJECT TERMS (Continue on reverse if necessary and identify by block number)
FIELD	GROUP	SUB-GROUP	Aircraft Transparency Systems Heat Transfer
01	01		Aerodynamic Heating Computer Programs
20	13		Wind Tunnel Testing Supersonic Speeds

19. ABSTRACT (Continue on reverse if necessary and identify by block number)
This report describes a wind tunnel test program and the STAPAT computer program which were used to study heat transfer rates on an analytic forebody at Mach 3.0. STAPAT, a Specific Thermal Analyzer Program for Aircraft Transparencies, defines aerodynamic heating environments over windshields and canopies of high-speed aircraft. As a check of its validity, STAPAT predictions were compared with measurements on an analytic forebody whose shape is representative of the forward fuselage of an aircraft. The measurements were obtained using a newly developed experimental technique for determining heat transfer rates at high Reynolds numbers and supersonic speeds in a cold flow wind tunnel. Basically, this technique incorporated a means for raising the temperature of the outer surface of the analytic forebody above the recovery temperature of the tunnel which was operated at stagnation temperatures near atmospheric. This technique required establishment of steady state conditions and use of a special three-wire, coaxial thermocouple probe inserted in the model wall to determine the temperature of the outer surface, which was in contact with the air flow, and the temperature of the backface, which was in contact with circulating hot water.

20 DISTRIBUTION/AVAILABILITY OF ABSTRACT ☒ UNCLASSIFIED/UNLIMITED ☐ SAME AS RPT. ☐ DTIC USERS	21 ABSTRACT SECURITY CLASSIFICATION UNCLASSIFIED
22a NAME OF RESPONSIBLE INDIVIDUAL CHARLES A. BABISH III	22b. TELEPHONE (Include Area Code) (513) 255-5060 22c OFFICE SYMBOL AFWAL/FIER

DD Form 1473, JUN 86   Previous editions are obsolete.   SECURITY CLASSIFICATION OF THIS PAGE

19 continued.

Heat transfer rates were significantly influenced by tunnel stagnation temperatures, gage surface temperatures and water temperatures. Use of a nondimensional heat transfer coefficient, the Stanton number, effectively eliminated heat transfer rate dependency upon these temperatures and therefore was shown to be the best way to evaluate heat transfer rates over the analytic forebody. There was very good agreement between the measured and STAPAT-calculated Stanton number relationships with tunnel stagnation pressure and angle of attack. Both showed slight but general decreases in Stanton number with increasing pressure and angle of attack.

The magnitudes of the measured heat transfer rates, their distribution over the analytic forebody and their good agreement with STAPAT calculations combined to provide validations of both the STAPAT program and the experimental technique for heat transfer testing in cold flow wind tunnels.

FOREWORD

This report describes a cooperative in-house program between the Aircrew Protection Branch (AFWAL/FIER) of the Vehicle Subsystems Division (AFWAL/FIE) and the High Speed Aero Performance Branch (AFWAL/FIMG) of the Aeromechanics Division (AFWAL/FIM). Both Branches are part of the Flight Dynamics Laboratory at the Air Force Wright Aeronautical Laboratories (AFWAL), Wright-Patterson Air Force Base, Ohio 45433-6553. The program was documented under Project 2402, "Vehicle Equipment Technology," Task 03, "Aerospace Vehicle Recovery and Escape Subsystems," Work Unit 50, "Analysis of Aircraft Transparencies."

The work reported herein was performed during the period October 1984 to September 1986, under the direction of the authors, Mr Charles A. Babish III (AFWAL/FIER) and Mr James R. Hayes (AFWAL/FIMG). The report was released by the authors in September 1987.

The authors wish to thank Mr Max E. Hillsamer of the AFWAL Wind Tunnel Facilities for his contributions to the successful operation of the Mach 3 wind tunnel. Special acknowledgement is made to Mr M. Joseph Rakolta, a student at the University of Cincinnati, for his assistance in STAPAT operation during the periods he served as an engineering aid at AFWAL.

The tunnel interference effects models were fabricated by the Fabrication/Modification Division of the 4950th Test Wing at Wright-Patterson Air Force Base, Ohio. The heat transfer rate test model was designed by Sverdrup Technology, Inc and fabricated by Schmiede Machine and Tool Corporation, both of Tullahoma, Tennessee. The support given by all personnel at these organizations is especially appreciated.

TABLE OF CONTENTS

TABLE OF CONTENTS (Concluded)

LIST OF FIGURES

LIST OF FIGURES (Continued)

11   Four Views of the STAPAT Model of the Analytic Forebody   30

12   Correlation Equation Relationships for Shadow Region   33
        Pressure Coefficients

13   Variation of Body Slope Angle Along the Top Centerline   34
        of the Analytic Forebody

14   Variation of Pressure Coefficient Along the Top Centerline   35
        Shadow Region of the Analytic Forebody

15   Sample of Part of the STAPAT Tabular Output — for Wind   38
        Tunnel Test Run 0657.

16   Typical Data Table — From Wind Tunnel Test Run 0657   40

17   Schlieren Photographs of the Flow Field Over the   41
        Analytic Forebody

18   STAPAT Predictions of Flow Field Properties   43

        a. Isolines of Mach Number   43
        b. Isolines of Static Temperature   43
        c. Isolines of Static Pressure   44
        d. Isolines of Pressure Coefficient   44

LIST OF FIGURES (Continued)

LIST OF FIGURES (Continued)

LIST OF FIGURES (Concluded)

LIST OF TABLES

SECTION I

INTRODUCTION

This report describes and documents the results from a wind tunnel test program and the STAPAT* computer program which were used to study aerodynamic heat transfer rates on an analytic forebody at Mach 3.0.

Air Force aircraft can be expected to operate at supersonic speeds where aerodynamic heating significantly affects the design and performance characteristics of their transparent windshield and canopy systems. STAPAT was developed to provide a valuable tool for the aerothermodynamic analysis of these transparency systems. A three-dimensional, external-forced convection module, STAHET, is included in STAPAT to define aerodynamic heating environments over forward fuselage sections of aircraft. During STAPAT development, a preliminary wind tunnel test program was accomplished to acquire heat transfer rate data for comparison with predictions from a generalized form of the STAHET code. This preliminary test program applied a newly developed experimental technique for obtaining heat transfer rate data at supersonic Mach numbers and high Reynolds numbers, but at ambient stagnation temperatures; i.e., in a "cold flow" wind tunnel. Because of problems with the heat transfer rate gages, only a limited amount of data was acquired. As a result of lessons learned during the preliminary test program, we recommended that the tests be reaccomplished using more suitable heat transfer rate gages to acquire data that could be used for comparison with predictions from the final form of the STAHET code. This report includes the information relative to the test program which incorporated the recommended gages.

Sections II and III present descriptions of the wind tunnel test program and the STAPAT computer program, respectively. Results from the programs, discussions of their significance, and comparisons of the wind tunnel data with STAPAT predictions are presented in Section IV.

---

* STAPAT is an acronym for Specific Thermal Analyzer Program for Aircraft Transparencies. STAPAT is documented in References 1 and 2.

SECTION II

DESCPIPTION OF THE TEST PROGRAM

1. TECHNIQUE FOR HEAT TRANSFER TESTING IN COLD FLOW WIND TUNNELS

A newly developed experimental technique for heat transfer testing in cold flow wind tunnels was used to acquire the data needed for this program. Standard heat transfer testing techniques require the use of wind tunnel test facilities where stagnation temperatures, and therefore recovery (adiabatic wall) temperatures, are significantly greater than ambient temperatures. These facilities do not provide desired Reynolds number ranges at supersonic speeds. Facilities that do provide high Reynolds numbers at supersonic speeds are cold flow facilities which operate at stagnation temperatures less than or equal to ambient temperatures. To use cold flow facilities for heat transfer testing required development of a new experimental technique. Such a technique was developed and is documented in Reference 3.

Basically, this experimental technique incorporates a means for raising the model outer wall temperature above the tunnel recovery temperature by means of hot water flow along the inner wall of the model. The temperatures of the outer and inner walls are measured after steady state conditions have been achieved. During this "steady state" heat transfer condition and for a homogeneous wall material of constant thermal conductivity, a linear temperature distribution exists through the model wall. From these temperatures and the properties of the wall material, the conductive heating rate can be determined. Because steady state conditions have been established, the forced convective heat transfer rate from the surface of the model into the air flow is equated to the conductive heat transfer rate through the wall.

2. AFWAL MACH 3 HIGH REYNOLDS NUMBER WIND TUNNEL TEST FACILITY

All tests were accomplished in the Mach 3 High Reynolds Number Wind Tunnel Test Facility at the Air Force Wright Aeronautical Laboratories (AFWAL), Wright-Patterson Air Force Base, Ohio. A perspective view of the facility is presented in Figure 1. The facility is an intermittent, cold flow wind tunnel that operates in a blowdown
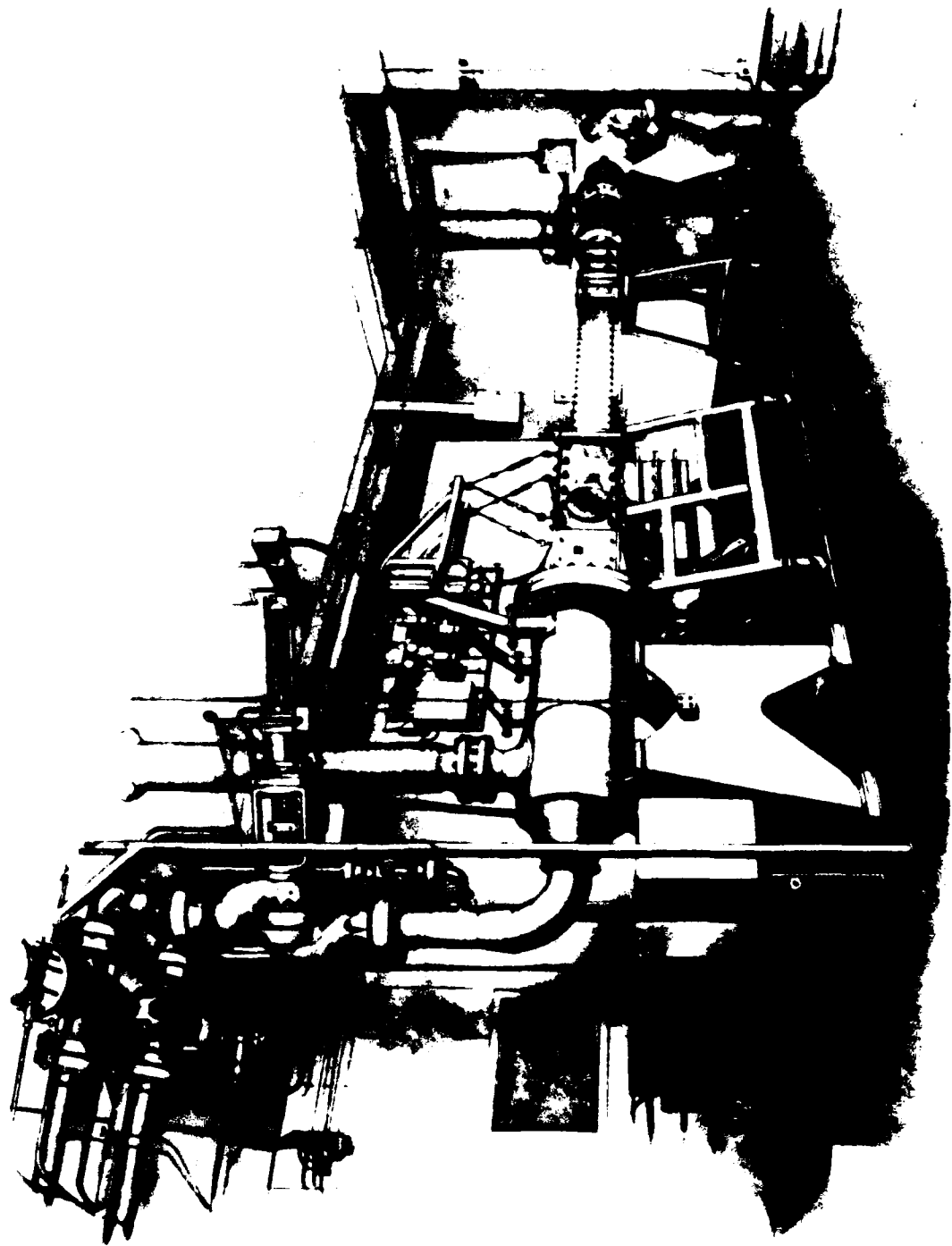
Figure 1. Perspective View of the AFWAL Mach 3 High Reynolds Number
Wind Tunnel Test Facility (From Reference 4)

mode using dry compressed air which is exhausted to the atmosphere through silencers. A diagram of the operating process is shown in Figure 2a. The tunnel has a constant area rectangular test section 8.0-in. wide and 8.2-in. high, with a test rhombus 23-in. long (Figure 2b). One set of test section side walls is furnished with 8-in.-diameter windows. These 2-in.-thick glass windows were used with the shadowgraph and schlieren systems for flow visualization.

The tunnel can be operated at stagnation pressures from approximately 70 to 570 psia for stagnation temperatures in the range from 400 to 560 R depending upon ambient conditions. The corresponding free-stream unit Reynolds numbers range from 13 to 140 million per ft.

Detailed descriptions of the AFWAL Mach 3 High Reynolds Number Wind Tunnel Test Facility can be found in References 4 and 5.

3. ANALYTIC FOREBODY WIND TUNNEL MODELS

a. Analytical Description of the Surface Shape

The developed cross-sections model (Forebody 4) of Reference 6 was selected for the shape of the wind tunnel models used in this test program. A sketch of Forebody 4 from Reference 6 is reproduced in Figure 3. Also shown in Figure 3 are the locations of the orifices which were used to obtain surface pressures during the test program reported in Reference 6. As required for verification of STAPAT (Reference 2), this shape is representative of the forward fuselage of an aircraft (with a canopy-like hump) and has sufficient surface curvature to induce three-dimensional flow and variable edge entropy effects.

ATMOSPHERIC
EXHAUST
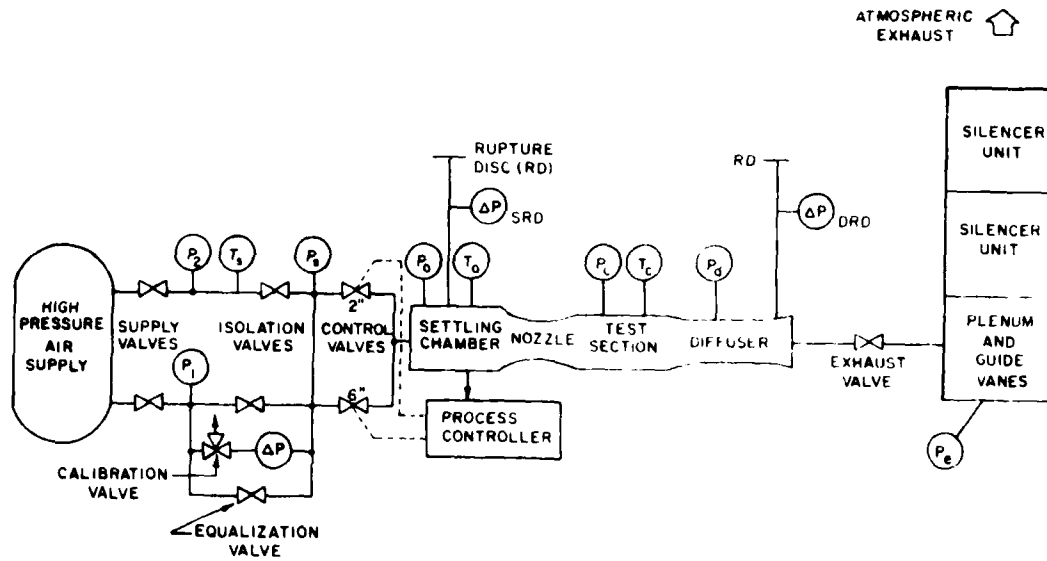
a. Sketch of the Operating Process (Symbols
are Defined in Reference 4)
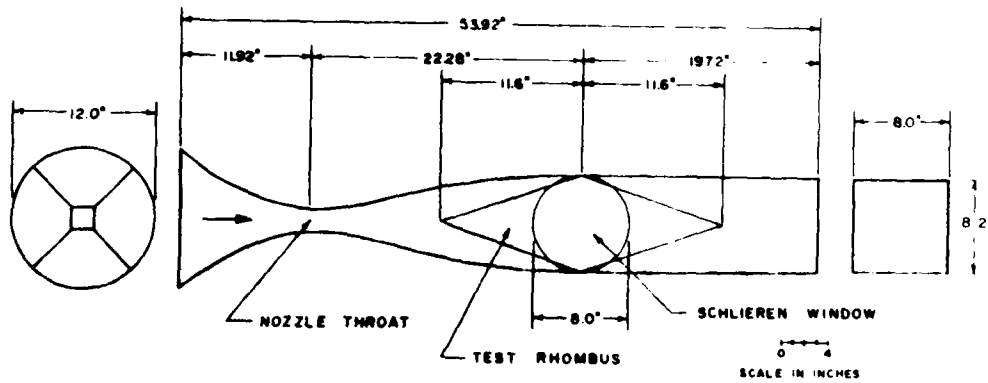
b. Sketch of the Test Section

Figure 2.   Sketches of the AFWAL Mach 3 High Reynolds Number Wind
Tunnel Test Facility (From Reference 4)

LOCATIONS OF THE
SURFACE PRESSURE
ORIFICES
(Reference 6)
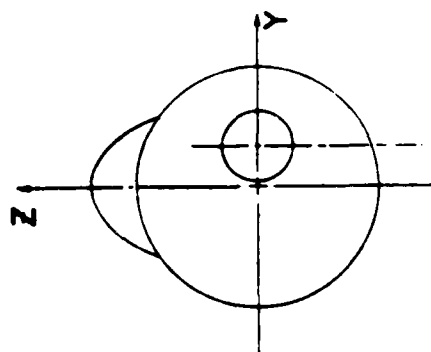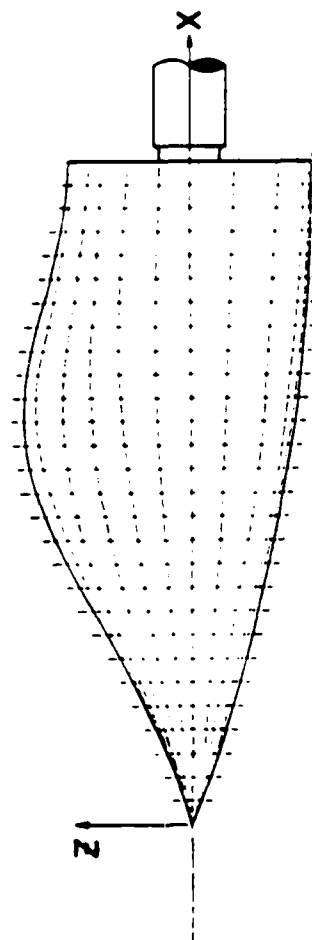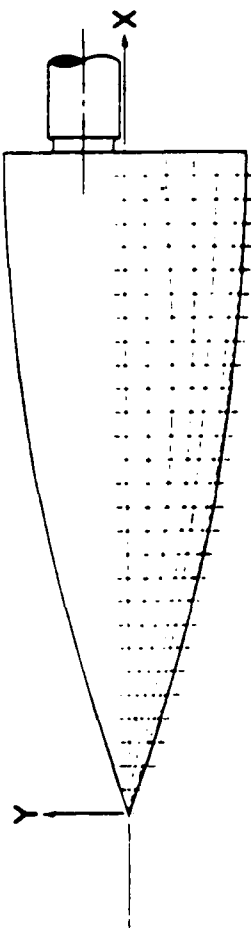
Figure 3. Surface Shape of the Analytic Forebody (From Reference 6, Forebody 4)

6

The surface of the analytic forebody is described parametrically by the following equations (Reference 6):

$$\frac{y}{r_1} = \left[1 + \left(1.35 \frac{r}{r_1} - 1\right) \sin^2\left(\frac{\pi x}{\ell}\right)\right] \sin \theta \tag{1}$$

$$\frac{z}{r_1} = \left[1 + \left(1.35 \frac{r}{r_1} - 1 + \frac{0.35}{\cos \theta}\right) \sin^2\left(\frac{\pi x}{\ell}\right)\right] \cos \theta \tag{2}$$

Where

$$\frac{r}{r_1} = \frac{1}{1.25 - 0.25 \cos 2\theta + 0.13174 (\cos \theta - \cos 3\theta)} \tag{3}$$

and

$$\frac{r_1(x)}{\ell} = \left(1 - \frac{x}{2\ell}\right)\left(\frac{x}{\ell}\right) \tan 20^\circ \tag{4}$$

Note that the radial distances r and r_1, and the polar angle θ are not the same as the polar coordinates R and ϕ of the analytic forebody cross section. (See Section III paragraph 3a(2).)

Since surface pressure data is available in Reference 6 for this analytic forebody, the scope of the wind tunnel program was reduced considerably by the elimination of the requirement for pressure measurements.

b. Tunnel Interference Effects Models

Determination of the model size for the tests was based on a compromise between selecting a large-size model, to provide high Reynolds numbers and room for instrumentation, and selecting a small-size model, to minimize wind tunnel interference effects such as those caused by reflected shock waves and solid blockage or tunnel choking. Selection of model size was aided by conducting wind tunnel tests using uninstrumented models of the analytic forebody. Two tunnel interference effects models were fabricated from aluminum and stainless steel, one 8-in. long and one 10-in. long (Figure 4). The interference models were placed in the wind tunnel (Figure 5) and tested over a range of Reynolds numbers and angles of attack. Based on observations of tunnel wall pressures and schlieren photographs of shock waves, we concluded that analytic forebody models as long as 10 in. could be tested at angles of attack from -5 to +5° with negligible interference effects.

The 10-in.-long model (not including the sting support) presents a frontal area of approximately 11 in.^{2} at 0° angle of attack. This area is 16.8 percent of the physical cross-sectional area of the test section and is well below the solid blockage limit of 28 percent recommended in Reference 4.

c. Heat Transfer Rate Model

With the shape and size of the heat transfer rate model determined, a method for providing hot water flow to the inner wall of the model and a means for measuring the temperature of the inner and outer walls had to be incorporated into the model design. The approach taken is illustrated in the sketches and photographs presented in Figure 6.

The model consists of four sections; an upper body, a lower body, a central plug and a sting mounting adaptor. The upper body forms the inner and outer walls (0.125 in. nominal wall thickness) that are instrumented for temperature measurements. Twenty locations were selected for measurement; eight along the top center-line of the model ($\phi = 0°$) and six each along the $\phi = 30°$ and $\phi = 60°$ rays. Temperature measurement (gage) locations are spaced at 1.0-in. intervals. (The photographs in Figure 6 show macor (glass) cylinders inserted in the gage location holes. These inserts were used in the preliminary test program (Reference 2) and

Figure 4.   Photograph of the 8- and 10-in.-Long Wind Tunnel Interference Effects Models
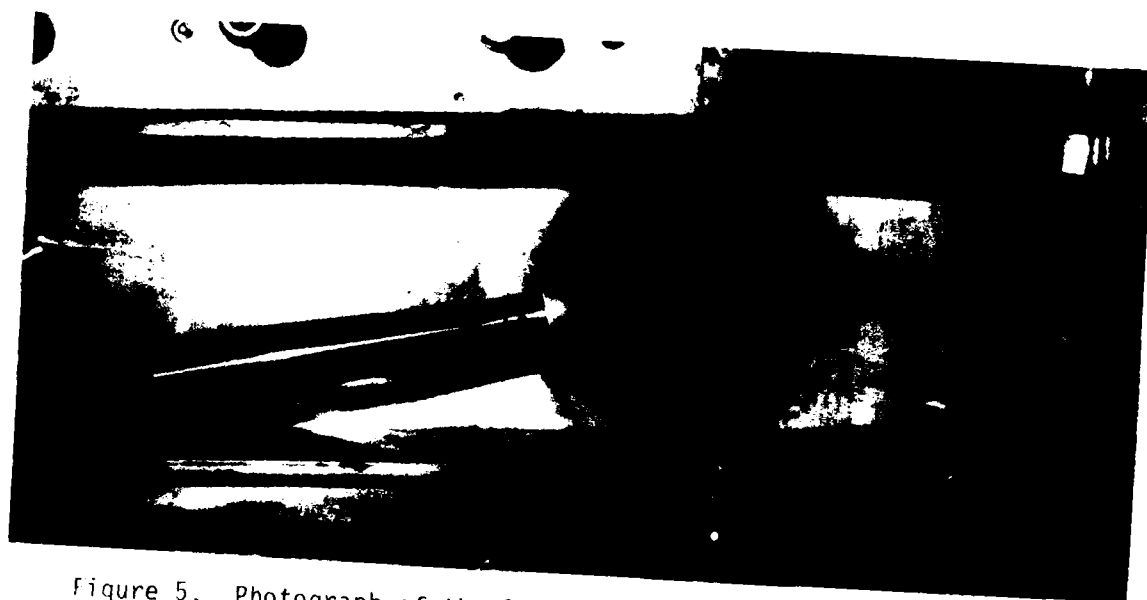
Figure 5.   Photograph of the 10-in.-Long Interference Effects Model in the AFWAL Mach 3 Wind Tunnel
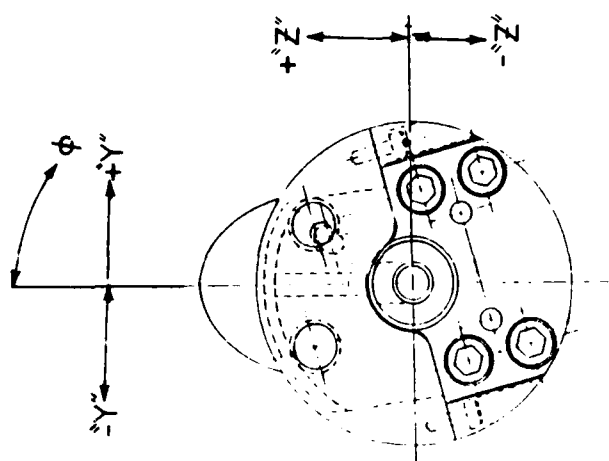
STING MOUNTING ADAPTOR

MODEL ASSEMBLY

+"Z"   -"Z"

φ   +Y

-Y

X

+ ALPHA   FLOW
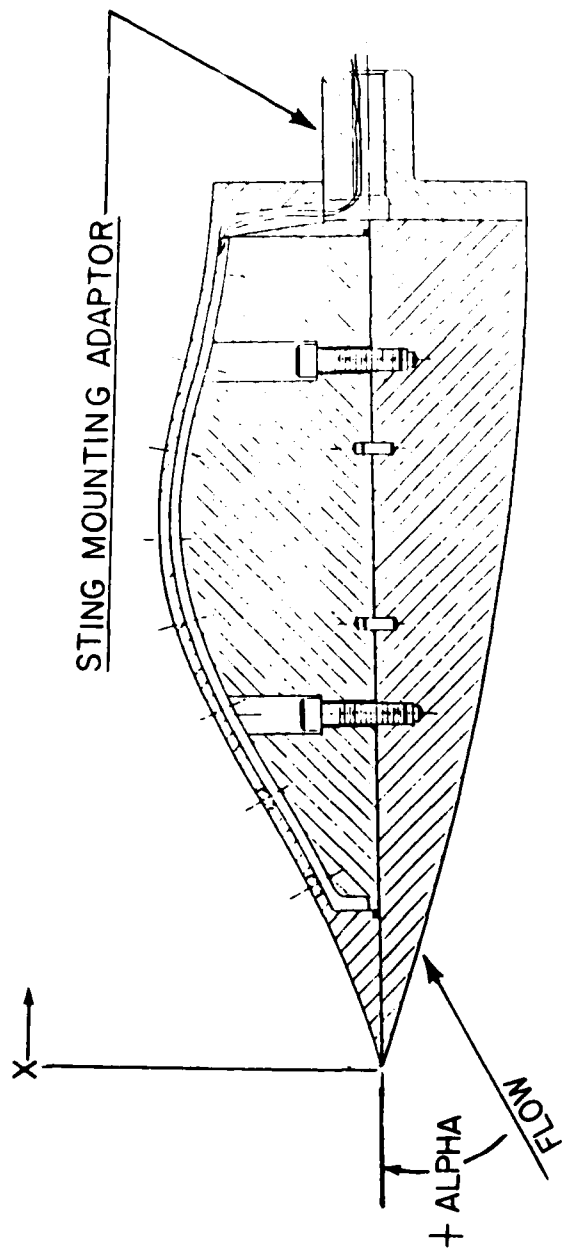
COORDINATES OF EXTERNAL SHAPE

STATION X INCHES	φ DEGREES	Y INCHES THEORETICAL	MEASURED	Z INCHES THEORETICAL	MEASURED
2.000	26.951	0.3417	0.3394	0.6641	0.6685
	54.090	0.5146	0.5415	0.3908	0.3916
	146.578	0.3655	0.3661	-0.5519	-0.5580
4.000	22.338	0.6295	0.6317	1.4591	1.4661
	70.809	1.0594	1.0641	0.1687	0.1704
	141.257	0.7540	0.7621	-0.9460	-0.9498
6.000	22.338	0.8282	0.8282	1.9150	1.9196
	70.809	1.3904	1.3950	0.4619	0.4855
	141.257	0.9962	0.9991	-1.2416	-1.2454
8.000	26.951	0.9005	0.9028	1.770	1.7754
	54.090	1.4390	1.4410	1.0427	1.0449
	146.578	0.9748	0.9741	-1.4	-1.4809
10.000	30.000	0.9099	0.9106	1.5760	1.5772
	60.000	1.5760	1.5792	0.9094	0.9918
	150.000	0.9094	0.9120	1.5760	1.5796

Figure 6. Sketches, Photographs and Coordinates of the Heat Transfer Rate Model

UPPER BODY ASSEMBLY
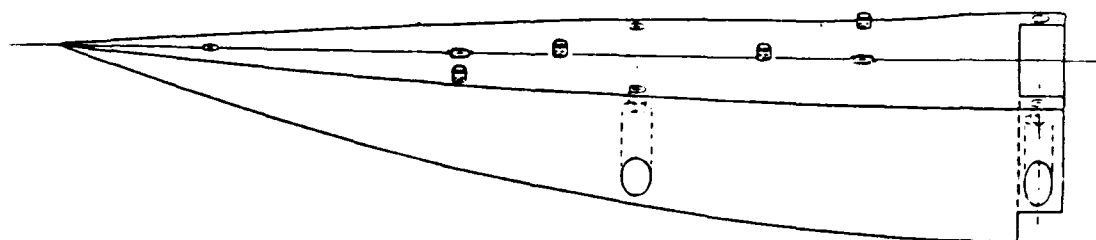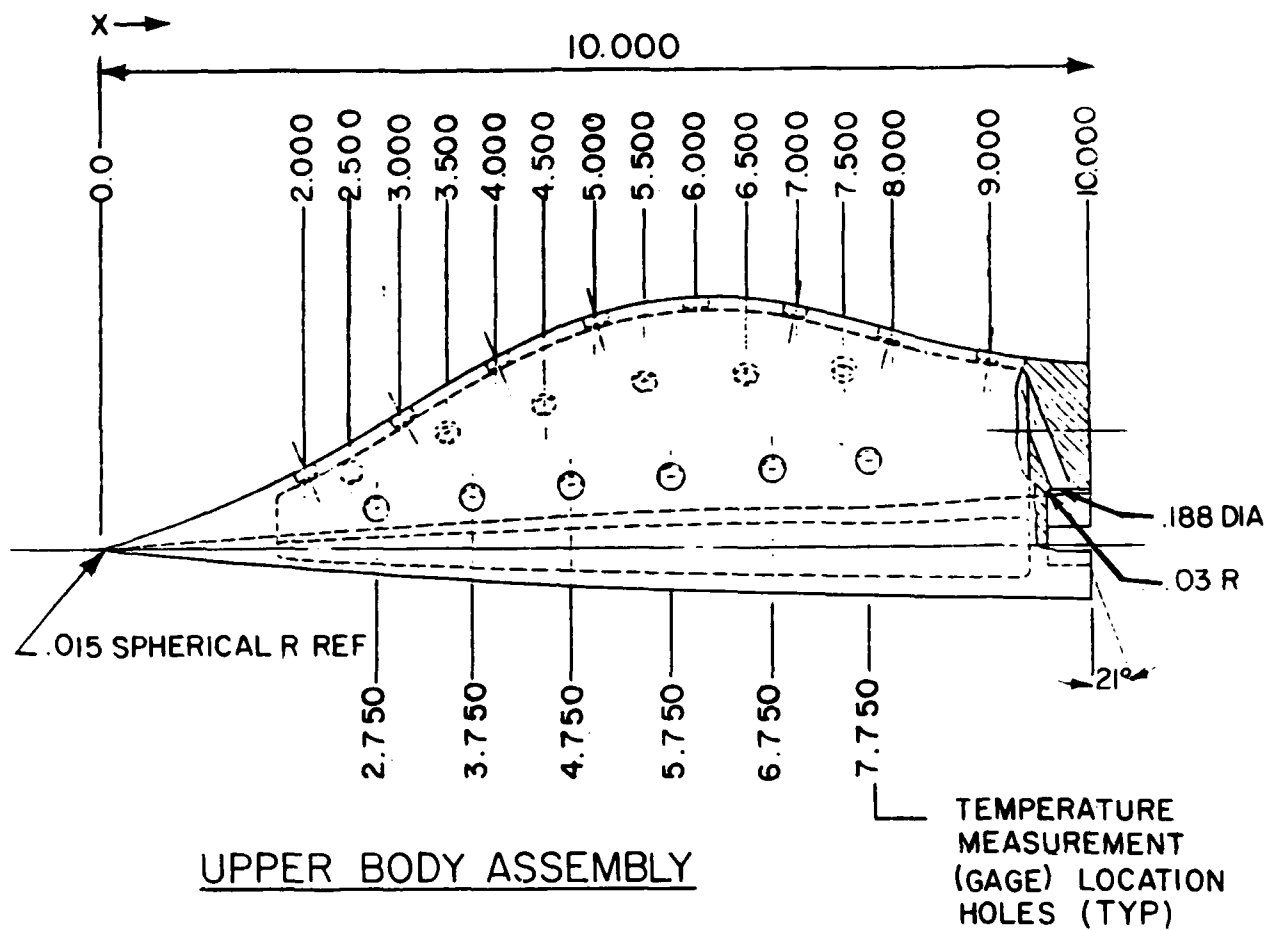
LOWER BODY ASSEMBLY

Figure 6. (Continued)

11
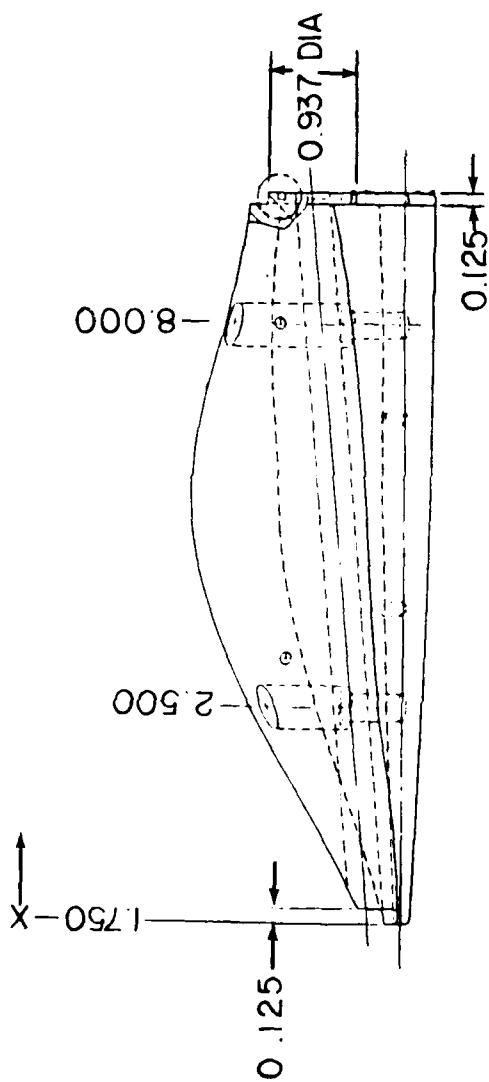
PLUG ASSEMBLY

Figure 6. (Concluded)

were replaced with the new heat transfer rate gages described in Section II paragraph 5.) The upper and lower bodies form the external shape of the analytic forebody and are joined with five cap screws. The central plug is used to form the water flow channels along the inner wall of the gages. The nominally 0.125-in.-thick cavity between the upper body and the central plug was first filled with a room temperature vulcanizing (RTV) silicone sealer. Then sections of the RTV sealer were cut away to form 0.50-in.-wide channels along the centerlines of the rows of gages. The design allows for water flow into the rear of the model, through the interior of the central plug toward the nose of the model, back through the RTV sealer channels, and out the rear of the model. The central plug is joined to the lower body with two cap screws. The sting mounting adaptor is fastened to the lower body with four cap screws.

The heat transfer rate model was designed by Sverdrup Technology, Inc and fabricated from aluminum and stainless steel by Schmiede Machine and Tool Corporation of Tullahoma, Tennessee. The as-built shape of the analytical forebody was very close to the desired (theoretical) shape. Differences between measured and theoretical coordinates did not exceed 0.0050 in., with an average difference of 0.00307 in. and a standard deviation of ±0.00115 in. (as obtained from the values presented in Figure 6).

4. MODEL SUPPORT SYSTEM

The model support system consisted of a hydraulically actuated pitch sector mounted in the test section downstream of the test rhombus. A linear potentiometer attached to the actuator arm was used to determine sting pitch angle. The output of the potentiometer was fed to a display in the control room and used to manually set sting pitch angle (and hence the model angle of attack) before each run. Calibration of the potentiometer was accomplished with an inclinometer placed on the pitch sector head. The calibration was performed at the beginning of each test day and is accurate to within 0.01° between -8 and +8° angle of attack.

5. INSTRUMENTATION AND DATA GATHERED

Different types of instrumentation were used to gather the data which was needed for comparison with STAPAT predictions. General descriptions of the instrumentation are given below; additional information can be found in the references cited.

a. Heat Transfer Rate Gage Temperatures

The primary data gathered was the temperature of the outer wall of the analytic forebody (the outer surface temperature) and the temperature of the inner wall (the backface temperature). These temperatures were measured at various locations on the analytic forebody using one heat transfer rate gage at each location (see Figure 6).

Each gage incorporated a three-wire, coaxial thermocouple probe swaged in a stainless steel cylindrical "button" as shown in Figure 7. The coaxial thermocouple probe consisted of a constantan center wire which was coated with a 0.0005-in. thickness of ceramic insulation and swaged in a tube of Chromel® material. The thermocouple was then swaged in the cylindrical button and its length cut to the thickness of the button. The thermocouple junction at the outer surface of the analytic forebody was formed by filing the probe/button to the contour of the forebody so that metallic slivers of the constantan and Chromel materials bridged the insulation. The thermocouple junction on the backface of the probe/button was formed at the juncture of a second constantan wire and the Chromel tube. Additional information on the coaxial thermocouple probes can be found in References 7 and 8.

b. Instrumentation for Other Data

The data needed to determine the free-stream flow conditions for the AFWAL Mach 3 wind tunnel was tunnel stilling chamber (stagnation) pressure,

---

® Registered - Hoskins Manufacturing Co
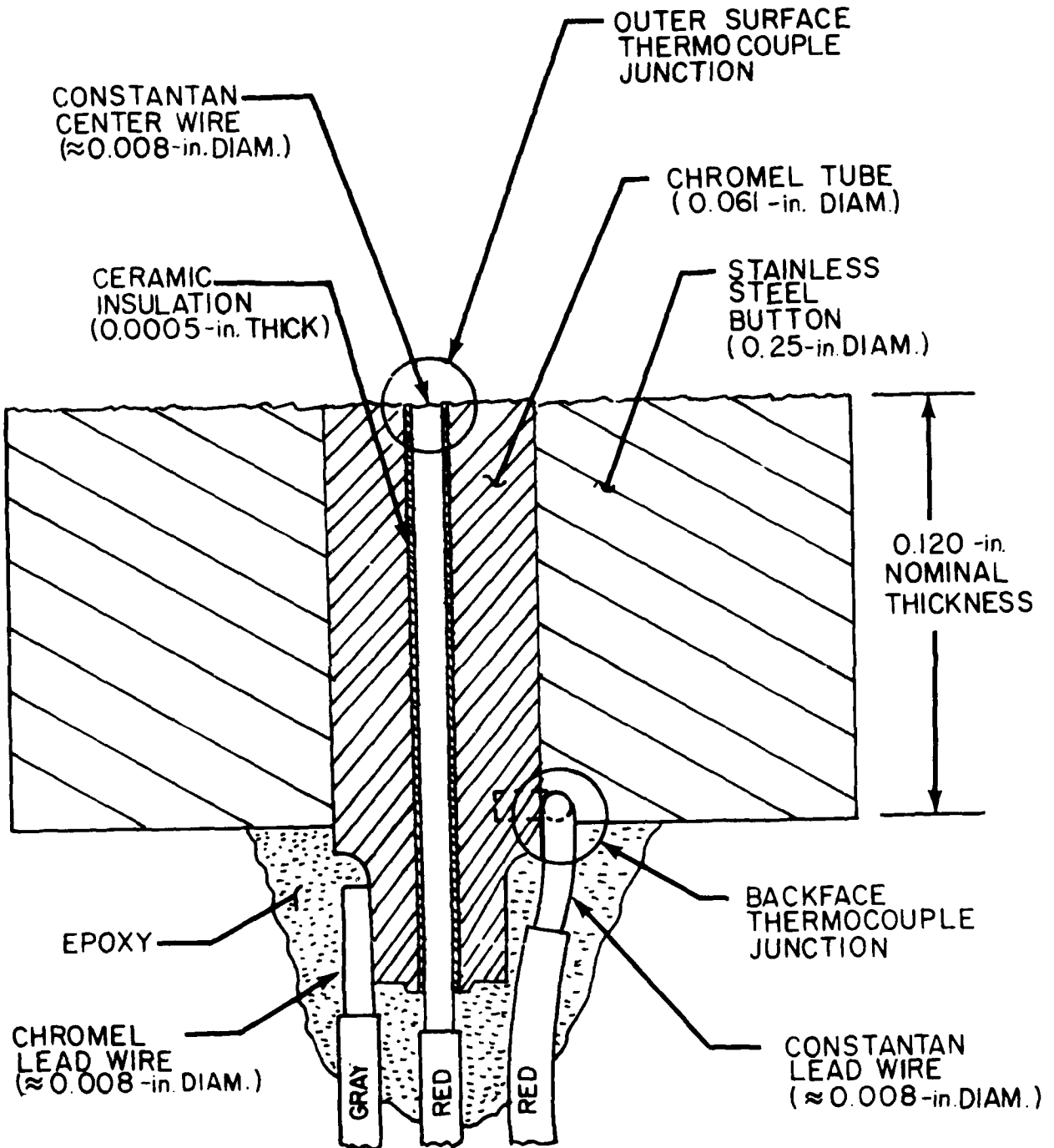
Figure 7. Cross Section of the Heat Transfer Rate Gages Showing
General Construction

15

PO, and tunnel stilling chamber (stagnation) temperature, TO. The stagnation pressure was measured using a 600-psia transducer and the stagnation temperature was measured using a Type J (iron vs constantan) thermocouple. Model angle of attack was obtained from the linear potentiometer which was attached to the pitch sector actuator arm. Axial station and circumferential locations of the heat transfer rate gages were determined during the machining of the model surface contours. Model inlet and outlet water temperatures were measured with type K (chromel vs alumel) thermocouples located in the water line attachment points at the base of the model.

A video camera was used to photograph the model during the tests. This camera was mounted on the schlieren system and was connected to a monitor and video recorder in the control room.

6. TEST PROCEDURES

Before each run the model was brought to a uniform and constant temperature by circulating water through the internal passages. The water temperature was regulated by a 10 gal hot water heater and was held at approximately 600 R. When all gage outputs indicated a constant temperature (both surface and backface measurements) the data acquisition system was started and then the tunnel was started. Several gages were selected for display on strip chart recorders and these were monitored during the run. Data were taken until these gages indicated that the surface to backface temperature difference was constant. The time to reach this steady state heating condition was approximately 15 s. The data acquisition rate was one sample per second and data were taken for about 30 s after the steady state condition was established.

Figure 8 shows a typical temperature-time history for one gage. The surface to backface temperature difference is shown in Figure 9. This figure shows that the steady state condition was reached in 12 s and maintained through the rest of the run. The heat transfer rate was computed from the average of the temperature difference during the steady state portion of the run.

7. DATA REDUCTION AND PRECISION
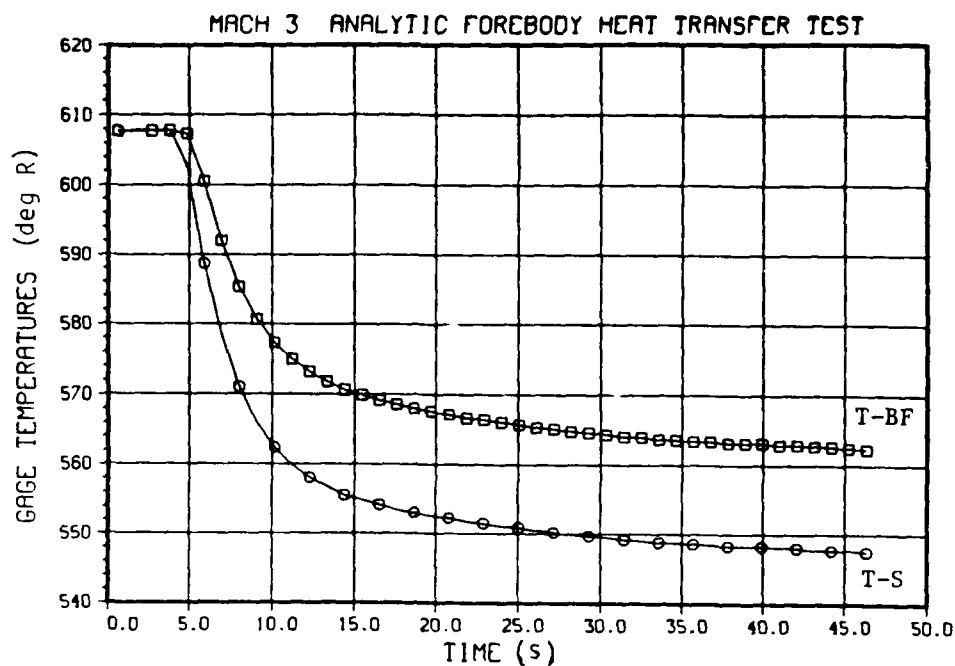
Figure 8. Typical Temperature-Time History From One Heat Transfer Rate Gage
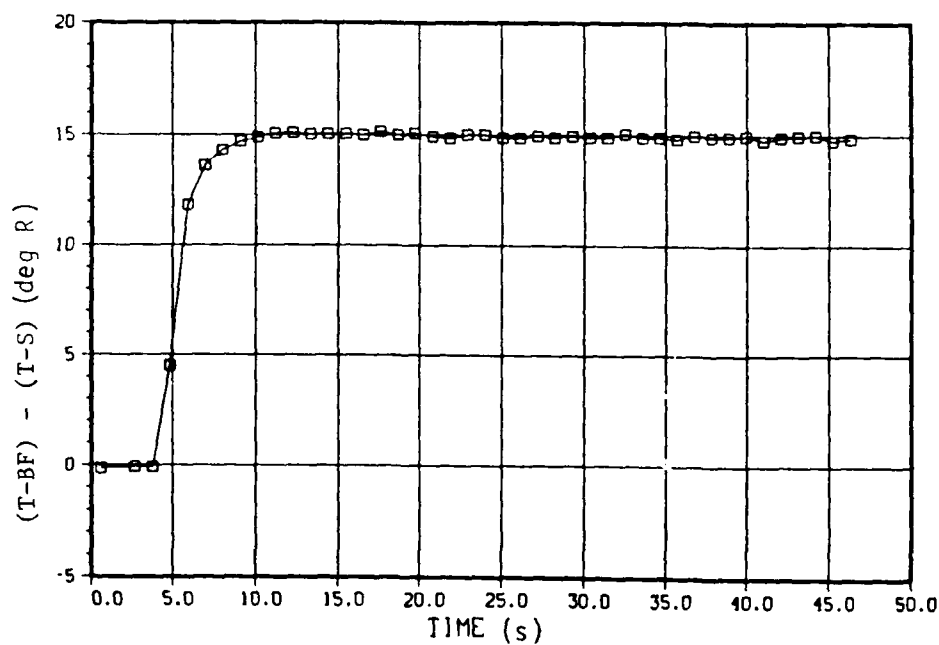
Figure 9. Typical Time History of the Difference in Gage Surface and Backface Temperatures

17

a. Data Reduction Methods and Equations

The data reduction methods, equations, symbols, and constants used during this test program are summarized below.

(1) Wind Tunnel Flow Conditions

The calibrated wind tunnel Mach number, M, the measured stagnation (settling chamber) pressure, P0, and the measured stagnation temperature, T0, were used to calculate the remaining free-stream wind tunnel flow conditions. The equations given in Reference 9 were applied. Static pressure, P-INF, and static temperature, T-INF, were calculated using the equations for perfect gas, isentropic expansion from the settling chamber to the test section. Static density, RHO-INF, was calculated using the thermal equation of state and the derived values for static pressure and temperature. Velocity, V-INF, was calculated using the equation for the speed of sound, the definition of Mach number and values for calibrated Mach number and derived static temperature. Absolute viscosity, MU-INF, was calculated using Sutherland's equation and the derived value for static temperature. Free-stream unit Reynolds number, RE-INF, was calculated based on the derived static density, velocity and absolute viscosity values.

(2) Model Characteristics and Heat Loads

Model heat load parameters at each measured axial, X, and circumferential, PHI, gage location were determined for various measured model angles of attack, ALPHA, and average inlet and outlet water temperatures, T-WATER.

Heat transfer rate, QDOT, was calculated based on the measured gage backface and surface temperatures, T-BF and T-S, using the data reduction method.

The heat transfer rate gages were placed in the wall of the upper body of the analytic forebody. During the wind tunnel tests, hot water was passed along the backface of the wall and air was passed over the outer surface (see Figure 10). This situation was maintained until a "steady state" condition was reached for all gages; i.e., until the difference between gage temperatures, T-BF and T-S, had stabilized. For this steady state condition, the rate of heat flow per unit area

18
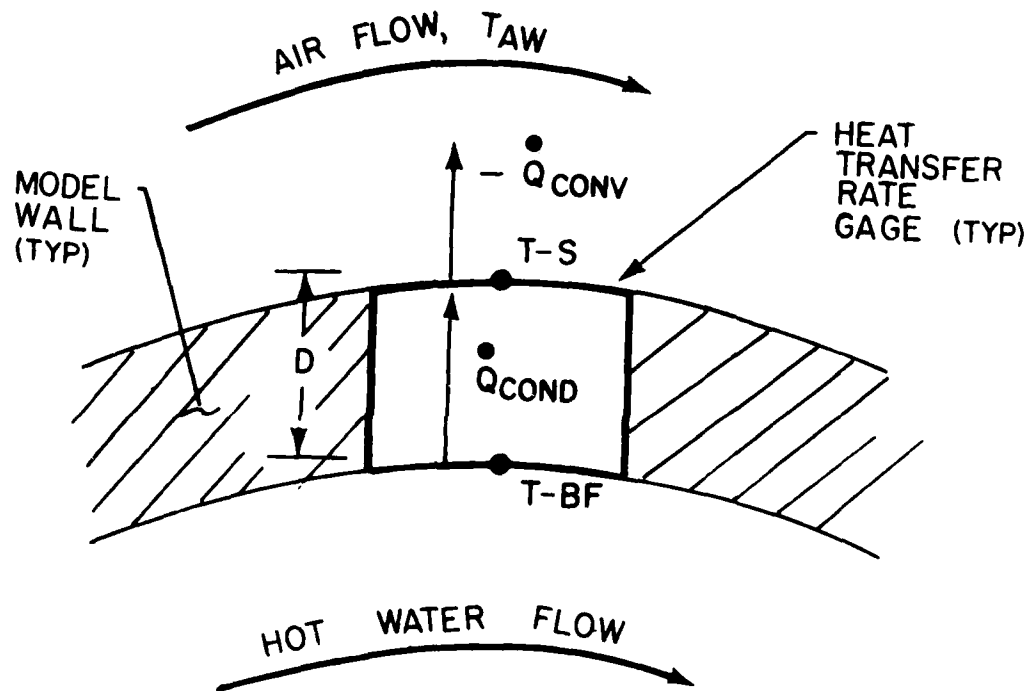
Figure 10.   Parameters Associated With the Heat Transfer Rate Gages

(heat flux or heat transfer rate) through the gage from the backface to the surface, $\dot{Q}_{COND}$, was assumed equal to the heat transfer rate from the gage surface to the airflow, $-\dot{Q}_{CONV}$.* That is,

$$-\dot{Q}_{CONV} = \dot{Q}_{COND} \tag{5}$$

These heat transfer rates (see Reference 10) can be expressed as follows:

$$\dot{Q}_{COND} = k \left[(T\text{-}BF) - (T\text{-}S) \right] / D \tag{6}$$

$$\dot{Q}_{CONV} = h \left[T_{AW} - (T\text{-}S) \right] \tag{7}$$

Where k is the thermal conductivity of the gage and D its thickness; h is the forced convection heat transfer coefficient; and T_{AW} is the adiabatic wall temperature of the flow over the gages.

---

*Since the thermophysical properties of the gage and model materials were similar, lateral heat transfer rates were considered negligible. Expected differences in thermal conductivities of the gage materials were included in the heat transfer rate uncertainty estimates. Radiation from the model surface to the tunnel walls was estimated to be an order of magnitude less than the uncertainty and was neglected.

For the purposes of this test program, then, the forced convection heat transfer rate can be obtained from

$$\dot{Q}_{CONV} = -k \lceil (T\text{-}BF) - (T\text{-}S) \rceil / D \qquad (8)$$

To obtain values for $\dot{Q}_{CONV}$, values for k, D, T-BF, and T-S must be known. The value for k was determined based on reported properties of the gage materials for the material temperature range encountered during this test program (References 8 and 11). Reported values for constantan and Chromel materials ranged from 0.0027 to 0.0039 Btu/(ft·s·R) for temperatures from 470 to 580 R. An average value of 0.0033 Btu/(ft·s·R) was used for all gages. Because each gage was inserted in the model wall and then filed to the surface contour of the model, the value of D was slightly reduced from its measured initial nominal value of 0.125 in. A thickness of 0.120 in. was chosen for each gage. Gage temperatures T-BF and T-S were obtained from gage thermocouple measurements and their differences were averaged over the steady state period. Values for the heat transfer rate, then, were calculated using the following equation:

$$QDOT = \dot{Q}_{CONV} = (-0.33) [(T\text{-}BF) - (T\text{-}S)]_{AVE} \qquad (9)$$

A forced convection heat transfer coefficient, H(.9 TO) = h, was calculated from Equation 7 using a measured-surface temperature, T-S, the derived value of heat transfer rate, QDOT, and an adiabatic wall temperature, T_{AW}, equal to 90 percent of the measured-stagnation temperature, TO. That is,

$$H(.9\ TO) = QDOT / \lceil (0.9) (TO) - (T\text{-}S) \rceil \qquad (10)$$

A Stanton number, ST, was calculated based on the derived values of heat transfer coefficient, free-stream static density, RHO-INF, and free-stream velocity, V-INF, and a value of 6006 ft^2/(s^2·R) for the specific heat of air at constant pressure, c_p (Reference 9) using the following equation:

$$ST = (778)\ H(.9\ TO) / \lceil (RHO\text{-}INF) (V\text{-}INF) (c_p) \rceil \qquad (11)$$

b. Precision of the Data

The maximum uncertainty in the specific heat of air at constant pressure, c_p, was conservatively estimated at ± 300 ft^2/(s$^2\cdot$R) (i.e., ± 5 percent of 6006 ft^2/(s$^2\cdot$R), the value used). This was to account for the general lack of data reported in the literature for the low temperatures and pressures encountered during these tests.

The estimated maximum uncertainty in Mach number was based on the results of aerodynamic tunnel calibration measurements made to determine the lateral and longitudinal Mach number distributions in the test rhombus (Reference 4).

The maximum uncertainties in the measured parameters were based on estimates, quoted instrument limits of error, and checks against secondary standards. (The maximum uncertainty in gage thickness, D, was conservatively estimated at ± 0.005 in. to account for unknown thickness changes due to filing of the gages to match the contour of the model.)

The estimated maximum uncertainty in gage thermal conductivity was taken as two-thirds of the range of values reported for the materials used and the temperature range encountered.

Maximum uncertainties in the derived data parameters were estimated by propagating the maximum uncertainties in the material property, calibrated, and measured parameters through the applicable relationships among the parameters. The method applied makes use of the Taylor's series and is described in detail in Reference 12.

The estimated maximum uncertainties of all measured and derived data parameters are listed in Table 1.

TABLE 1. Precision of the Data

Data Parameter, Symbol, Units	Typical Value	Maximum Uncertainty (+ and -)
WIND TUNNEL FLOW CONDITIONS		
Material Property Parameter		
Specific heat of air, c_p, $ft^2/(s^2 \cdot R)$	6006	5%*
Calibrated Parameter		
Mach number, M	3	0.075
Measured Parameters		
Stagnation pressure, PO, psia	300.09	0.15
Stagnation temperature, TO, R	497.74	1.8
Derived Parameters		
Static pressure, P-INF, psia	2.80	11.2%
Static temperature, T-INF, R	179.29	3.2%
Static density, RHO-INF, $slug/ft^3$	0.3940E-02	11.6%
Velocity, V-INF, ft/s	1955.8	3.0%
Absolute viscosity, MU-INF, $lbf \cdot s/ft^2$	0.14421E-06	6.4%
Reynolds number, RE-INF, ft^{-1}	0.5344E+08	13.2%
MODEL CHARACTERISTICS AND HEAT LOADS		
Material Property Parameter		
Gage thermal conductivity, k, $Btu/(ft \cdot s \cdot R)$	0.33E-02	0.4E-03

* % means percent of value

TABLE 1. Precision of the Data — Continued

Measured Parameters

Angle of attack, ALPHA, deg	-0.01	0.01
Gage thickness, D, in.	0.120	0.005
Gage axial station location, X, in.	2.75	0.05
Gage circumferential location, PHI, deg	60.0	0.5
Backface temperature, T-BF, R	552.60	1.8
Surface temperature, T-S, R	524.61	1.8
Water temperature, T-WATER, R	600.83	1.3

Derived Parameters

Ratio T-S and T0, T-S/T0	1.054	0.5%
Heat transfer rate, QDOT, Btu/(ft^2·s)		
a. QDOT $\leq$ -5.000	-9.320	0.54 + 10%
b. QDOT $>$ -5.000	-2.656	0.79 + 5%
Heat transfer coefficient, H(.9 T0), Btu/(ft^2·s·R)		
a. H(.9 T0) $<$ 0.7000E-01	0.5538E-01	0.63E-02 + 11%
b. H(.9 T0) $\geq$ 0.7000E-01	0.1216E+00	20%
Stanton number, ST		
a. ST $<$ 0.1000E-02	0.3644E-03	0.10E-03 + 14%
b. ST $\geq$ 0.1000E-02	0.2044E-02	24%

8. RUN SUMMARY

Fifty-one wind tunnel test runs were made in support of this program. Table 2 presents a chronological summary of the test runs in terms of selected parameters of the test matrix.

The tests were accomplished over a period of days and hence for different atmospheric conditions. Essentially, the outside air temperature fixed the temperature of the high-pressure air supply and therefore the tunnel stagnation temperature, T0. Values for T0 ranged from approximately 450 to 498 R. Test were also accomplished at tunnel stagnation pressures, P0, of nominally 100, 200, 300 and 400 psia. Since all tests were conducted at a free-stream Mach number of 3.0, these tunnel conditions provided a range of free-stream unit Reynolds numbers, RE-INF, from approximately 16 million to 76 million per ft.

To assure different levels of heat transfer rates for given free-stream conditions, the temperature of the water flowing along the backface of the outer wall of the analytic forebody, T-WATER, was adjusted to provide nominal T-WATER values of 580, 590, 600 and 610 R.

Tests at model angles of attack, ALPHA, of -4, -3, 0, +3 and +4° were accomplished to determine the effect of variations in this parameter on flow field properties and heat transfer rates over the analytic forebody.

TABLE 2. Test Run Summary

RUN	ALPHA (deg)	P0 (psia)	T0 (R)	T-WATER (R)
0654	0	200	497	601
0655	0	300	498	601
0656	0	400	497	600
0657	0	100	474	601
0658	0	200	473	601
0659	0	300	475	601
0660	0	400	477	600
0661	-3	100	468	600
0662	-3	200	471	600
0663	+4	100	469	601
0664	+4	200	474	601
0665	0	100	493	610
0666	0	200	495	611
0667	+4	100	491	611
0668	+4	200	493	611
0669	-4	100	490	611
0670	-4	200	491	611
0671	-3	100	488	611
0672	-3	200	490	610
0673	+3	100	487	611
0674	+3	200	489	611
0675	0	100	467	593
0676	0	200	463	592

RUN	ALPHA (deg)	P0 (psia)	T0 (R)	T-WATER (R)
0677	+3	100	459	592
0678	+3	200	460	591
0679	-3	100	457	591
0680	-3	200	461	590
0681	-4	100	458	589
0682	-4	200	462	588
0683	+4	100	460	588
0684	+4	200	462	587
0685	0	100	466	583
0686	0	200	461	583
0687	+3	100	458	582
0688	+3	200	459	582
0689	-3	100	457	582
0690	-3	200	459	582
0691	-4	100	456	582
0692	-4	200	459	581
0693	+4	100	458	581
0694	+4	200	461	580
0695	+4	100	463	611
0696	+4	200	456	610
0697	+3	200	454	610
0698	+3	100	451	609
0699	0	100	451	609
0700	0	200	453	609
0701	-3	200	452	608
0702	-3	100	450	608
0703	-4	100	451	608
0704	-4	200	454	608

NOTE: All values are nominal values.

SECTION III

DESCRIPTION OF THE STAPAT PROGRAM

1. GENERAL CHARACTERISTICS OF STAPAT

STAPAT is a Specific Thermal Analyzer Program for Aircraft Transparencies. The code merges state-of-the-art technology with functional and accuracy requirements, resulting in an efficient aerothermodynamic analytical technique that is specifically applicable to the study of high-temperature resistant transparencies for high-speed aircraft. STAPAT is a modular software package consisting of four discrete program modules. The STAHET module is used for generation of the forced, external convection environment surrounding a body for specific points within a wind tunnel or flight mission. The TAP module is a transient, three-dimensional, finite element thermal analyzer program that generates temperature-time histories within a transparency system. The STABLD module is a preprocessor program that allows interactive generation of the finite-element grid. The STAPLT module is an interactive, postprocessor program that provides visual display of the STAHET and TAP solution results. References 1 and 2 provide general descriptions of the STAPAT computer program and its development; Reference 2 also includes the users manuals and sample problems.

2. STAHET CAPABILITIES AND LIMITATIONS

The STAHET module is a modified version of the DeJarnette heating code as described in References 13 through 15. For flight mission environments, at subsonic and low-to-moderate supersonic speeds, STAHET provides solutions for sharp-nose forebody configurations at zero angles of attack and yaw. For the specific applications intended, nonzero angles of attack and yaw were not required to be included in STAPAT. A streamline tracing approach is used to define the heat transfer and flow field parameter variations along specified streamlines traced from a point near the forebody nose. Only one-half of the forebody (divided along its plane of symmetry) is used in STAHET. Pressure distributions are based on application of the modified Newtonian theory with pressure coefficient values set to

zero in shadow regions of the forebody. Input data required for implementation of STAHET includes control parameters, forebody and transparency system coordinates, Mach number, altitude, atmosphere type (standard, high- or low-temperature atmospheres), and ratios of body surface (wall) temperature to tunnel stagnation temperature.

For wind tunnel mission environments, STAHET includes routines to compute heating rate and flow field parameter variations over two-dimensional, wedge-shaped configurations. Input data includes control parameters and time histories of wedge angle of attack and tunnel Mach number, pressure, and temperature.

Output from STAHET consists of heating rate and flow field parameter distributions over the body for all conditions specified in the input data stream, and at two specified wall temperature conditions.

3. STAHET MODIFICATIONS

a. Nonwedge Shaped Wind Tunnel Models

Because the thermal performance of aircraft transparency system materials are often evaluated in high speed wind tunnels on wedge-shaped test fixtures (References 16 through 24), STAHET includes the capability to calculate the forced, external convection environment surrounding those type configurations during wind tunnel tests. However, and in keeping with the scope of the STAPAT development program, STAHET does not provide a capability for computing the convection environment over nonwedge shaped wind tunnel models.

(1) Code Changes

For the purpose of this test program, STAHET was modified to provide solutions for the analytic forebody at constant wind tunnel conditions. This was accomplished with minimal code changes by combining flight and wind tunnel mission capabilities. Conceptually, the problem was treated as one where the analytic forebody was in a flight mission environment at free-stream conditions equal to the wind tunnel flow conditions.

(2) STAHET Model of the Analytic Forebody

A model of the analytic forebody was prepared for use in the STAHET module of STAPAT. STAHET requires a description of the geometry of the forebody in terms of the polar coordinates R and ϕ at each axial station X. The required coordinate data file was obtained using Equations 1 through 4 which describe the forebody surface parametrically, and the following geometric relationships:

$$R = (y^2 + z^2)^{\frac{1}{2}} \tag{12}$$

$$\phi = \cos^{-1} (7/R) \tag{13}$$

Figure 11 shows four views of the analytic forebody used in STAHET as generated by the STAPAT postprocessor. The model has 20 axial stations over its 10-in. length and 20 circumferential stations over half its circumference. (A model using 10 axial and 10 circumferential stations was also tried but the grid was apparently too coarse since the curve fit in STAHET yielded pressures which were not sufficiently close to the desired full modified Newtonian pressures.)

b. Nonzero Pressure Coefficients in Shadow Regions

STAHET calculations of the inviscid surface streamlines and heating rates are dependent upon surface pressure distributions. These distributions were determined from a modified Newtonian pressure coefficient relationship (Reference 2), that is

$$C_p = C_{p_S} \sin^2 \delta \tag{14}$$

where

$$C_{p_S} \equiv \left(P_{t_2} - P_\infty \right) \bigg/ \left(0.5 \, \gamma \, P_\infty \, M_\infty^2 \right) \tag{15}$$

and

$$C_p = \left(P - P_\infty \right) \bigg/ \left(0.5 \, \gamma \, P_\infty \, M_\infty^2 \right) \tag{16}$$

29
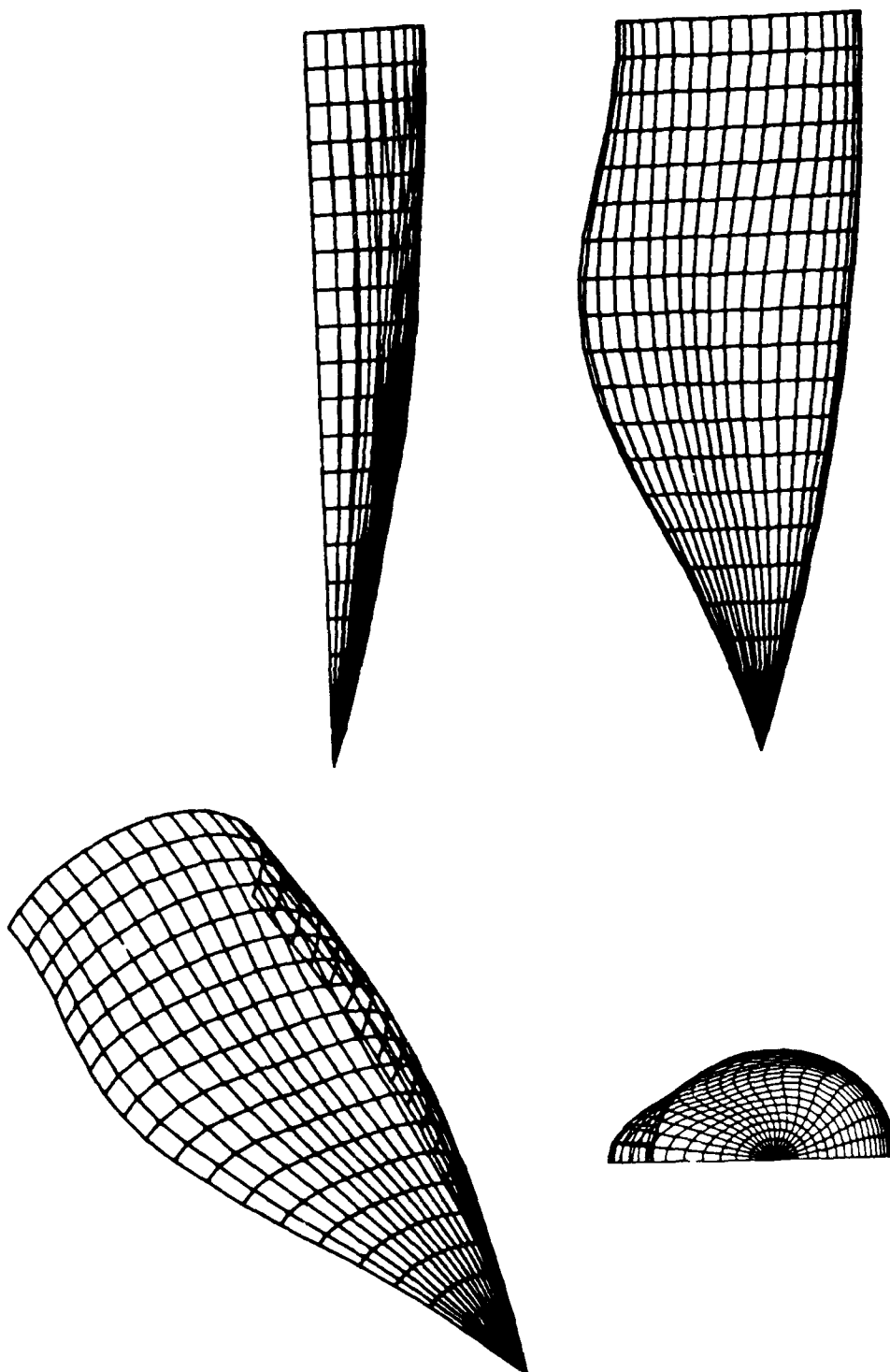
Figure 11. Four Views of the STAPAT Model of the Analytic Forebody

30

In shadow regions of the forebody (where $\delta < 0.0°$) the surface pressure, P, is set equal to the free-stream static pressure, P_∞ , that is, $C_{p_{SHADOW}}$ = 0.0.

(1) Correlation Equation

To investigate the effects of this feature, STAHET was modified to include nonzero pressure coefficients in shadow regions. Rather than incorporating flow expansion type calculation techniques which would require extensive code modifications, a correlation equation for pressure coefficient, C_p, in terms of Mach number M_∞ , and body slope, δ, was sought which would

1. be continuous in M_∞ for $0 \leq M_\infty \leq \infty$,

2. be continuous in δ for $-90 \leq \delta \leq 0°$,

3. yield negative C_p values for negative δ values,

4. yield larger negative C_p values for larger negative δ values,

5. yield C_p values that follow the general trend of, and are bounded by, the $C_{p_{MIN}}$ (i.e., C_p for P = 0) versus M_∞ relationship for $M_\infty > 1.0$, and

6. yield C_p values that agree reasonably well with available data in terms of magnitude and variation with M_∞ .

31

Figure 12 shows the relationships among $C_{P_{SHADOW}}$, M_∞ and δ which were

obtained using the correlation equation derived for use in STAHET. The shadow
region pressure coefficient correlation equation selected was

$$C_{P_{SHADOW}} = -AR\ (0.7)\ M^{1/2}\ \sin^{1/3}\ (-\delta) \qquad (17)$$

for $-90 \leq \delta \leq 0°$ and where

$$AR = 1\ /\ [\ (\ 1 - M_\infty^2\ )^2\ +\ M_\infty^2\ ]^{1/2} \qquad (18)$$

Also shown on Figure 12 are test data and the curve for the minimum pressure
coefficient for supersonic flow, that is, for

$$C_{P_{MIN}} = -2\ /\ (\ \gamma\ M_\infty^2\ ) \qquad (19)$$

as evaluated for $\gamma = 1.4$. Basically, the derivation of the correlation equation
was based on the application of a magnification ratio, AR (Reference 25), to the
$C_{P_{MIN}}$ curve so that a reasonable fit to the available data would be obtained,
especially at $M_\infty = 3.0$.

(2) Comparisons With Experimental Data

Evaluation of the shadow region pressure coefficients using the
correlation equation (Equation 17) requires values for the slope of the body surface
at each point of interest. Since the surface of the analytic forebody is described
by a set of parametric equations, surface slopes are readily obtained by
differentiation, especially along the plane of symmetry (e.g., along the top
centerline where $\phi = 0$). This variation of body slope angle along the top
centerline of the analytic forebody is shown in Figure 13.

Comparisons of experimental and calculated pressure coefficients in the
shadow region of the analytic forebody can be obtained from Figure 14. The
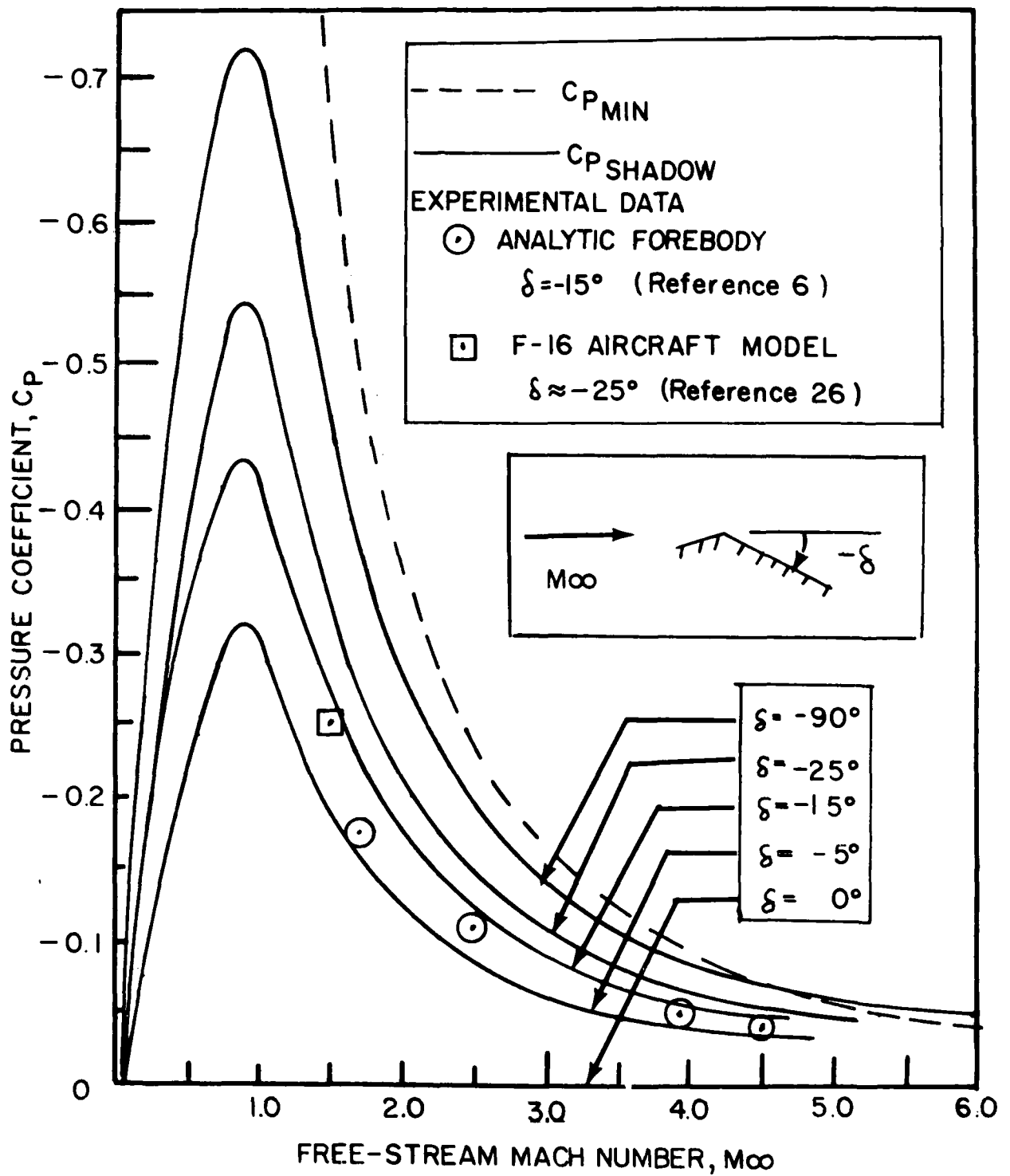
Figure 12. Correlation Equation Relationships for Shadow Region
Pressure Coefficients
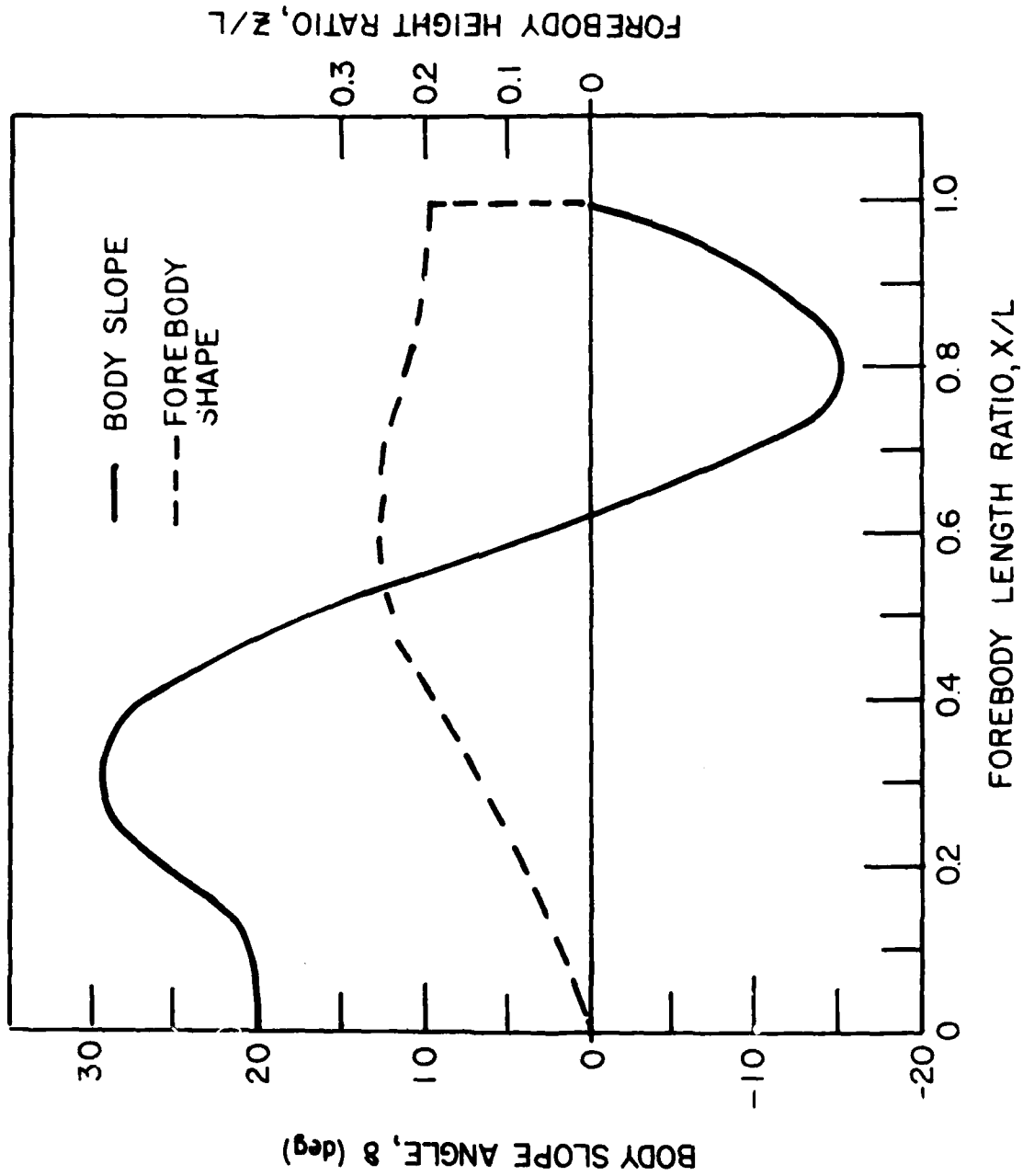
Figure 13. Variation of Body Slope Angle Along the Top Centerline of the Analytic Forebody
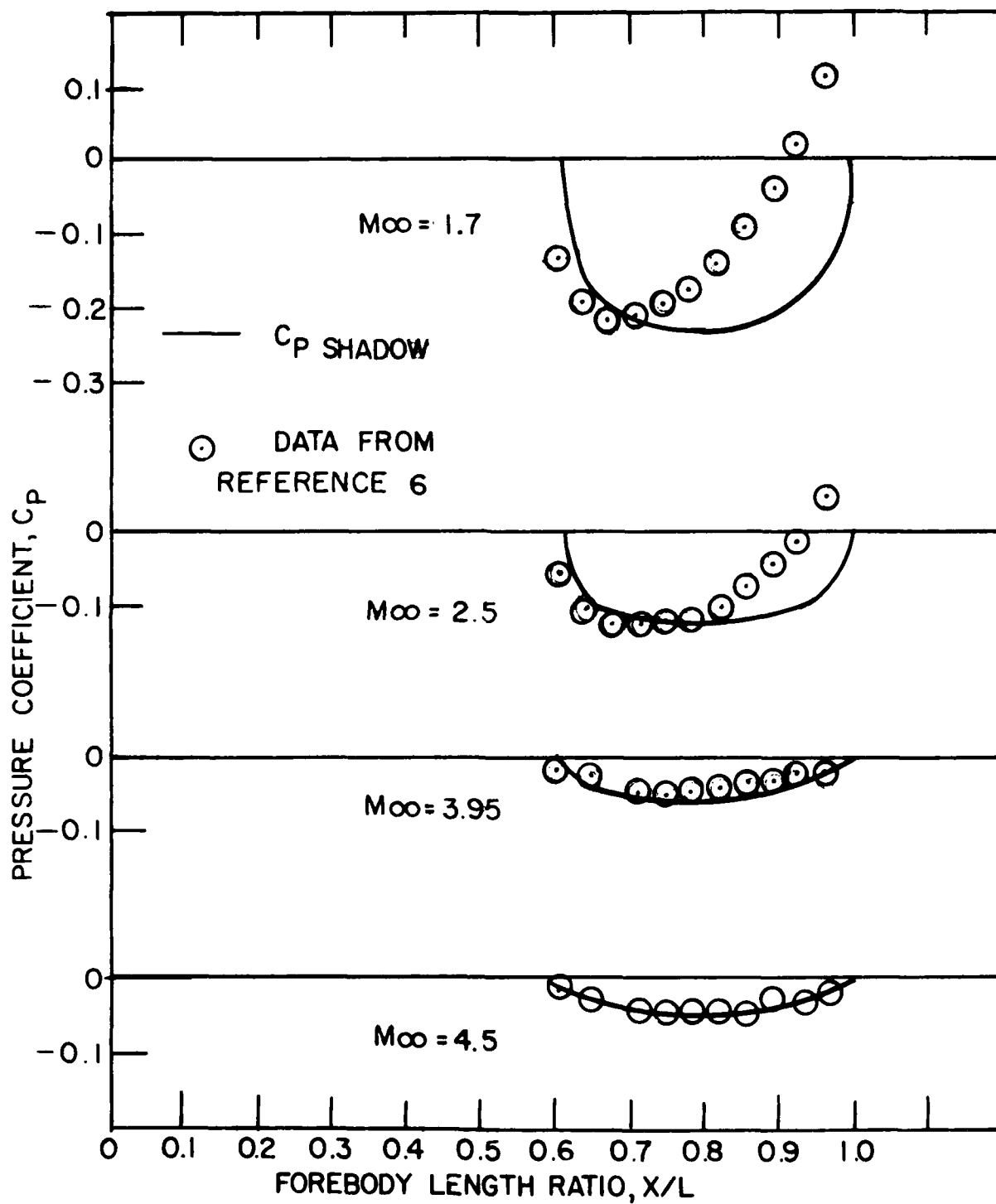
Figure 14. Variation of Pressure Coefficient Along the Top Centerline Shadow Region of the Analytic Forebody

experimental data was taken from Reference 6. The calculated values were determined using the correlation equation evaluated at the body slope angles presented in Figure 13. Agreement is very good at Mach numbers of 4.5 and 3.95, and becomes progressively worse for the lower Mach numbers of 2.5 and 1.7. The calculated pressure coefficient values are nearly symmetrical about a forebody length ratio of X/L = 0.8 at all Mach numbers since the body slope angle is almost symmetrical (see Figure 13). The experimental data does not show this symmetry at the lower Mach numbers.

(3) Code Changes

The STAHET module was modified to incorporate the shadow region pressure coefficient correlation equation so that nonzero pressure coefficients would be obtained on regions of the analytic forebody where the body slope angle, s, was less than zero.

c. Nonzero Angles of Attack

During the development of STAHET, a number of modifications were made to the DeJarnette code to meet the objective and functional requirements of STAPAT. One modification was the elimination of the angle-of-attack input option. The STAHET code, however, still includes angle of attack, ALPD, as a variable in the equations. The modification apparently only removed ALPD as an input variable from NAMELIST FLTIN, leaving ALPD always equal to its default value of 0.0°.

In an attempt to provide calculated values for comparison with wind tunnel data acquired at nonzero angles of attack, STAHET was first modified to once again read ALPD from NAMELIST FLTIN and then run for angles of attack from -3.0 to +3.0°. STAHET only ran successfully for zero and negative angles of attack. It is postulated that either (1) other modifications made during the conversion from the DeJarnette code to the STAHET code (such as the change from blunt to sharp-nose forebodies) eliminated the full angle of attack capability or (2) the correct combination of body mesh size, step size and number of smoothing operations was never found for the particular body shape and test conditions tried.

4. FORMS OF THE STAPAT RESULTS

Output from the STAHET module of STAPAT was provided in the forms of tables of values for listing and a file of values for postprocess plotting. A sample of part of the STAPAT tabular output is shown in Figure 15; STAPAT plots are given in the next section of the report. Definitions of the symbols listed in Figure 15 are as follows:

PØ = Free-stream stagnation pressure, psia

MACH = Free-stream Mach number

NSL = Number of streamlines used in the calculation

TIN = Free-stream static temperature, R

PIN = Free-stream static pressure, lbf/ft^2

RHOIN = Free-stream static density, $slug/ft^3$

PR = Prandtl number

TW1/TØ = Ratio of wall temperature, TW, and free-stream stagnation temperature, TØ, for TW less than the expected local adiabatic wall temperature, TAW (temperatures in degrees Rankine)

TW2/TØ = Ratio of wall temperature, TW, and free-stream stagnation temperature, TØ, for TW greater than the expected local adiabatic wall temperature, TAW (temperatures in degrees Rankine)

X = Axial location along a streamline, in.

PHI = Circumferential angle location along a streamline, deg

RHOE = Local, boundary layer edge, static density, $slug/ft^3$

TE = Local, boundary layer edge, static temperature, R

MACHE = Local, boundary layer edge, Mach number

REC FACT = Local recovery factor

STAN NO = Local Stanton number, ST, based on free-stream conditions

That is

$$ST = QDOT / \lceil (RHOIN) (UIN) (CP) (TAW - TW) \rceil \qquad (20)$$

where

QDOT = Local heat transfer rate, lbf/(ft·s)

UIN = Free-stream velocity, ft/s

CP = Specific heat of air at constant pressure, $ft^2/(s^2 \cdot R)$

37

PQ psia	MACH	NSL	TIN deg R	PIN lbf/ft^2	RHOIN slug/ft^3	PR	TW1/T0	TW2/ T0
100	3.00	10	169.30	392.00	0.1349E-02	0.752	1.143	1.200

X in.	PHI deg	RHOE/RHOIN	TE/TIN	MACHE	REC FACT	STAN NO	TW/T0
0.097	0.000	1.754	1.289	2.421	0.852	0.2448E-02	1.143
0.118	0.000	1.753	1.289	2.422	0.852	0.2228E-02	
0.138	0.000	1.753	1.289	2.422	0.852	0.2059E-02	
0.157	0.000	1.752	1.289	2.423	0.852	0.1923E-02	
0.197	0.000	1.752	1.288	2.423	0.852	0.1718E-02	
0.237	0.000	1.752	1.288	2.423	0.852	0.1569E-02	
0.277	0.000	1.753	1.289	2.422	0.852	0.1454E-02	
0.314	0.000	1.755	1.289	2.421	0.852	0.1454E-02	
0.316	0.000	1.755	1.289	2.421	0.864	0.1495E-02	
0.321	0.000	1.755	1.289	2.421	0.868	0.2298E-02	
0.331	0.000	1.756	1.289	2.422	0.894	0.3787E-02	
0.349	0.000	1.761	1.287	2.426	0.898	0.3948E-02	
0.387	0.000	1.765	1.286	2.427	0.898	0.3729E-02	
0.462	0.000	1.773	1.287	2.425	0.898	0.3475E-02	
0.499	0.000	1.778	1.288	2.424	0.898	0.3393E-02	
0.574	0.000	1.788	1.290	2.419	0.898	0.3273E-02	
0.723	0.000	1.813	1.297	2.407	0.898	0.3134E-02	
0.957	0.000	1.867	1.312	2.381	0.898	0.3045E-02	
1.073	0.000	1.900	1.322	2.366	0.898	0.3034E-02	
1.305	0.000	1.976	1.342	2.331	0.898	0.3050E-02	
1.534	0.000	2.060	1.365	2.294	0.898	0.3099E-02	
1.762	0.000	2.145	1.388	2.257	0.898	0.3165E-02	
1.987	0.000	2.228	1.409	2.222	0.898	0.3235E-02	
2.211	0.000	2.303	1.428	2.192	0.898	0.3301E-02	
2.433	0.000	2.365	1.445	2.166	0.898	0.3356E-02	
2.653	0.000	2.413	1.457	2.147	0.898	0.3395E-02	
2.872	0.000	2.442	1.466	2.134	0.898	0.3413E-02	
2.982	0.000	2.449	1.468	2.130	0.898	0.3413E-02	
3.201	0.000	2.446	1.470	2.128	0.898	0.3394E-02	
3.420	0.000	2.420	1.466	2.134	0.898	0.3347E-02	
3.639	0.000	2.370	1.457	2.148	0.898	0.3270E-02	
3.861	0.000	2.294	1.441	2.173	0.898	0.3161E-02	
4.085	0.000	2.190	1.417	2.209	0.898	0.3017E-02	
4.311	0.000	2.061	1.386	2.259	0.898	0.2838E-02	
4.541	0.000	1.908	1.347	2.323	0.898	0.2626E-02	
4.774	0.000	1.736	1.299	2.404	0.898	0.2384E-02	
5.012	0.000	1.547	1.242	2.504	0.898	0.2117E-02	
5.253	0.000	1.354	1.179	2.623	0.898	0.1839E-02	
5.498	0.000	1.192	1.121	2.737	0.898	0.1599E-02	
5.745	0.000	1.086	1.082	2.819	0.898	0.1434E-02	
5.994	0.000	0.985	1.041	2.907	0.898	0.1275E-02	
6.244	0.000	0.838	0.975	3.061	0.898	0.1054E-02	
6.494	0.000	0.690	0.902	3.245	0.898	0.8436E-03	
6.742	0.000	0.618	0.863	3.352	0.898	0.7328E-03	
6.989	0.000	0.592	0.849	3.391	0.898	0.6841E-03	
7.235	0.000	0.570	0.836	3.427	0.898	0.6388E-03	
7.479	0.000	0.549	0.824	3.464	0.898	0.5954E-03	
7.722	0.000	0.537	0.817	3.484	0.898	0.5636E-03	
7.964	0.000	0.533	0.815	3.489	0.898	0.5410E-03	
8.206	0.000	0.535	0.817	3.486	0 898	0.5232E-03	
8.448	0.000	0.542	0.821	3.471	0.898	0.5098E-03	
8.691	0.000	0.557	0.831	3.443	0.898	0.5007E-03	
8.936	0.000	0.577	0.843	3.407	0.898	0.4912E-03	
9.182	0.000	0.601	0.857	3.366	0.898	0.4744E-03	
9.430	0.000	0.641	0.881	3.301	0.898	0.4471E-03	
9.554	0.000	0.673	0.899	3.262	0.898	0.4129E-03	

Figure 15. Sample of Part of the STAPAT Tabular Output — for Wind Tunnel Test Run 0657

38

SECTION IV

RESULTS, DISCUSSION, AND COMPARISONS

1. FORM OF THE TEST DATA

Wind tunnel test results which were used to evaluate the heat transfer rates on the analytic forebody were presented in the forms of schlieren photographs and data tabulations. One data table was generated for each of the 51 test runs and they are presented in the Appendix. Figure 16 shows a typical data table, the one for Test Run 0657. The tabulated data consisted of a heading and columns of data. The heading listed the tunnel conditions, model angle of attack, and water temperature. The data columns listed the locations, temperatures and heat transfer rates associated with each working gage on the model. (Gage numbers 4, 10, 11, and 20 malfunctioned and yielded no useable data.)

Note that the backface (inner wall) temperature T-BF, was not the same for each heat transfer rate gage. For Test Run 0657, T-BF ranged from 529 to 573 R. This shows the importance of having a backface thermocouple junction to determine T-BF for this technique of heat transfer testing in cold flow wind tunnels — rather than relying on a single value of T-BF for all gages which may be obtained from measurement of inlet and/or outlet water temperature(s).

2. FLOW FIELD

a. Schlieren Photographs

A qualitative assessment of the flow field over the analytic forebody can be obtained from the schlieren photographs presented in Figure 17. The photographs clearly show the strong bow shock waves which eminated from the sharp nose of the model at the various angles of attack. The bow shock waves, while asymmetric, were essentially conical in shape. The 8-in.-diameter schlieren windows almost enclose the 8.2-in.-high tunnel walls. The bow shock waves can be seen to intersect the top and bottom walls, with reflected shock waves trailing downstream. The intersections of the bow shock waves with the schlieren windows can also be discerned; they would produce trailing shock waves similar to those from the top and bottom walls. It is

MACH 3 CANOPY TEST   RUN= 0657

	T-INF	P-INF	RHO-INF	V-INF	ALPHA
	170.80	2.80	0.1376E-02	1908.9	-0.07
	deg R	psia	slug/ft^3	ft/s	deg

	TO	PO	MU-INF	RE-INF	T-WATER
	474.16	99.83	0.13717E-06	0.1915E+08	600.83
	deg R	psia	lbf·s/ft^2	1/ft	deg R

GAGE	X in.	PHI deg	T-BF deg R	T-S deg R	T-S/TO	QDOT Btu/ (ft^2·s)	H(.9 TO) Btu/ (ft^2·s·R)	ST
1	2.75	60.0	572.80	555.31	1.171	-5.769	0.4487E-01	0.2213E-02
2	3.75	60.0	558.30	548.47	1.157	-3.242	0.2664E-01	0.1314E-02
3	4.75	60.0	563.29	554.29	1.169	-2.969	0.2328E-01	0.1148E-02
5	6.75	60.0	555.14	548.10	1.156	-2.321	0.1913E-01	0.9435E-03
6	7.75	60.0	557.25	550.75	1.162	-2.147	0.1731E-01	0.8538E-03
7	2.00	0.0	533.83	517.84	1.092	-5.277	0.5793E-01	0.2857E-02
8	3.00	0.0	528.66	515.00	1.086	-4.509	0.5109E-01	0.2520E-02
9	4.00	0.0	542.42	523.09	1.103	-6.381	0.6624E-01	0.3267E-02
12	7.00	0.0	568.24	564.81	1.191	-1.133	0.8201E-02	0.4045E-03
13	8.00	0.0	572.19	569.83	1.202	-0.779	0.5441E-02	0.2683E-03
14	9.00	0.0	565.44	562.86	1.187	-0.853	0.6267E-02	0.3091E-03
15	2.50	30.0	555.01	538.90	1.137	-5.317	0.4741E-01	0.2338E-02
16	3.50	30.0	556.59	541.31	1.142	-5.044	0.4403E-01	0.2171E-02
17	4.50	30.0	548.57	540.73	1.140	-2.587	0.2270E-01	0.1120E-02
18	5.50	30.0	548.82	542.62	1.144	-2.045	0.1764E-01	0.8702E-03
19	6.50	30.0	552.69	544.44	1.148	-2.721	0.2311E-01	0.1140E-02

Figure 16. Typical Data Table — From Wind Tunnel Test Run 0657

ALPHA = 4°　　　　　　　ALPHA = -4°

CONICAL BOW
SHOCK WAVE
(TYPICAL)

REFLECTED
BOW SHOCK
WAVE (TYPICAL)

MODEL AND
TUNNEL
CENTERLINE

INTERSECTION
OF BOW SHOCK
WAVE WITH
TUNNEL WINDOWS
(TYPICAL)

ALPHA = 0°
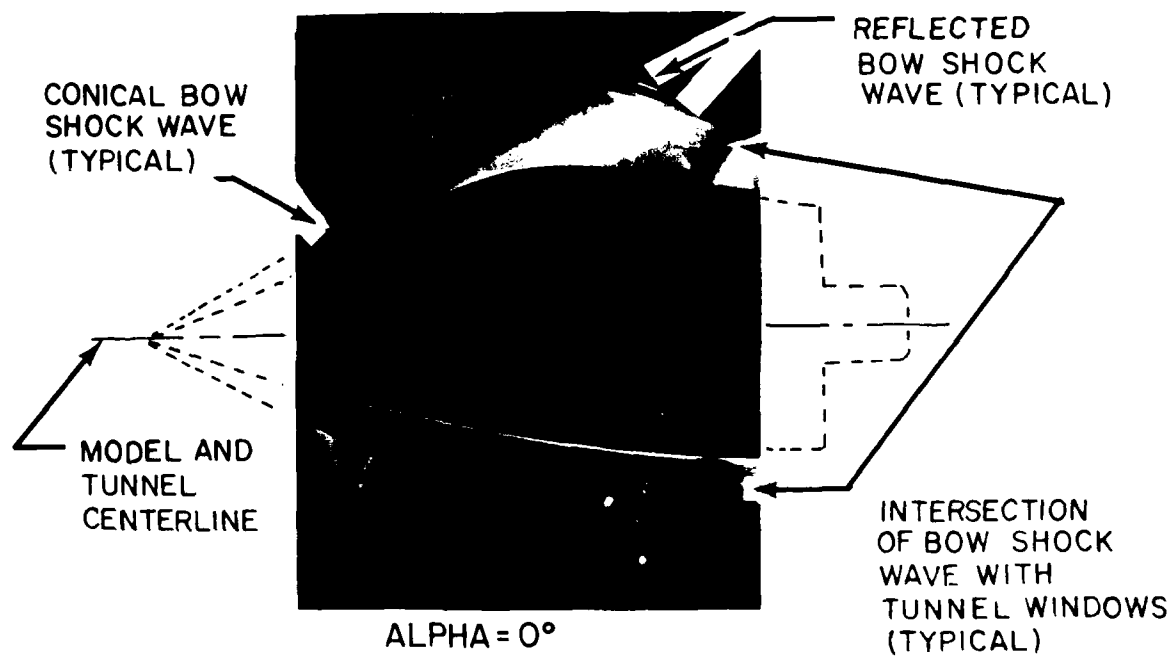
Figure 17.　Schlieren Photographs of the Flow Field Over the
Analytic Forebody

41

clear that the reflected bow shock waves did not interfere with the flow over the model at any of the angles of attack tested.

The bright areas surrounding the silhouette of the model highlight the boundary layers along the top and bottom centerlines of the analytic forebody. Boundary layer type, either laminar, transitional or turbulent, cannot be absolutely determined. A definite change in the flow field can be seen near the surface along the top centerline as the flow expands into the shadow region.

Based on analysis of the schlieren photographs, the flow fields surrounding the analytic forebody during the tests were free from anomalies which would invalidate the data.

b. STAPAT Predictions of Boundary Layer Edge Conditions

STAPAT predictions of the flow field properties at the edge of the boundary layer over the analytic forebody at zero angle of attack are shown in Figure 18. Isolines of Mach number, static temperature, static pressure and pressure coefficient are shown from near the nose to near the base for radial locations from the top centerline, $\phi = 0°$, to approximately $\phi = 100°$. Mach numbers behind the bow shock wave were less than the Mach 3.00 free-stream value as expected, with a minimum value of Mach 2.13 located on the top centerline at an axial location of approximately 3 in. Local Mach numbers increased to the free-stream value at an axial location of approximately 6 in. and increased further to a value of Mach 3.49 after the flow expanded into the shadow region. Static temperatures and pressures followed an opposite pattern. They were greater than free-stream values behind the bow shock wave, decreased to free-stream values near an axial location of 6 in., and decreased further in the expansion region.

Figure 19 is presented to show the effect of modification of the STAHFT module of STAPAT to allow nonzero pressure coefficient, C_p, values in the shadow region. The results from the unmodified code, Figure 19a, show C_p values of approximately 0.0 in all areas of the forebody aft of an axial location of 6.0 in. The results from the modified code, Figure 19b, show negative C_p values in the shadow region and both axial and radial C_p gradients aft of an axial location of 6.0 in.

42
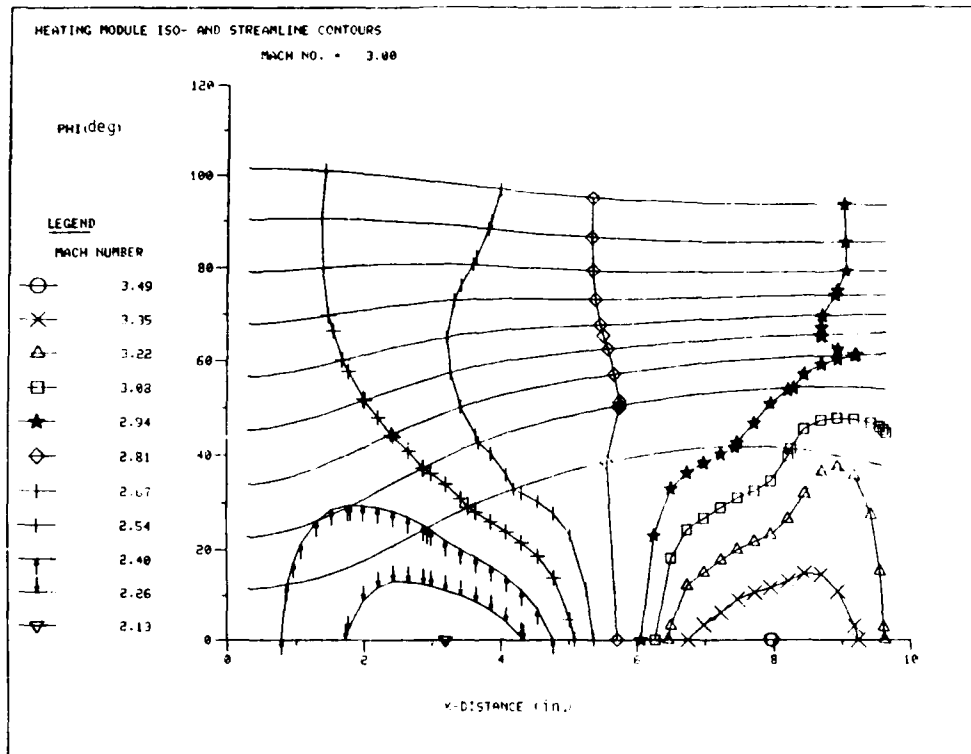
a. Isolines of Mach Number
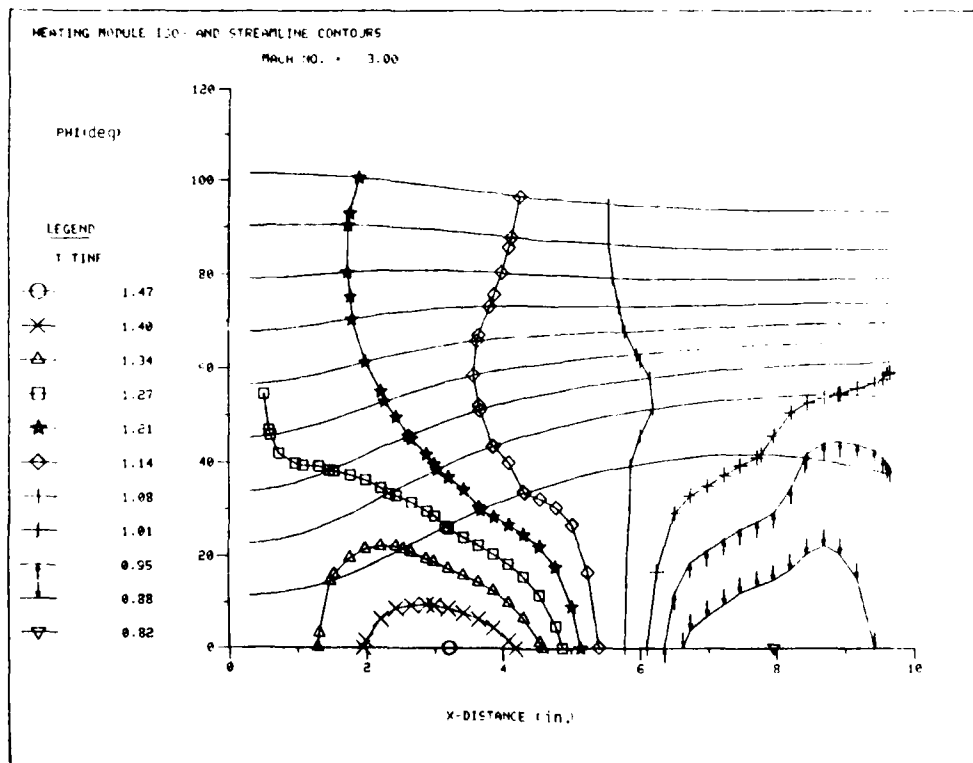
b. Isolines of Static Temperature

Figure 18. STAPAT Predictions of Flow Field Properties

c Isolines of Static Pressure

d Isolines of Pressure Coefficient

Figure ??. STAPAT Predictions of Flow Field Properties (Concluded)
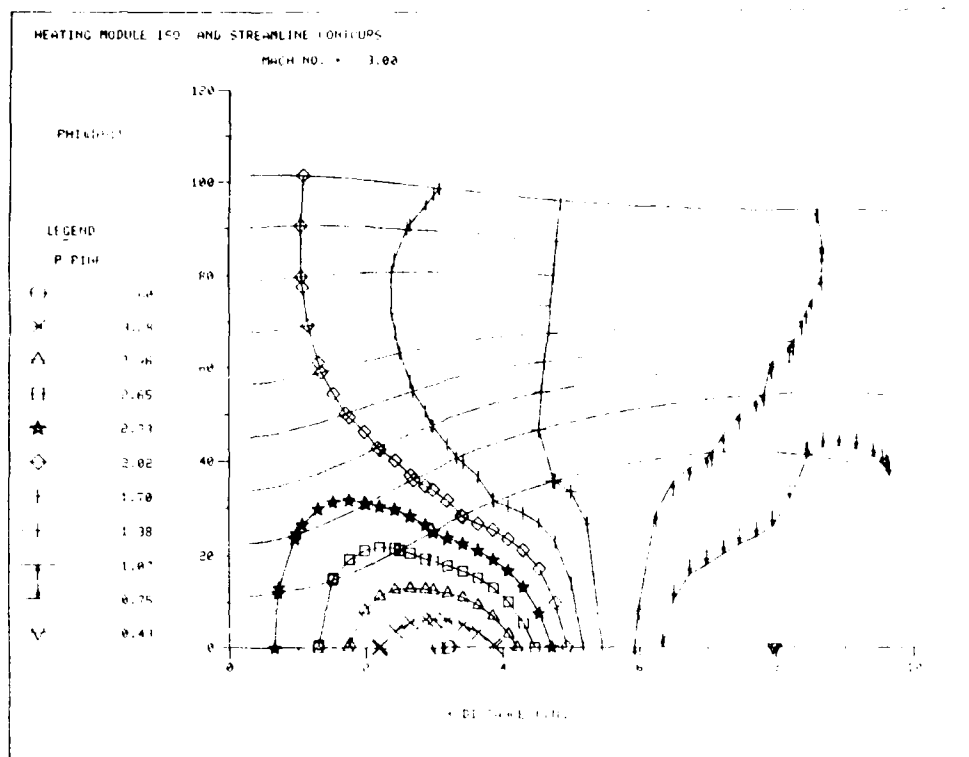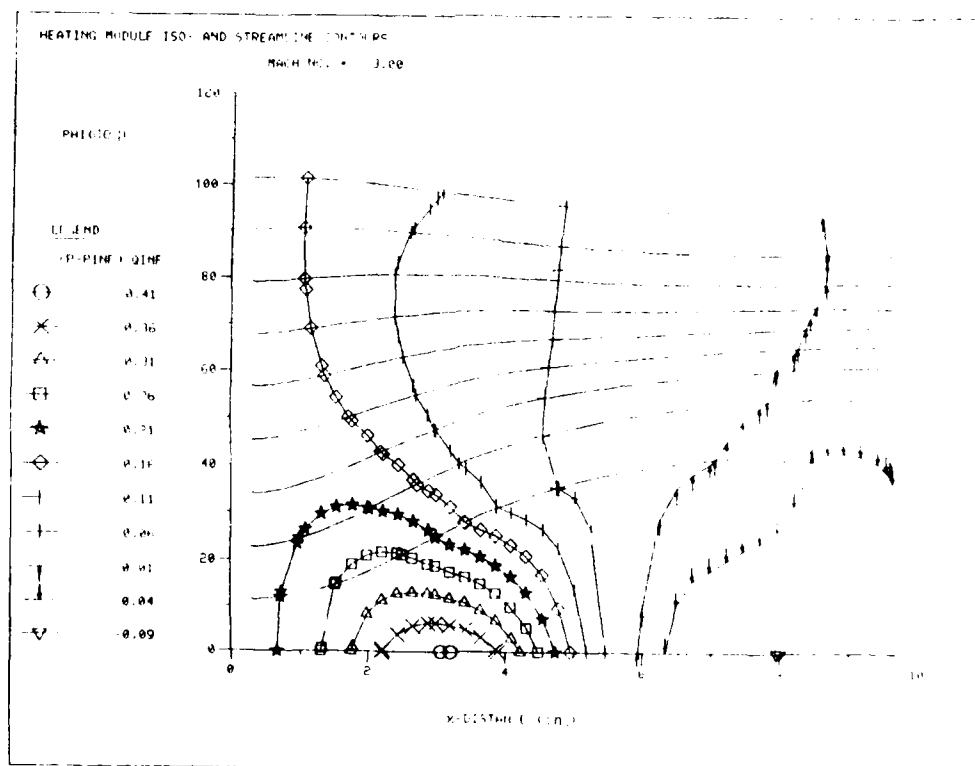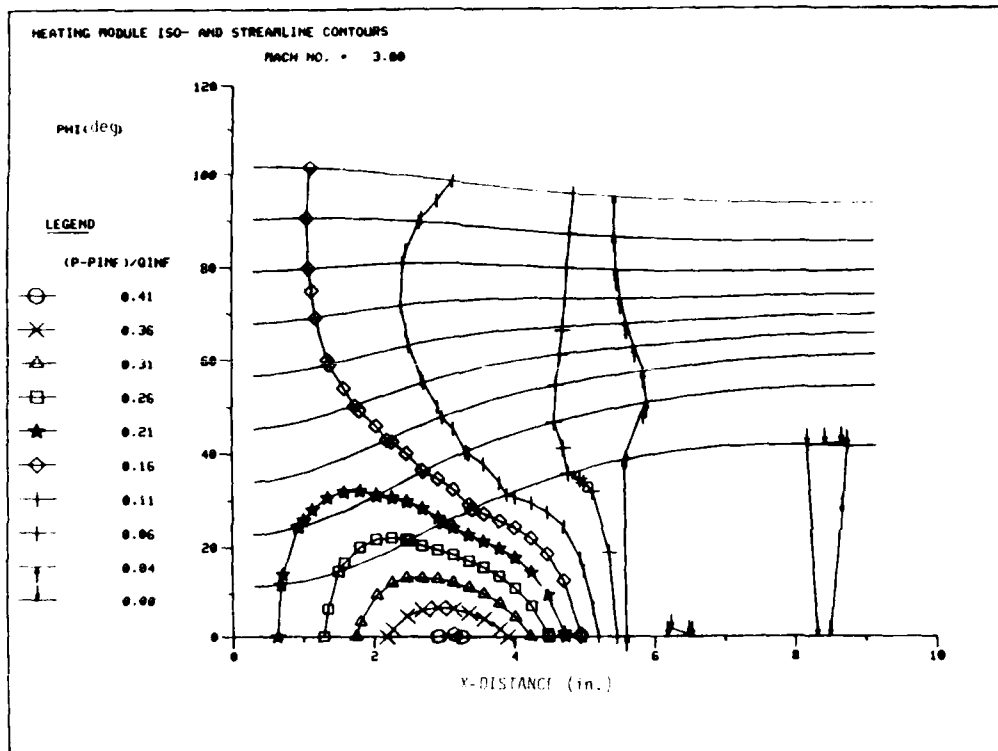
a. Unmodified STAHET Code
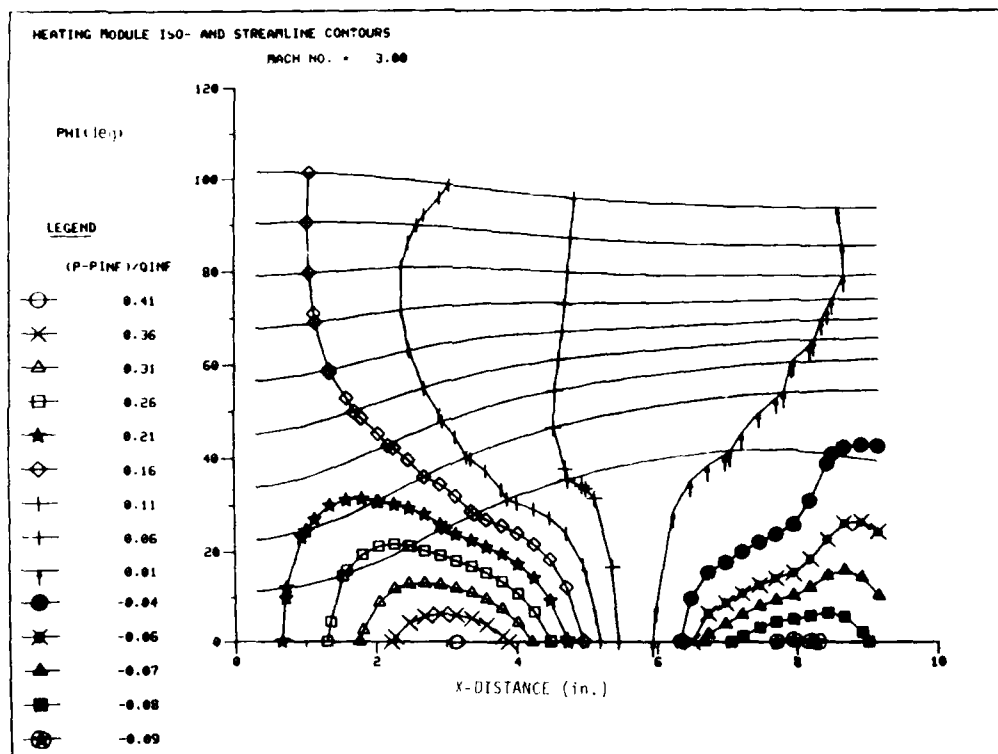
b. Modified STAHET Code

Figure 19. Comparison of STAPAT Predictions of Pressure Coefficient in the Shadow Region

45

Figure 20 is presented for information only to show a more complete picture of the distribution of streamlines over the analytic forebody. The streamlines in these two plots can be combined with those plotted in Figure 18a to give a total of at least 27-separate streamlines over the whole forebody. Figure 20b clearly shows how the streamlines wrap around the canopy-like hump of the analytic forebody (i.e., how they turn back toward the top centerline). Review of the other two plots shows that the streamline wraparound only takes place in this region of the forebody.

c. Surface Pressures

Figure 21 is presented to provide comparisons of measured and predicted pressures on the surface of the analytic forebody at zero angle of attack. Figure 21a shows plots of C_p values as functions of axial location for three-radial locations and Figure 21b shows C_p values as functions of radial location at an axial station of 4 in. The measured C_p values were obtained from the data presented in Reference 6 for the analytic forebody. Values for ϕ = 30 and 60° were obtained using linear interpolation of the values for ϕ = 20 and 35° and ϕ = 50 and 70°, respectively. Interpolations for Mach number, M, were not made; C_p data for both M = 2.5 and 3.95 are plotted.

Also shown along the bottom of the figure (and on most subsequent figures) is a sketch of the top half of the analytic forebody with the heat transfer rate gage numbers and their approximate locations included. The symbols help locate the circumferential angles, the circles are for ϕ = 0°, the squares for ϕ = 30°, and the triangles for ϕ = 60°. The cross section shape of the analytic forebody at an axial distance of 4 in. is also shown.

In general, STAPAT adequately predicted the pressure distribution over the surface of the analytic forebody. Both the data and predictions showed a sharp rise in pressure along the centerline from the nose to a maximum value near an axial station of 3.3 in. This was followed by sharp decreases in pressure in both the axial and radial directions to levels which produced negative C_p values near the base of the forebody. STAPAT under-predicted the pressure levels on the forward portion of the forebody (axial stations less than 4 in.) but showed good agreement with the measured values for axial stations greater than 4 in. (STAPAT predictions are expected to be good in the shadow region, because the data from Reference 6
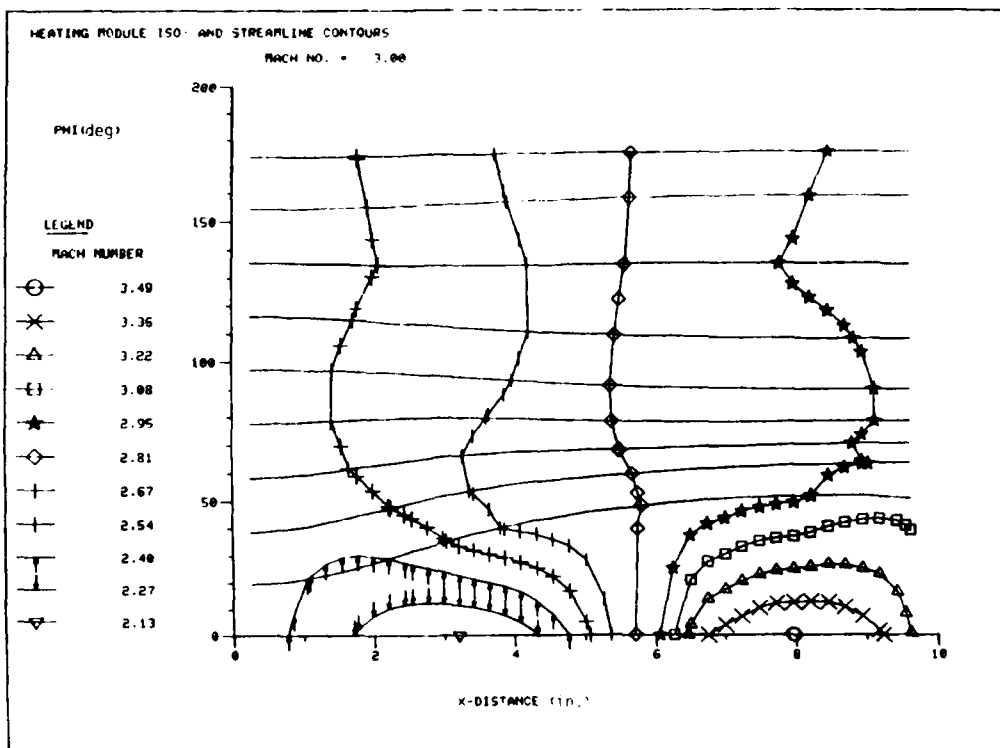
a. Streamlines Over the Entire Forebody
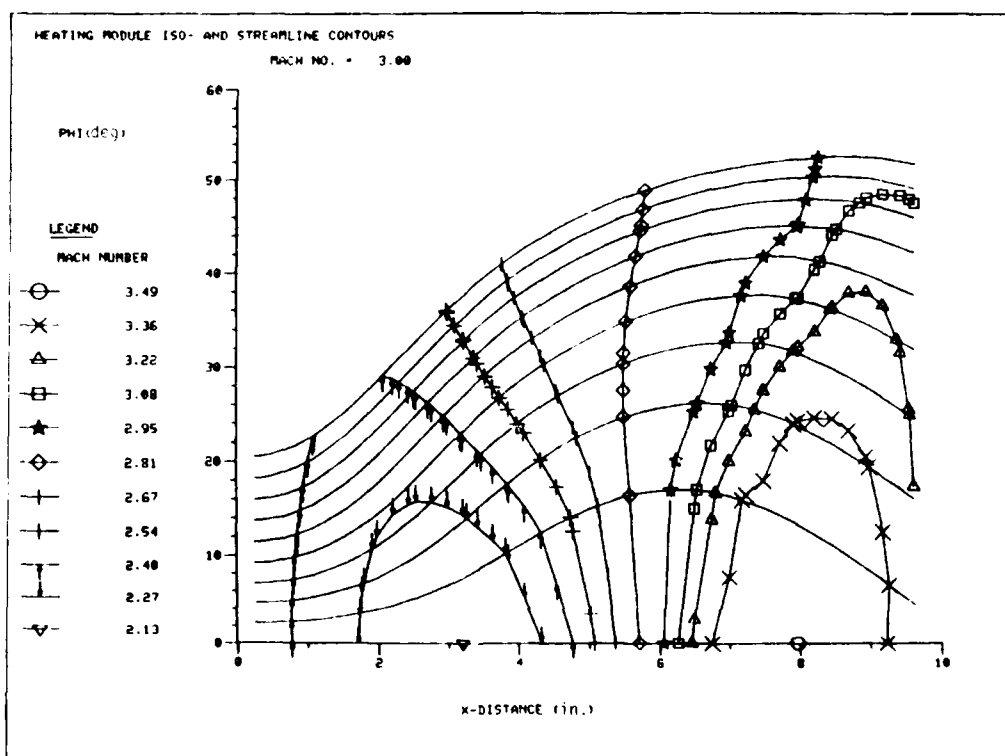
b. Streamlines Over the Canopy-Like Hump

Figure 20. STAPAT Predictions of Streamline Distributions

42

X = 4 in

POLAR COORDINATE ANGLE, φ (deg)

b Cp Versus Radial Location

φ = 0°
φ = 30°
φ = 60°

AXIAL DISTANCE, X (in)

SYMBOLS — DATA
FROM REFERENCE 6

OPEN — M = 2.5

CLOSED — M = 3.95

—— STAPAT
PREDICTIONS

φ = 60°

φ = 30°

φ = 0°

AXIAL DISTANCE, X (in.)

a Cp Versus Axial Location
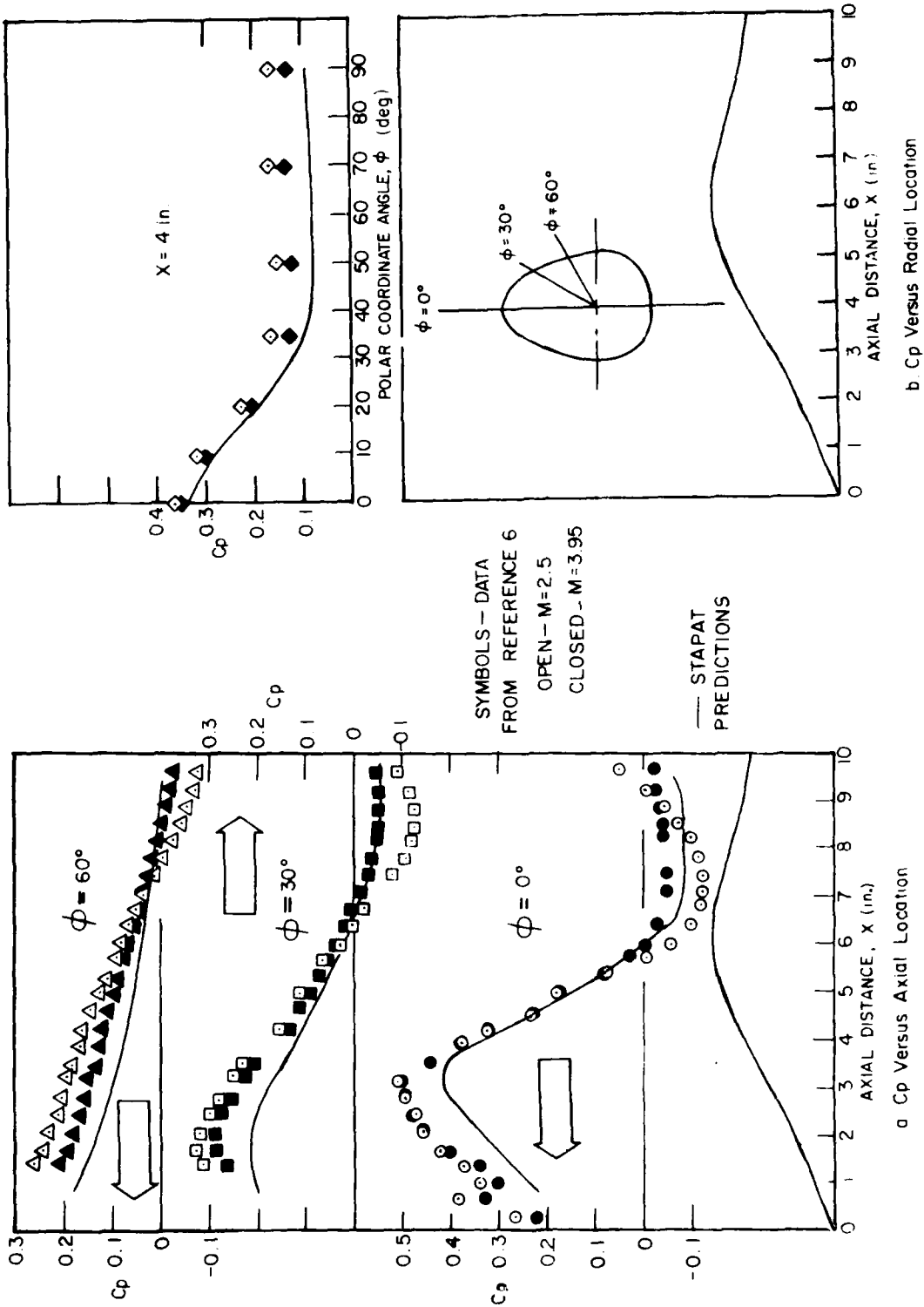
Figure 21 Comparisons of Measured and Predicted Surface Pressures

59

influenced the development of the shadow region pressure coefficient correlation equation used in the STAHET module of STAPAT.)

3. HEAT TRANSFER RATES

   a. Typical Distributions From Wind Tunnel Data

The tabulated data from Figure 16 (for Run 0657) is plotted in Figure 22 to show typical heat transfer rate distributions over the analytical forebody. The heating rate values are in terms of QDOT and ST and include symbolic representations of the estimated maximum uncertainties listed in Table 1. While the uncertainties were relatively large, they did not mask the overall level of heat transfer rates nor their relationships with axial and radial locations.

The distributions for QDOT and ST were similar. The highest heating rates occurred on the top centerline of the forebody at axial locations from 2 in. to 4 in. and the lowest occurred in the shadow region. Heating rates along the $\phi = 30°$ and $\phi = 60°$ radial locations were generally characterized by gradual decreases in heating rates with increasing axial locations. These relationships of heat transfer rates with axial and radial locations followed the same relationship just presented for the measured and predicted surface pressures (Figure 21). Therefore, the measured heat transfer rates were strongly dependent upon surface pressures.

   b. Typical Distributions from STAPAT Predictions

STAPAT predictions of heat transfer rate distributions over the analytic forebody for the typical test, Run 0657, are presented in Figures 23 and 24. Figure 23 shows isolines of QDOT and ST over the top half of the analytic forebody. Figure 24 incorporates a finer grid of isolines to show more details of the Stanton number distribution.

These STAPAT-predicted distributions were similar to both the measured heat transfer rate distributions and to the measured and predicted surface pressure distributions. Strong gradients in heat transfer rates were predicted along the axial direction for all radial locations, and significant gradients were predicted along the radial direction for axial locations from 2 in. to 4 in. and from 7 in. to 9 in.
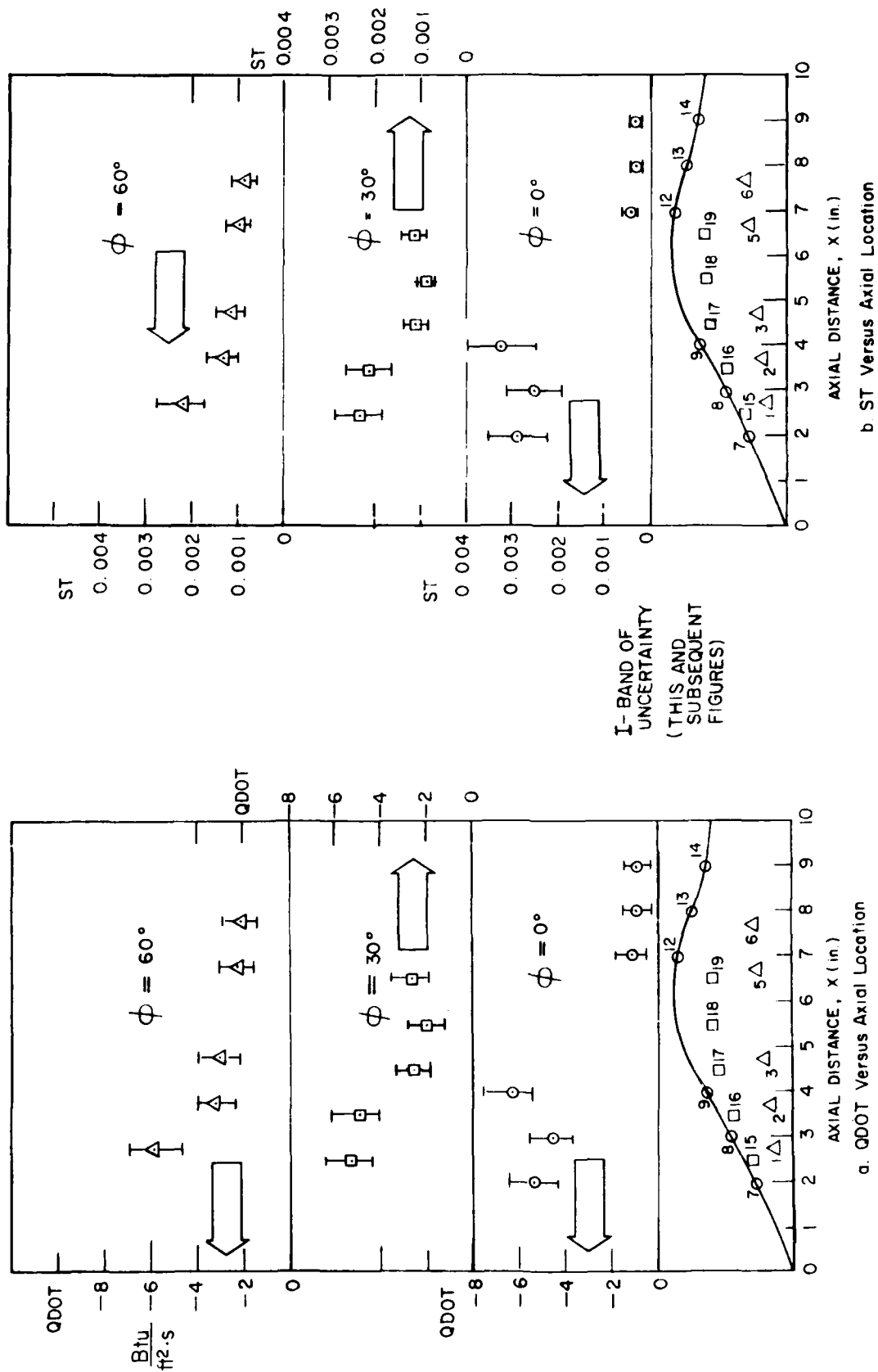
Figure 30. Typical Measured Heat Transfer Rate Distributions
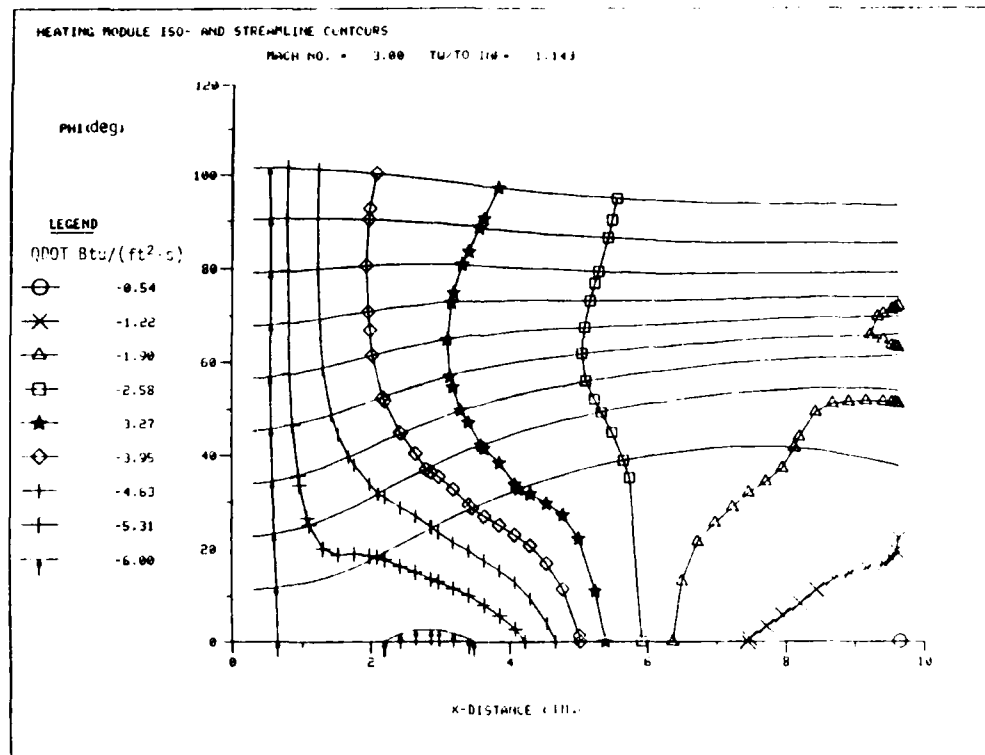
a. Isolines of QDOT
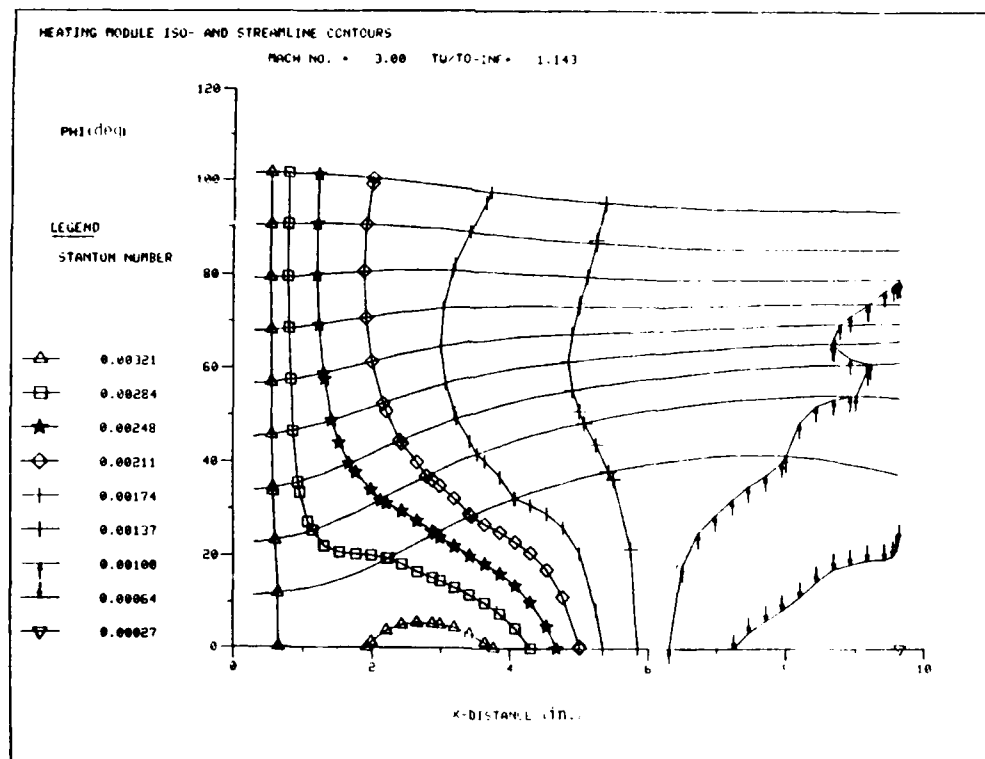
b. Isolines of ST

Figure 23. Typical STAPAT Predictions of Heat Transfer Rate Distributions
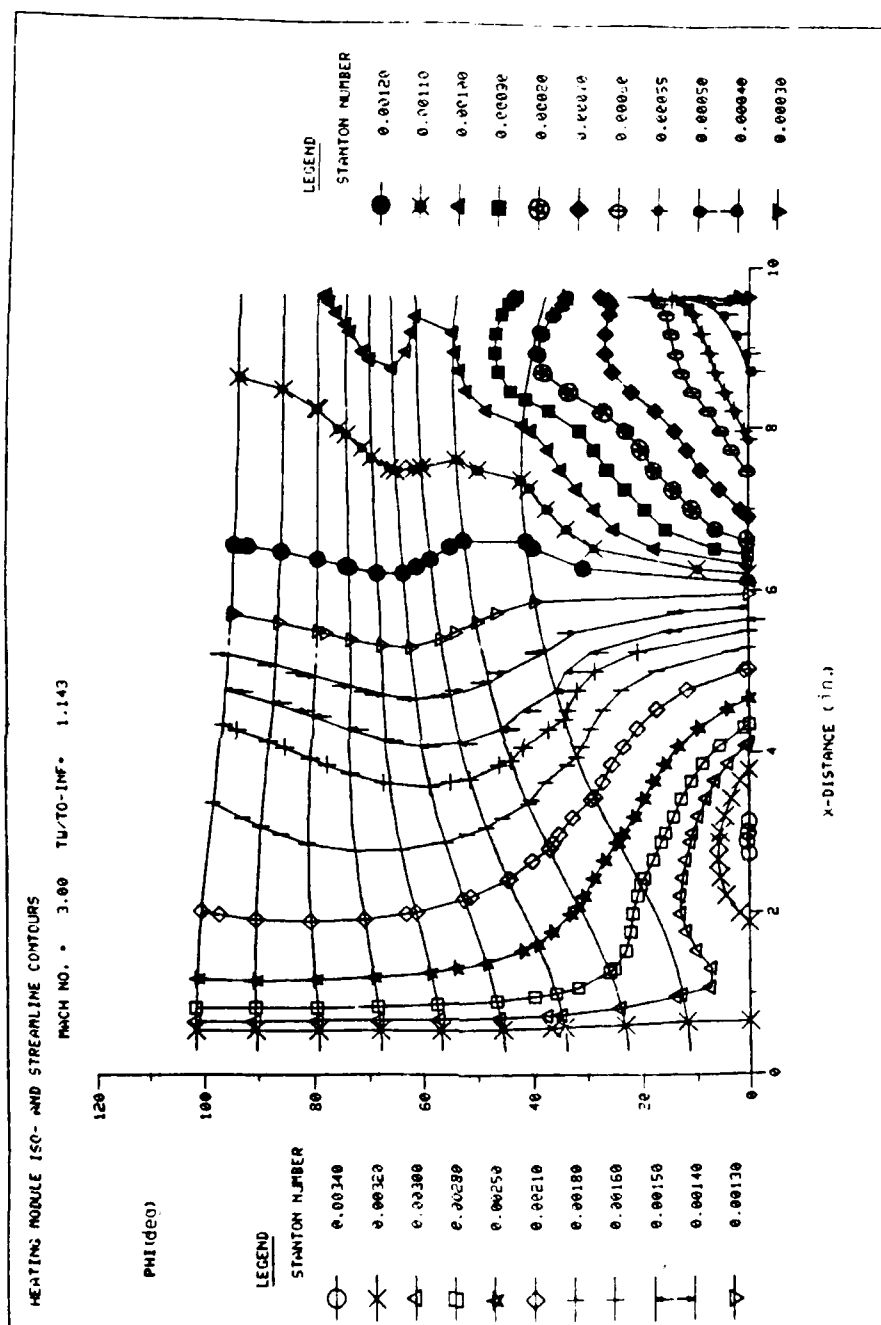
Figure 24. STAPAT Predictions of Stanton Number Distribution — Typical Fine Grid of Isolines

c. Effect of STAPAT Input Variables

For heat transfer rate calculations, operation of the STAHET module of STAPAT allows user selection of values for a number of input variables. Three that may influence results for this program are the amount of forebody smoothing (input variable ISMO), the streamline type (KP) and the skin friction law (KCF). The degrees of influence of these variables on heat transfer rate, QDOT, and Stanton number, ST, were evaluated by repeating STAPAT predictions for Run 0657 using different values for the variables. ISMO values of 1 (no body smoothing, the default value), 2 (intermediate body smoothing), and 3 (smoothing to a cone-like body) were used. KP values of 0 (simplified streamlines) and 1 (modified Newtonian streamlines, the default value) were used. KCF values of 0 (Spalding - Chi), 1 (Van Driest I), 2 (Van Driest II, the default value), and 3 (White and Christoper) were used.

STAPAT predictions showed essentially no differences due to body smoothing (ISMO) and no differences due to streamline type (KP) up to an axial location of 6 in. After this (in the shadow region), the simplified streamlines (KP = 0) gave slightly larger QDOT and ST values than did the modified Newtonian streamlines (KP = 1). The type of skin friction law had a slight influence on heat transfer rates. The KCF = 0 value yielded the smallest QDOT and ST values, with KCF = 2, KCF = 1, and KCF = 3 yielding successively larger QDOT and ST values.

The results from this evaluation are summarized in Figure 25. The STAPAT predictions of QDOT and ST values for all variations in input variables are contained between the two solid lines (except in the shadow region where values obtained using simplified streamlines deviated from the other values). These bands represent very small variations in heat transfer rate from the mean values, approximately ± 0.4 Btu/(ft^2·s) for QDOT and ± 0.0002 for ST. These variations are well below the estimated uncertainties in the measured QDOT and ST values.

For these reasons, the default values for these three-input variables were selected for all subsequent STAPAT runs. Predictions for Run 0657 using the default values are given by the dashed lines in the figure and show that using the default values yielded QDOT and ST values that were near the means.
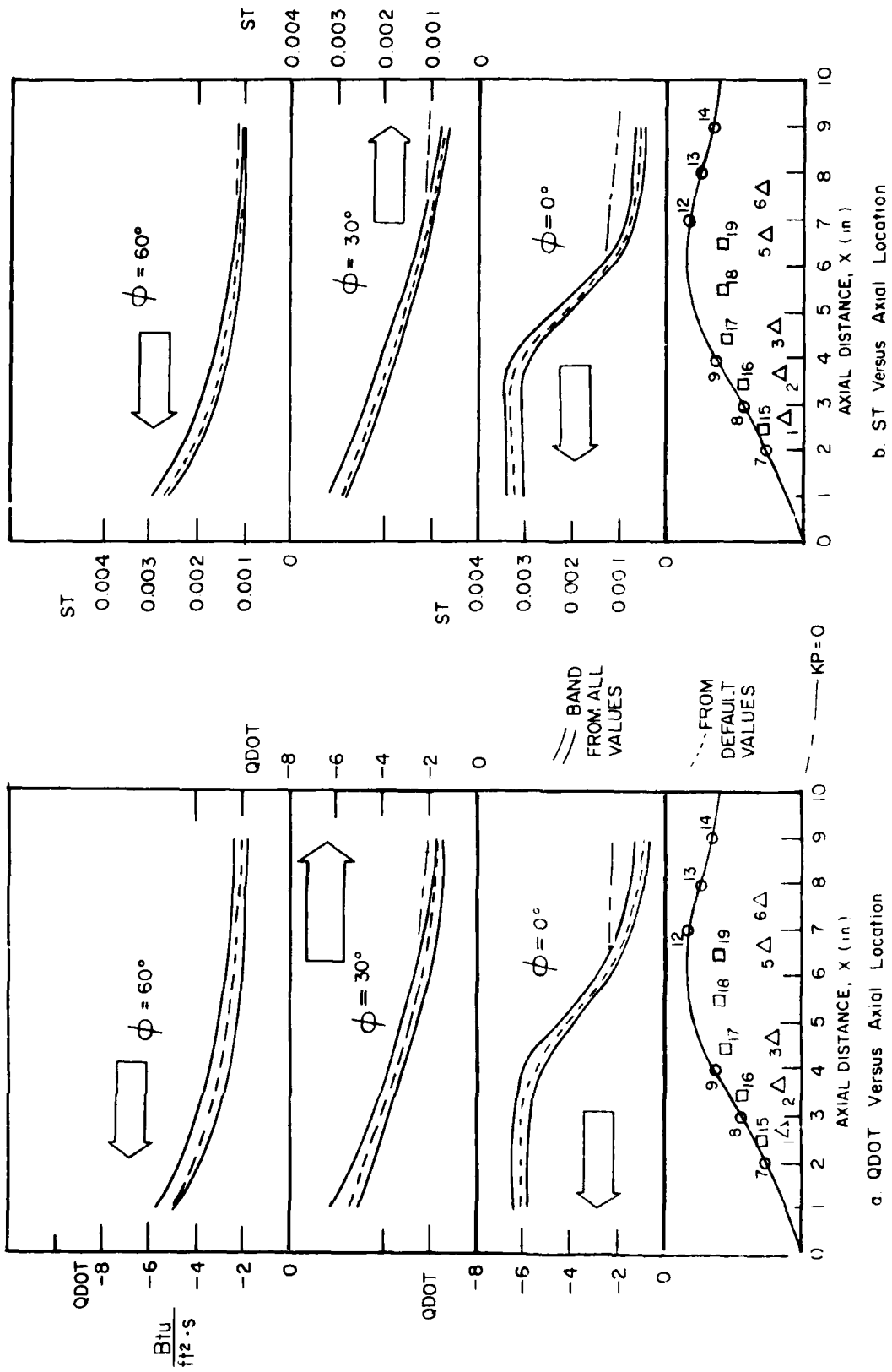
Figure 25. Effect of Input Variables on S_T, ΔT Predictions of Heat Transfer Rate.

a. QDOT Versus Axial Location

b. S_T Versus Axial Location

(Computer run times were influenced by selection of values for the input variables. Run times on the Digital Equipment Corporation, VAX 8650 computer using a KP value of 0 (simplified streamlines) ranged from 54 CPU s to 57 CPU s for all values of forebody smoothing (ISMO) and skin friction law (KCF). Run times using KP = 1 (modified Newtonian streamlines) ranged from 89 CPU s to 94 CPU s, a 65 percent increase in run times over the run times for KP = 0.)

d. Temperature Effects

As indicated by the equations used for wind tunnel data reduction and for STAPAT calculations, the heat transfer rate (in terms of QDOT and ST) at each gage location is dependent upon the values of, and the relationship between, a number of temperatures. Measured-QDOT values are proportional to differences between gage surface and backface temperatures. These temperatures are influenced by the temperature of the water flowing through the model and by the adiabatic wall temperature. STAPAT-calculated QDOT values are proportional to differences between gage surface and adiabatic wall temperatures. Measured and STAPAT-calculated ST values are dependent upon surface, adiabatic wall, and tunnel stagnation temperatures. The tunnel stagnation temperature was used to nondimensionalize other temperatures.

(1) Ratio, T-S/TO

The effects of variations in the ratio of gage surface temperature to tunnel stagnation temperature, T-S/TO, on STAPAT-calculated heat transfer rates were evaluated by repeating STAPAT predictions for Run 0657 using all 16 tabulated values for T-S/TO. The results from this evaluation are summarized in Figures 26 and 27.

The STAPAT predictions of QDOT and ST values using minimum, average and maximum values of T-S/TO are shown in Figure 26. There were large variations in QDOT with T-S/TO. For example, at an axial location of 3 in. on the top centerline, QDOT varied from approximately 4.3 Btu/(ft$^2 \cdot$s) at a T-S/TO ratio of 1.086 to approximately 7.5 Btu/(ft$^2 \cdot$s) at a T-S/TO ratio of 1.202. STAPAT predictions of QDOT using the average value of T-S/TO ratio were midway between the QDOT values predicted using the minimum and maximum values of T-S/TO. There were very small

Figure 26. Effect of the Ratio T-S/T0 on STAPAT Predictions of Heat Transfer Rates.
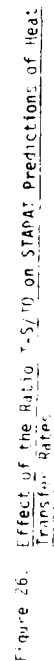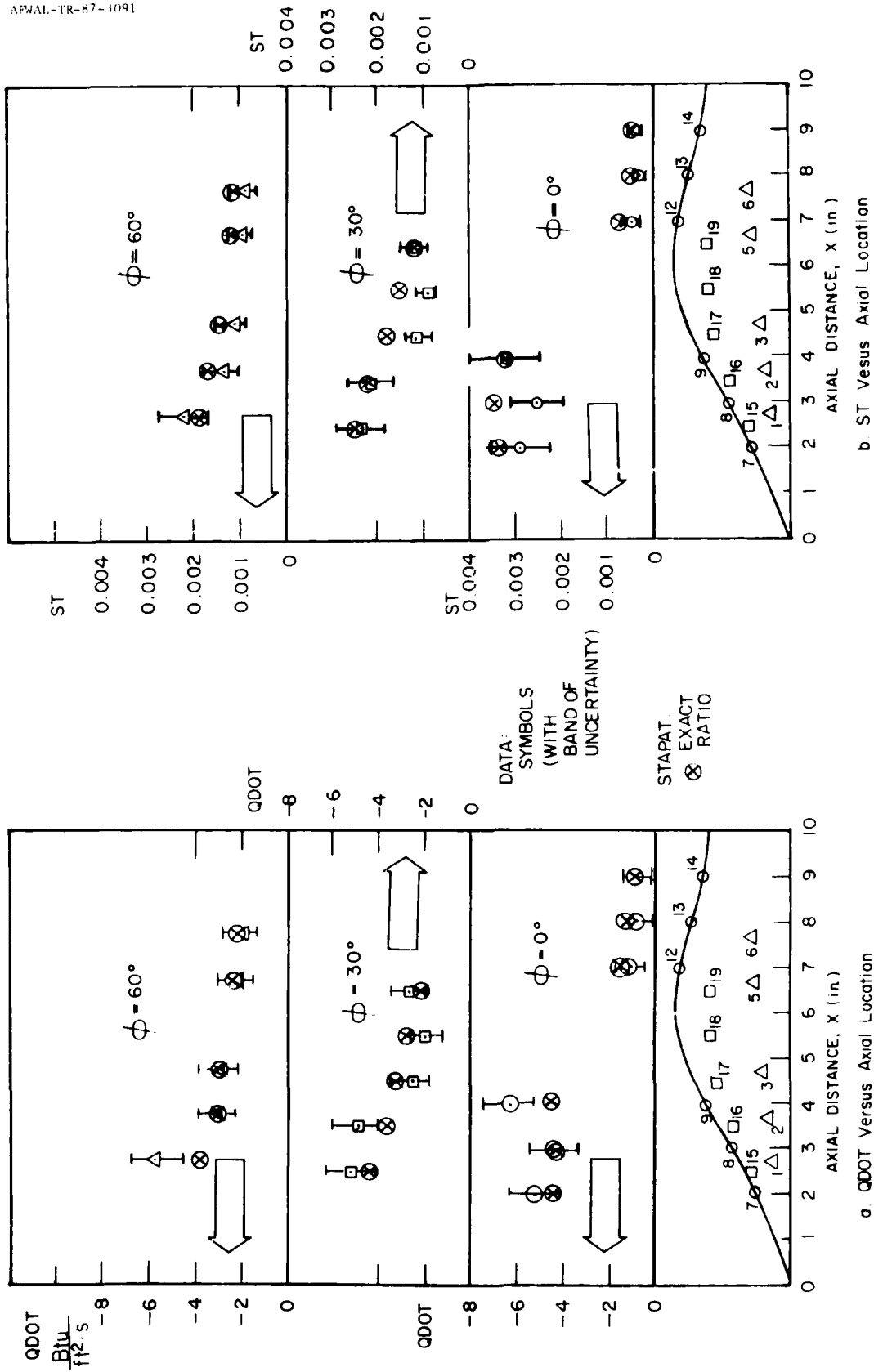
Figure 27. Comparison of Heat Transfer Rates for Exact Ratios of 1.0 to 10

variations in ST with T-S/TO; the predicted Stanton numbers were essentially independent of the ratio of gage surface temperature to tunnel stagnation temperature.

Also shown on Figure 26 are the measured values of QDOT and ST with their associated uncertainty estimates. The STAPAT-predicted values of QDOT essentially bounded the measured values and generally followed the trends indicated by the measured values. The STAPAT-predicted values of ST showed good agreement with the magnitude of the measured values and with their distribution over the upper surface of the analytic forebody.

Figure 27 shows that there was little to gain by using exact T-S/TO values for STAPAT calculations of QDOT and ST for a particular gage. Using the exact T-S/TO ratio gave no closer agreement with the measured values than using any value (greater than 1.0) for the temperature ratio T-S/TO. All subsequent STAPAT runs were made with a single value for T-S/TO, equal to 1.143.

(2) Water Temperature, T-WATER

The effects of variations in backface temperatures on measured heat transfer rates were evaluated by adjusting the temperature of the water circulating through the internal passages of the model. Hot water heater temperatures were varied to yield average inlet to exit water temperature, T-WATER, values of nominally 580, 590, 600, and 610 R. Typical results from this evaluation are summarized in Figure 28.

Measured values of QDOT and ST are shown in the figure for a T-WATER value of 583 R (Test Run 0686) and a T-WATER value of 609 R (Test Run 0700). For a tunnel stagnation pressure of 200 psia and zero angle of attack, these temperatures were near the minimum and maximum values tested and represented the outer bounds of the test data. The QDOT and ST data from the intermediate T-WATER temperatures were between the values plotted. (The tunnel stagnation temperatures, TO, for Runs 0686 and 0700 were 461 R and 453 R, respectively. This small difference effectively eliminated TO as an influencing parameter for these two test runs.) Also plotted in the Figure are STAPAT-calculated QDOT and ST values for these runs for comparison.
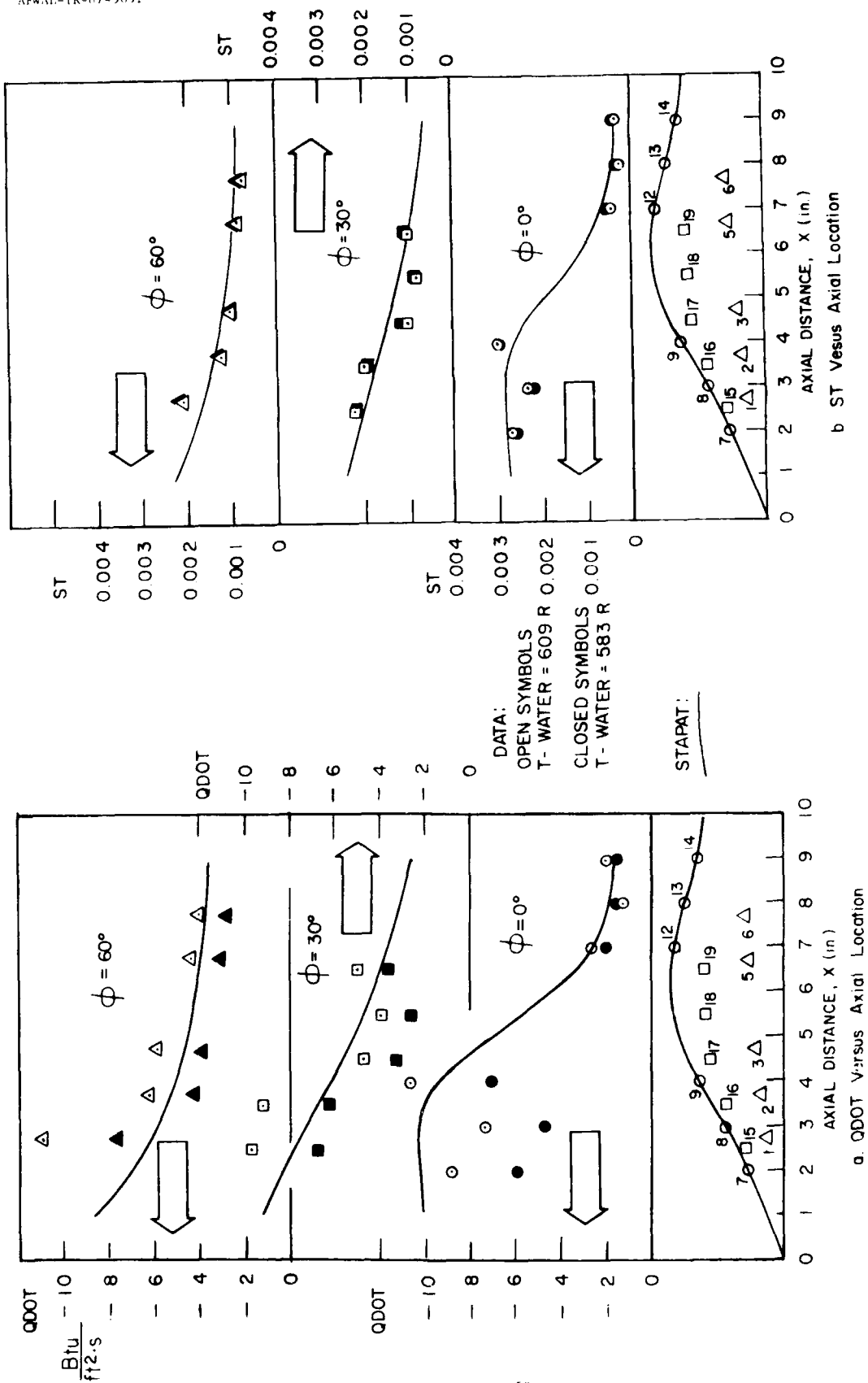
Figure 30. Effect of Water Temperature on Measured Heat Transfer Rates

a. QDOT Versus Axial Location

b. ST Versus Axial Location

DATA:
OPEN SYMBOLS
T-WATER = 609 R

CLOSED SYMBOLS
T-WATER = 583 R

STAPAT:

(Only one set of curves each for QDOT and ST are presented since T-WATER is not a variable in STAPAT calculations.)

Measured-QDOT values were significantly influenced by backface water temperature. For a given gage, QDOT increased with increasing T-WATER except in the shadow region where QDOT values were essentially the same. Measured-ST values were independent of backface water temperature for the range of temperatures studied. This means that the use of the nondimensional heat transfer coefficient, the Stanton number, effectively eliminated T-WATER as an influencing parameter.

(3) Tunnel Stagnation Temperature, TO

The effects of variations in tunnel stagnation temperatures, TO, on measured and STAPAT-calculated heat transfer rates were evaluated by studying tests run with values of TO from 453 R to 495 R, Runs 0658, 0666, 0676, and 0700. Typical results from this evaluation are summarized in Figure 29.

Measured and STAPAT-calculated values of QDOT and ST are shown in the Figure for a TO value of 453 R (Test Run 0700) and a TO value of 495 R (Test Run 0666). The QDOT and ST values from intermediate TO temperatures were between the values plotted. (The backface temperature, in terms of T-WATER, for Runs 0700 and 0666 were essentially the same (610 R), thus eliminating T-WATER as an influencing parameter for these two test runs.)

For a given gage, both the measured and STAPAT-calculated QDOT values increased with decreasing tunnel stagnation temperature except in the shadow region where QDOT values were essentially the same. The measured increases in QDOT were slightly larger than the increases calculated by STAPAT. Both the measured and calculated-ST values were independent of tunnel stagnation temperature for the range of temperatures studied. Agreement was good between the measured and the STAPAT-calculated Stanton numbers.

(4) Adiabatic Wall Temperature, T_{AW}

The effects of uncertainties in adiabatic wall temperature, T_{AW}, or measured-Stanton numbers were evaluated by consideration of the differences among
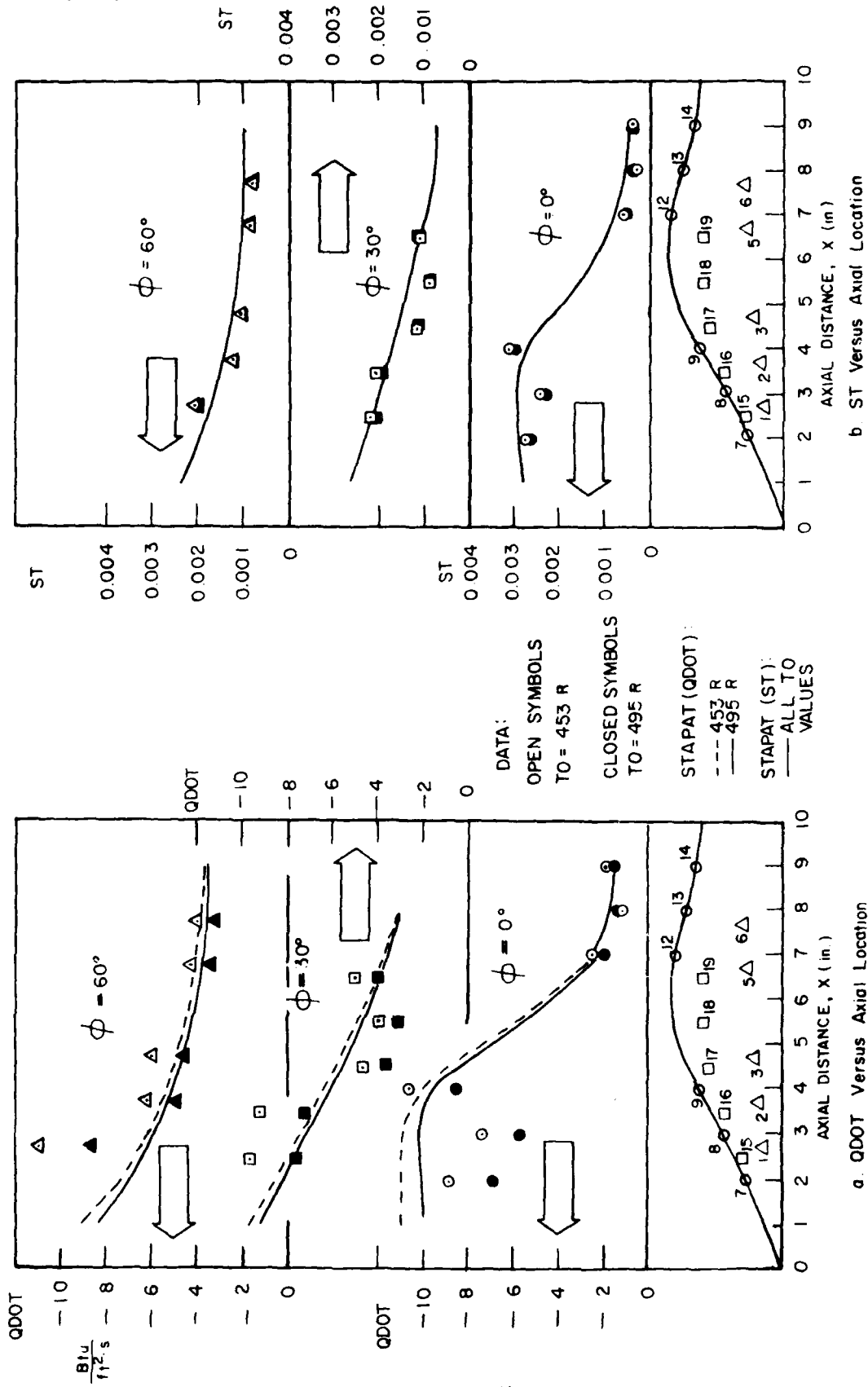
Figure 23. Effect of Tunnel Stagnation Temperature on Heat Transfer Rates

theoretical, calculated, and experimentally determined values of T_{AW}. The adiabatic wall (or recovery) temperature is the equilibrium surface temperature that would be reached, in the case of a high-velocity gas flow past a surface, when the rate-of-heat input by frictional dissipation equals the rate-of-heat convection away from the surface (Reference 10). Adiabatic wall temperatures can be calculated (estimated) using boundary layer edge flow conditions and a recovery factor whose value is determined from experimentally derived correlations involving flow conditions which are usually expressed in terms of the Prandtl number. Adiabatic wall temperatures can also be obtained experimentally by measuring the wall temperature (T-S in the case of these tests) when the heat transfer rate (QDOT in this case) equals zero.

The measured Stanton number, ST, values tabulated herein were determined using a (somewhat arbitrary and constant) theoretical value of T_{AW} equal to 0.90 TO. For wind tunnel Test Run 0700 and using a T-S/TO value of 1.143, STAPAT calculated T_{AW} values equal to 0.94 TO for gages 7, 8 and 9 (at axial locations of 2, 3 and 4 in., respectively). Gross extrapolations of data plots of heat transfer rate, QDOT, versus gage surface temperature, T-S, were made for Runs 0686 and 0700 from the QDOT and T-S values measured to the T-S value where QDOT would be zero. This yielded experimentally determined T_{AW} values of approximately 0.94 TO, 0.96 TO and 0.98 TO for gages 7, 9, and 8, respectively.

This means that the STAPAT-calculated value of T_{AW} equal to 0.94 TO is closer to the experimentally determined values of from 0.94 TO to 0.98 TO than to the theoretical value of 0.90 TO which was used to determine the measured-ST values. Use of a larger theoretical value, say 0.94 TO, would yield measured Stanton number values that are approximately 20 percent larger than the values tabulated. While this might give closer agreement between measured and STAPAT-calculated Stanton numbers, the differences fall within the band of estimated uncertainty and therefore do not justify making any correction to the tabulated data.

(5) Use of Stanton Number to Eliminate Temperature Effects

The measured values of heat transfer rate, QDOT, were shown to be influenced by test dependent temperatures T-WATER and TO. The STAPAT-calculated values of QDOT

were shown to be influenced slightly by the test dependent temperature TO and significantly by the unknown (apriori) surface (outer wall) temperature, T-S. Even though the measured Stanton number (based on free-stream conditions) was dependent on the unknown (not measured) temperature TAW and the STAPAT-calculated Stanton number (also based on free-stream conditions) was dependent on the unknown temperatures TAW and T-S, the use of this nondimensional heat transfer coefficient, the Stanton number, ST, was shown to be the best way to evaluate heat transfer rates over the analytic forebody for these tests. It effectively eliminated heat transfer rate dependency upon temperatures that were test dependent and/or unknown. Therefore, all subsequent test evaluations and comparisons were made using only the Stanton number.

    e. Effect of Tunnel Stagnation Pressure

    (1) Stanton Number Distributions
    The effects of variations in tunnel stagnation pressures, PO, on measured and STAPAT-calculated Stanton numbers were evaluated by studying Test Runs 0657, 0658, 0659, and 0660 which were conducted at nominal PO values of 100, 200, 300 and 400 psia, respectively. Typical results from this evaluation are summarized in Figure 30.

    Measured and STAPAT-calculated values of ST are shown in the figure for PO values of 100 and 400 psia. The STAPAT-calculated ST values from intermediate PO pressures were between the values plotted. The measured-ST values for PO values of 300 and 400 psia were essentially the same; the measured ST values for a PO of 200 psia were approximately midway between the values plotted.

    Both the measured and STAPAT-calculated Stanton numbers decreased with increasing tunnel stagnation pressure, except for the measured Stanton numbers in the shadow region where the values were essentially the same. STAPAT predicted slightly larger Stanton number decreases with increasing stagnation pressure than were measured. Overall, there was very good agreement between measured and STAPAT-calculated Stanton numbers for all stagnation pressures tested.
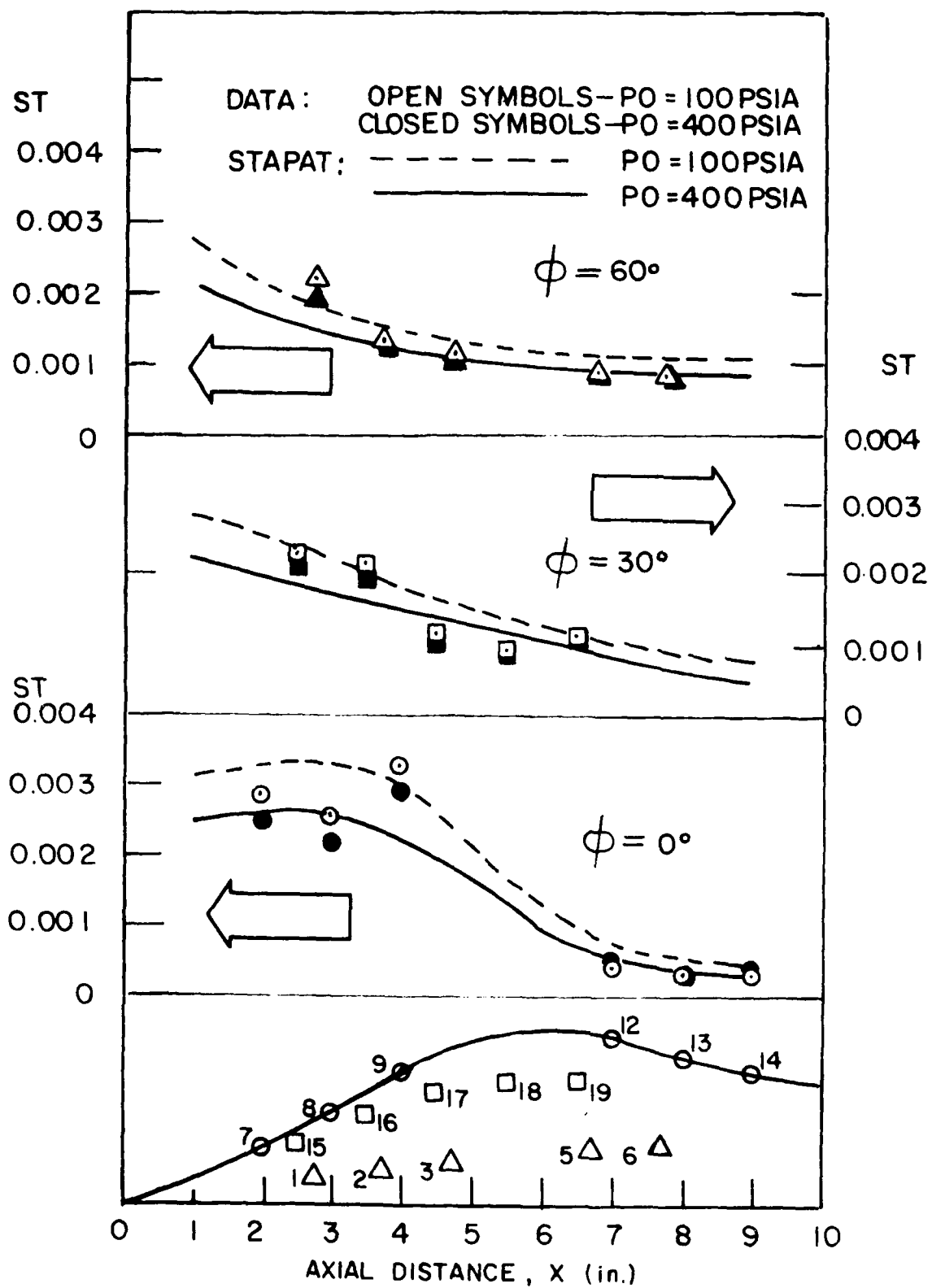
Figure 30. Effect of Tunnel Stagnation Pressure on Heat Transfer Rates

(2) Boundary Layer Type

The relatively large variation in tunnel stagnation pressure, which was accompanied by a correspondingly large free-stream unit Reynolds number variation of from 16 to 76 million per ft, did not affect the general distribution of Stanton number over the analytic forebody. This result, coupled with the good agreement between the measured values and the values calculated by STAPAT (which assumes a turbulent boundary layer), leads to the conclusion that the boundary layer over the analytic forebody was turbulent throughout the test program.

f. Spanwise Gradients

(1) Stanton Number Distributions

As the typical distributions from STAPAT calculations showed (Figures 23 and 24), STAPAT predicted large spanwise gradients in Stanton number over the forward portion of the analytic forebody. This variation is also illustrated in Figure 31 for Run 0657 at an axial location of 4 in. Stanton number decreased from a value of 0.0030 on the top centerline where $\phi = 0$, to a value of approximately 0.0016 for $40 \le \phi \le 90°$. Also shown on the figure are the measured values of ST. The values at $\phi = 30$ and $60°$ were obtained from linear interpolation of the values from the gages on either side of $X = 4$ in. There was very good agreement between the measured and STAPAT-calculated spanwise distributions of Stanton number.

(2) Strong Influence of Surface Pressures

In STAPAT calculations, Stanton numbers are directly proportional to surface Mach numbers, static pressures and static temperatures. Figure 18 shows that the Mach number can be expected to increase in the spanwise direction while the static pressures and temperatures decrease. The increase in Mach number and the decrease in static temperature were relatively small and effectively cancelled out each other. The decrease in static pressure was large, approximately 47 percent, and is almost equal to the spanwise decrease in Stanton number. Therefore, the magnitudes of the Stanton number values and their distributions over the analytic forebody were primarily dependent on surface pressures for these tests.

DATA: SYMBOLS
STAPAT:————

X = 4 in.

POLAR COORDINATE ANGLE, ϕ (deg)

$\phi =$ 0°

$\phi =$ 30°

$\phi =$ 60°

$\phi =$ 90°

AXIAL DISTANCE, X (in.)
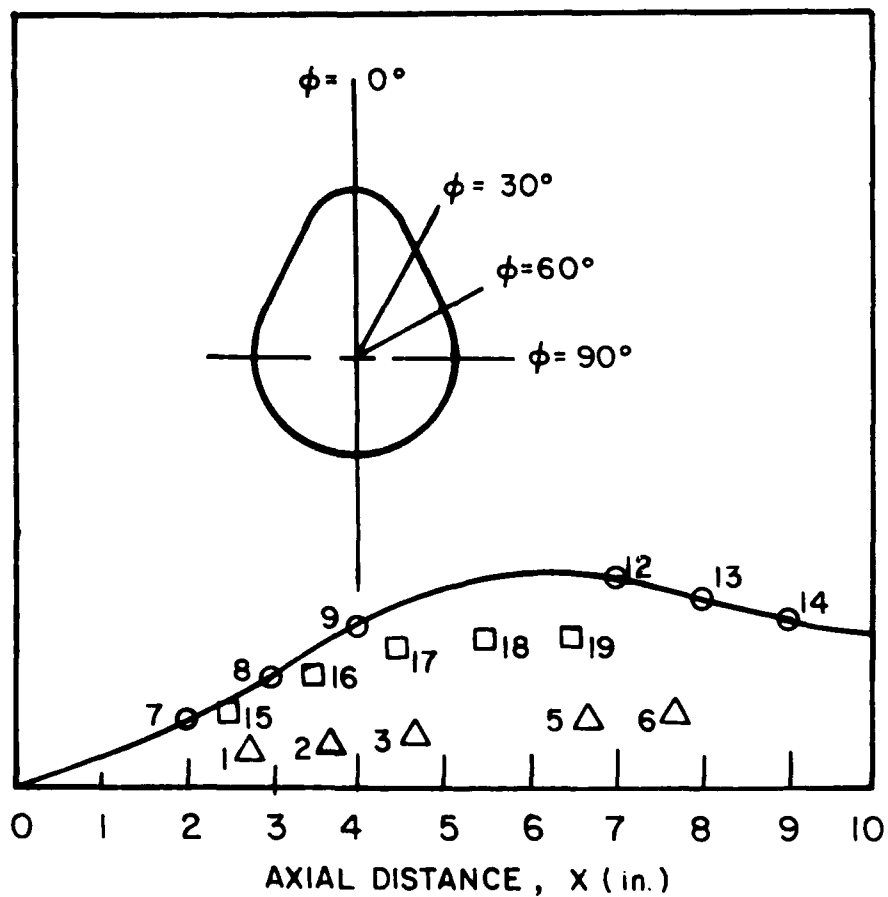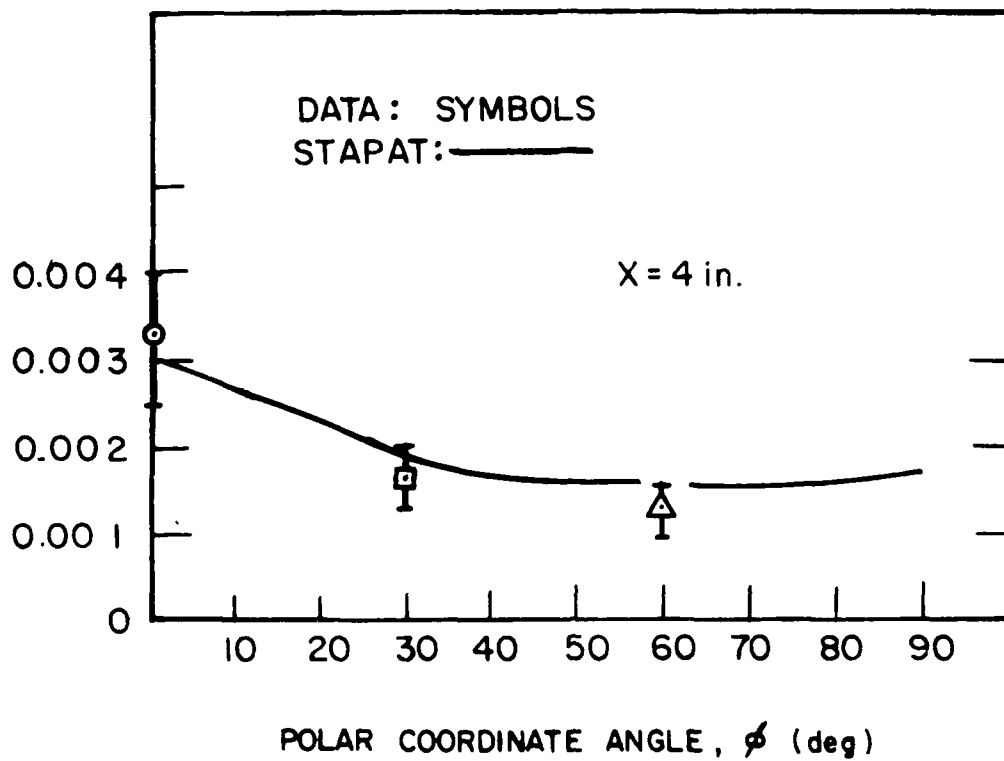
Figure 31. Spanwise Distribution of Heat Transfer Rates

66

4. Angle-of-Attack Effects

To study the effects of angle of attack, ALPHA, on heat transfer rates and other flow field properties, wind tunnel tests and STAPAT calculations were accomplished at zero and nonzero angles of attack of the analytic forebody. Angles of attack of -4, -3, 0, +3 and +4° were tested for various combinations of backface water temperature, tunnel stagnation pressure and tunnel stagnation temperature. Since STAPAT would only operate at negative nonzero angles of attack, calculations were made at ALPHA = -3° for comparison with (1) measured-heat transfer rate data, (2) zero angle-of-attack predictions, and (3) surface pressure data reported in Reference 6.

a. Heat Transfer Rates

The effects of variations in angle of attack of the analytic forebody on measured and STAPAT-calculated Stanton numbers were evaluated by studying Test Runs 0670, 0672, 0666, 0674, and 0668 which were conducted at values of -4, -3, 0, +3 and +4°, respectively. Typical results from this evaluation are summarized in Figure 32.

Measured values of Stanton number are shown in the figure for ALPHA values of -3 and +3°. Measured Stanton numbers for ALPHA values of -4 and +4° were essentially the same as the ST values for ALPHA values of -3 and +3°, respectively. Measured-ST values for zero angle of attack were between the values plotted. STAPAT-calculated values of Stanton number for ALPHA = -3° were obtained from the heat transfer rate distributions shown in Figure 33.

Both the measured and STAPAT-calculated Stanton numbers decreased only slightly with increasing angle of attack. Agreement was good between the measured and the STAPAT-calculated Stanton numbers for variations in angle of attack.

b. Flow Field

The effects of variations in angle of attack of the analytic forebody on flow field properties were determined by comparison of the streamline and isoline
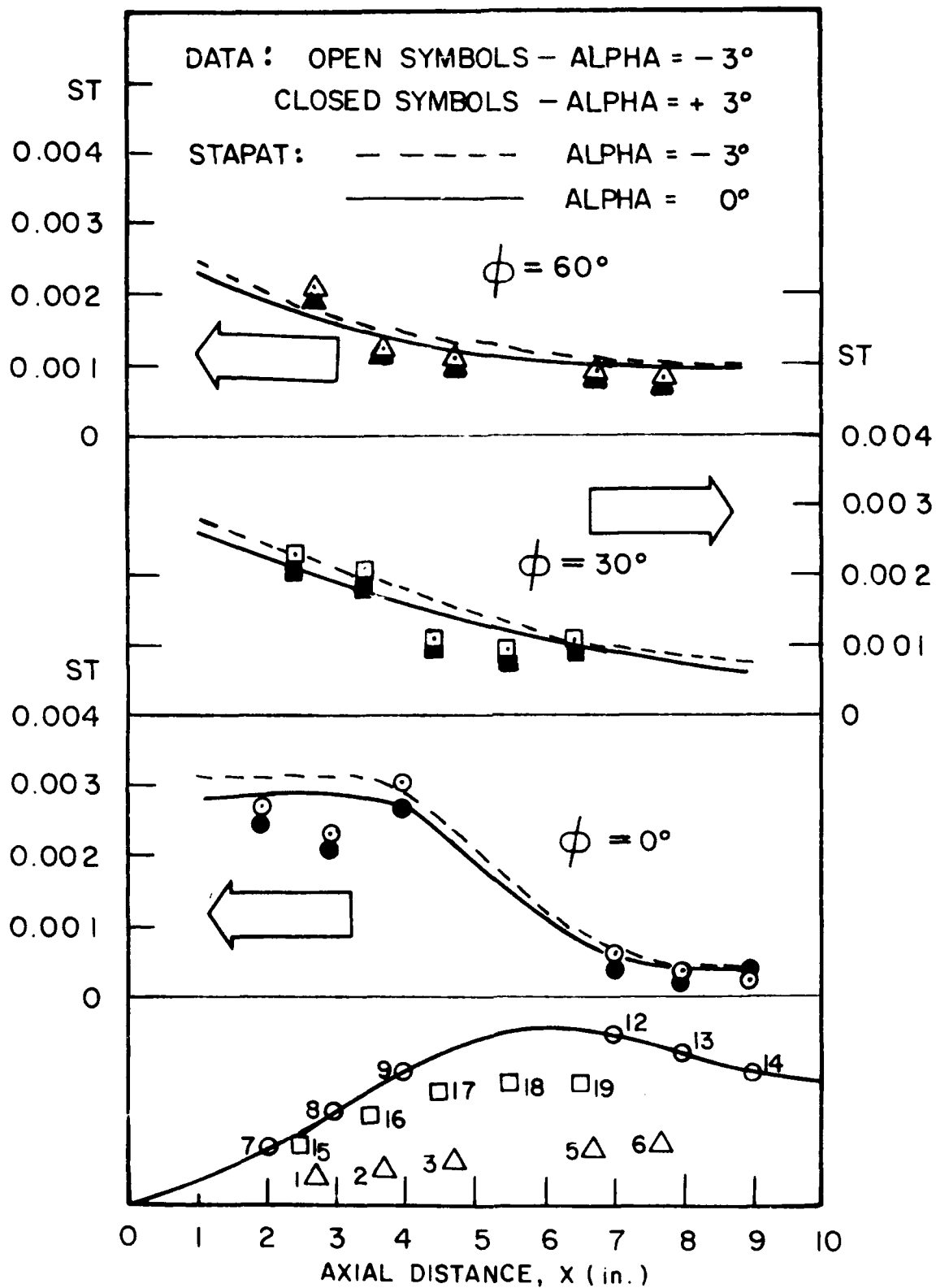
Figure 32. Effect of Angle of Attack on Heat Transfer Rates
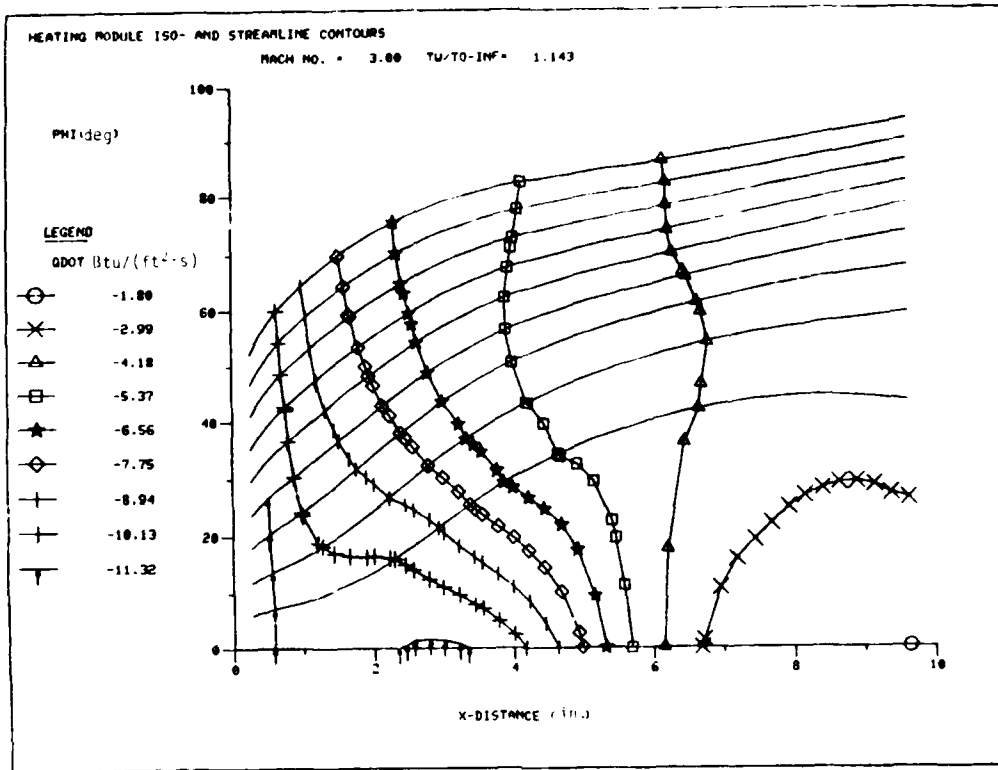
a Isolines of QDOT
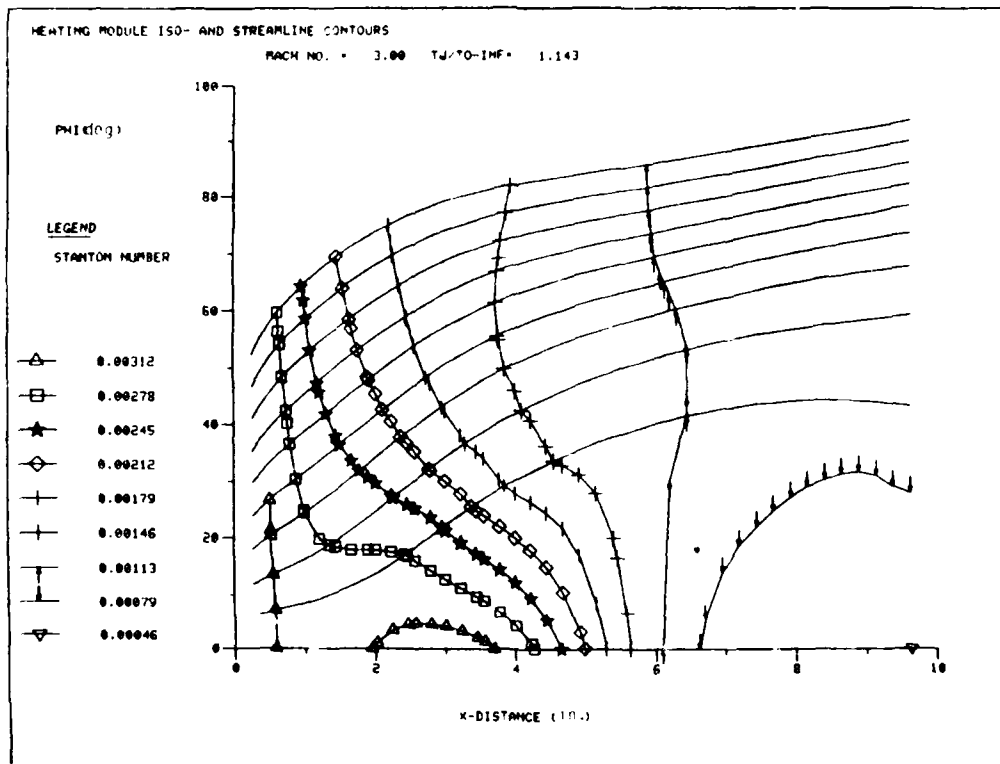
b. Isolines of ST

Figure 33. STAPAT Predictions of Heat Transfer Rate Distributions
for -3° Angle of Attack

69
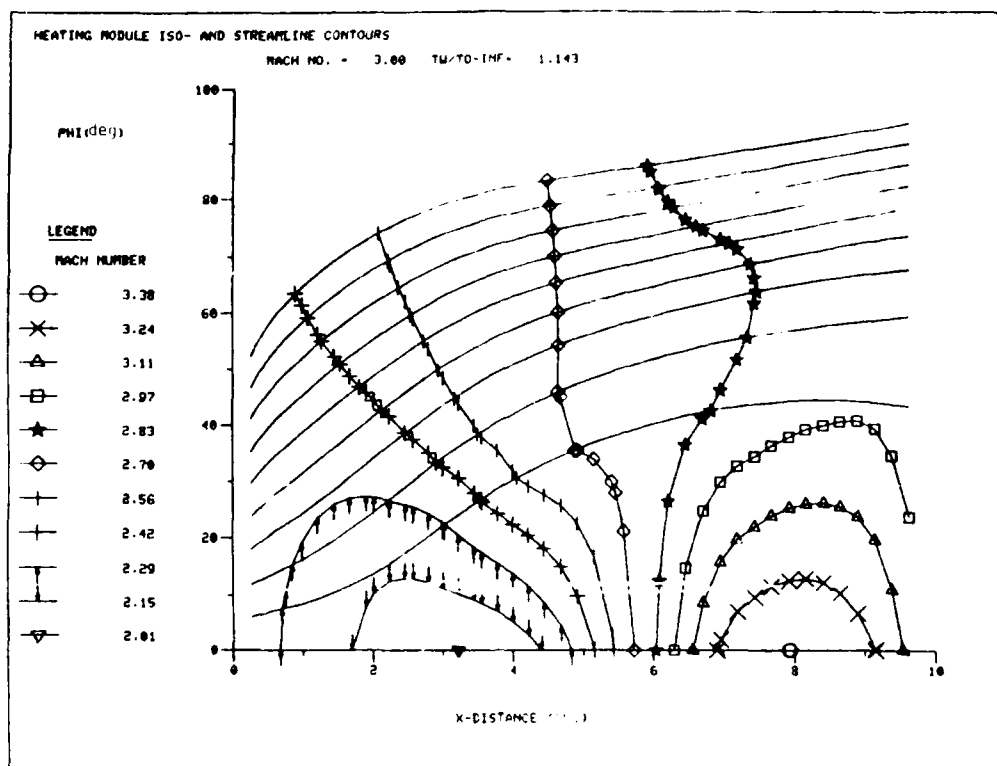
a. Isolines of Mach Number
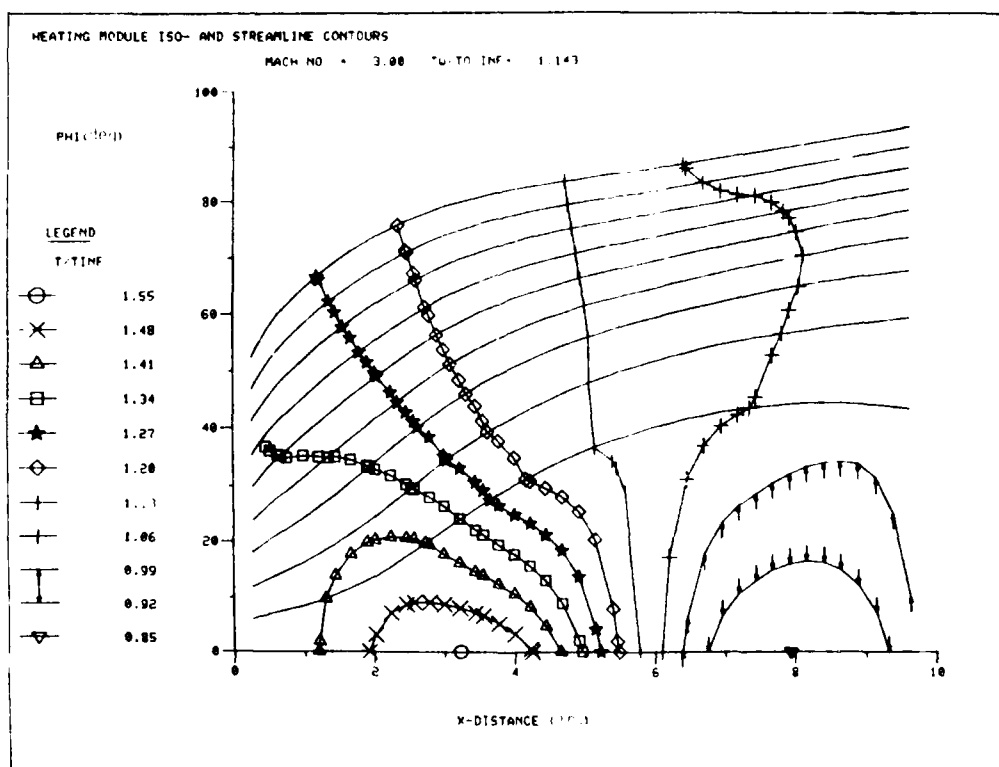
b. Isolines of Static Temperature

Figure 34. JAPAI Predictions, Below Fuel Proper at
Angle of Attack
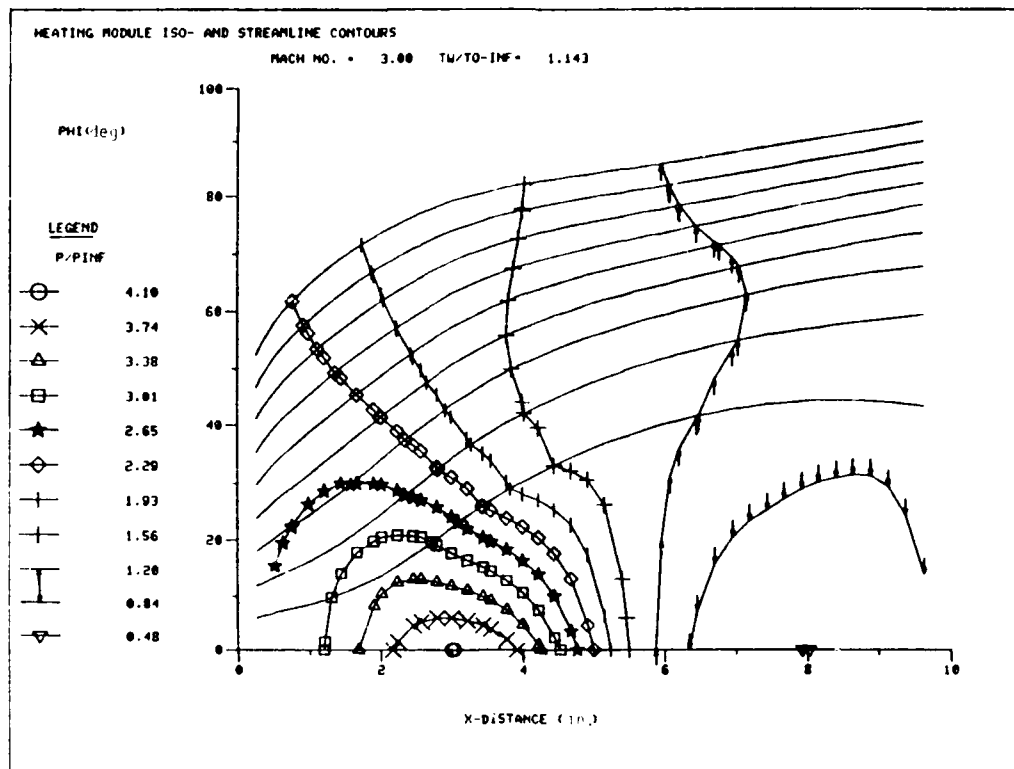
c. Isolines of Static Pressure
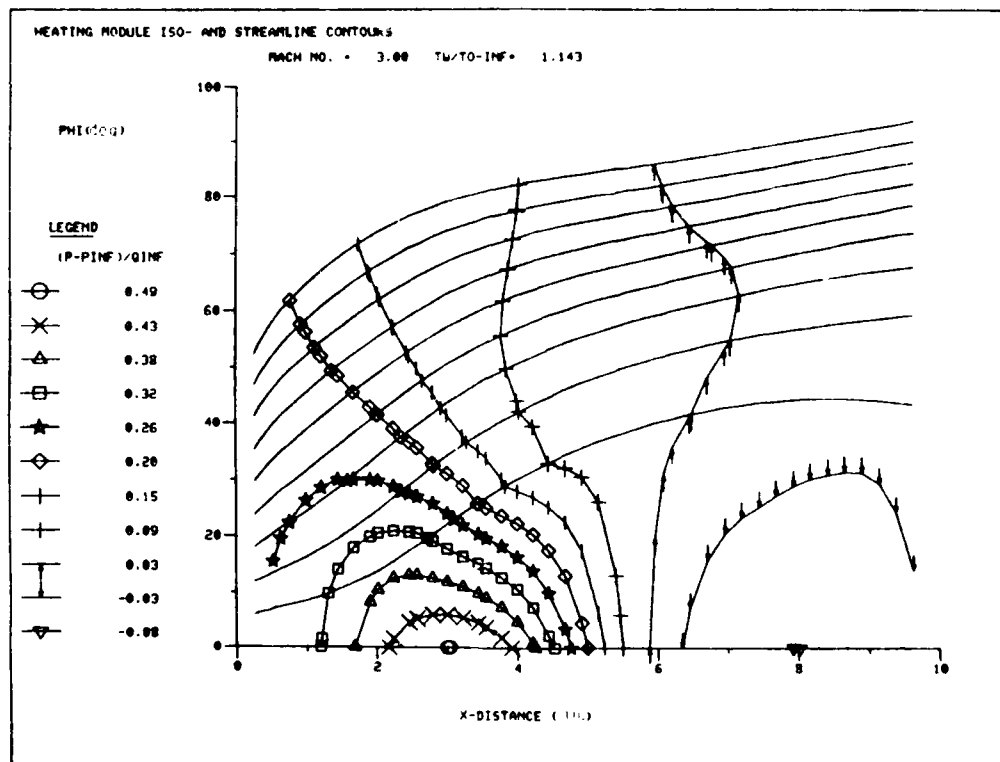
d. Isolines of Pressure Coefficient

Figure 14. (Concluded)

contours presented in Figure 34 for ALPHA = -3° with those in Figure 18 for ALPHA = 0°. The effects of ALPHA variations on surface pressures were determined by comparison of the pressure values in these figures with those values reported in Reference 6.

Most striking was the effect angle-of-attack variations had on the shape of the streamlines. At zero angle of attack, Figure 18, the streamlines came off the nose with essentially zero slope in the ϕ, X plane, while at an angle of attack of -3°, Figure 34, the radial location of a given streamline increased significantly with increasing axial location.

Overall, the shapes of the distributions of Mach number, temperature and pressure were independent of angle of attack for the two angles studied. A slight difference was in the axial location where the pressure coefficient, C_p, decreased to zero. On the top centerline the axial location where C_p equaled zero was approximately 6.0 in. for zero angle of attack and slightly greater than 6.0 in. for an angle of attack of -3°.

While the distributions were similar, the magnitudes of the values were different. Along the top centerline and at axial location of 3 in. for example, the STAPAT-calculated values of Mach number, static temperature, and static pressure for ALPHA = -3° were approximately 6 percent lower, 5 percent higher, and 14 percent higher, respectively, than those calculated for zero angle of attack. This STAPAT-calculated increase in static (surface) pressure of 14 percent at this location agreed very well with the approximately 16-percent increase in surface pressure which was reported in Reference 6.

SECTION V

CONCLUSIONS AND RECOMMENDATIONS

1. CONCLUSIONS

Based on results from tests with the tunnel interference effects models and from analysis of schlieren photographs taken during the test program, the flow fields surrounding the analytic forebody were determined to be free from anomalies which would invalidate the data.

The wide range of measured-backface temperatures showed that a separate thermocouple junction on the backface of each heat transfer rate gage was required for application of the technique for heat transfer testing in cold flow wind tunnels using the analytic forebody.

The boundary layer over the analytic forebody was determined to be turbulent throughout the test program.

While the estimated maximum uncertainties of the heat transfer data were relatively large, they did not mask the overall level of heat transfer rates nor their relationships with axial and radial locations over the analytic forebody.

Variations in values for input variables of forebody smoothing, streamline type, and skin friction law had negligible effect on STAPAT-calculated heat transfer rates. However, computer run times for runs using modified Newtonian streamlines were 65 percent longer than for runs using simplified streamlines. Forebody smoothing and skin friction law variations had negligible effects on computer run times.

In general, STAPAT correctly predicted the pressure distribution over the surface of the analytic forebody. STAPAT under-predicted the pressure levels on the foreward portion of the forebody but showed very good agreement with the data elsewhere. The magnitudes of the Stanton number values and their distributions over the analytic forebody were primarily dependent on surface pressures.

Both measured and STAPAT calculations showed strong gradients in pressure and heat transfer rates along the axial direction for all radial locations and significant gradients along the radial direction for axial locations from 2 in. to 4 in. and from 7 in. to 9 in.

Heat transfer rates, in terms of QDOT, were significantly influenced by tunnel stagnation temperatures, gage surface temperatures and backface (water) temperatures. Use of the nondimensional heat transfer coefficient, the Stanton number, ST, effectively eliminated heat transfer rate dependency upon temperatures that were test dependent and/or unknown and therefore was shown to be the best way to evaluate heat transfer rates over the analytic forebody for these tests.

Agreement was very good between the measured and STAPAT-calculated Stanton number relationships with tunnel stagnation pressure. Both showed a slight but general decrease in Stanton number with increasing pressure.

Stanton number decreased only slightly with increasing angle of attack; Agreement was good between the measured and STAPAT-calculated Stanton numbers for variations in angle of attack.

The STAPAT computer program, as modified in the STAHET module to include nonwedge shaped wind tunnel models, nonzero pressure coefficients in shadow regions and nonzero angles of attack, has been shown to predict surface pressures and heat transfer rates over the analytic forebody that are in good agreement with experimental data.

The magnitudes of the measured-heat transfer rates, their distribution over the analytic forebody and their good agreement with STAPAT calculations combined to provide validations of both the STAHET module of the STAPAT program and the experimental technique for heat transfer testing in cold flow wind tunnels.

2. RECOMMENDATIONS

All copies of the STAHET module of STAPAT should be modified to include nonwedge shaped wind tunnel models, nonzero angles of attack and nonzero pressure coefficients in body shadow regions. For calculation of pressures in body shadow regions, the correlation equation given in Section III should be considered for use.

When running STAHET, the user should verify that the STAPAT-predicted surface pressures are sufficiently close to the desired modified Newtonian pressures using known values for free-stream conditions and body surface slope angles. If the pressures are not close enough, the number of axial and/or circumferential stations of the forebody model should be adjusted (increased).

When selecting test methods and facilities for simulation of aerothermodynamics at supersonic speeds, the experimental technique for heat transfer rate testing in cold flow wind tunnels as described in this report should be considered for use.

REFERENCES

1. Varner, M.O., and Babish III, C.A., Status of a New Aerothermodynamic Analysis Tool for High-Temperature Resistant Transparencies, a paper published in Air Force Wright Aeronautical Laboratories, Wright-Patterson Air Force Base, Ohio 45433, AFWAL-TR-83-4154, "Conference on Aerospace Transparent Materials and Enclosures," edited by S.A. Marolo, December 1983.

2. Varner, M.O., et al., Specific Thermal Analyzer Program for High-Temperature Resistant Transparencies for High-Speed Aircraft (STAPAT), Volume I - Methodology, Volume II - Users Manual, Main Text and Volume III - Appendices of Sample Problems, Air Force Wright Aeronautical Laboratories, Wright-Patterson Air Force Base, Ohio 45433, AFWAL-TR-84-3086, (AD B089 497, AD B090 894L and AD B090 895L), October 1984.

3. Hayes, J.R., A Water Heated Platinum Thin-Film Heat Transfer Gage For Use In Cold Flow Wind Tunnels, Air Force Wright Aeronautical Laboratories, Wright-Patterson Air Force Base, Ohio 45433, AFWAL-TM-83-158 FIMG, November 1982.

4. Fiore, A.W., et al., Design and Calibration of the ARL Mach 3 High Reynolds Number Facility, Aerospace Research Laboratories, Wright-Patterson Air Force Base, Ohio 45433, ARL TR 75-0012, January 1975.

5. Scaggs, N., The Mach 3, Mach 6 High Reynolds Number and the 20 Inch Hypersonic Wind Tunnels - Information for Users, Air Force Flight Dynamics Laboratory, Wright-Patterson Air Force Base, Ohio 45433, Internal Report, August 1977.

6. Townsend, J.C., et al., Surface Pressure Data on a Series of Analytic Forebodies at Mach Numbers From 1.70 to 4.50 and Combined Angles of Attack and Sideslip, National Aeronautics and Space Administration, Langley Research Center, Hampton, Virginia 23365, NASA Technical Memorandum 80062, (N79-29145), June 1979.

7. Anon, Measure Surface Temperature With a Response Time as Little as 1 Microsecond, Medtherm Corporation, Huntsville, Alabama 35804, Bulletin 500.

8. Anon, Application Notes for Medtherm CO-AX^{TM} Thermocouple Probes, Medtherm Corporation, Huntsville, Alabama 35804, MEDTHERM AN-TCS-1.

9. Ames Research Staff, Equations, Tables, and Charts for Compressible Flow, National Advisory Committee for Aeronautics, Report 1135, 1953.

10. Chapman, A.J., Heat Transfer, The Macmillan Company, New York, New York, 1960.

11. Tauloukian, Y.S. (Director), et al., Thermophysical Properties of Matter, Volume I, Thermal Conductivity - Metallic Elements and Alloys, The TPRC (Thermophysical Properties Research Center) Data Series, IFI/Plenum, New York, New York, 1970.

12. Beers, Y., Introduction to the Theory of Error, Addison-Wesley Publishing Company, Inc., Reading, Massachusetts, June 1962.

13. DeJarnette, F.R., Calculation of Inviscid Surface Streamlines and Heat Transfer on Shuttle Type Configurations, Part I - Description of Basic Method, National Aeronautics and Space Administration, Langley Research Center, Hampton, Virginia 23365, NASA CR-111921, (N71-36186), August 1971.

14. DeJarnette, F.R. and Jones, M.H., Calculation of Inviscid Surface Streamlines and Heat Transfer on Shuttle Type Configurations, Part II - Description of Computer Program, National Aeronautics and Space Administration, Langley Research Center, Hampton, Virginia 23365, NASA CR-111922, (N72-11828), August 1971.

15. DeJarnette, F.R., Calculation of Heat Transfer in Shuttle-Type Configurations Including the Effects of Variable Edge Entropy at Boundary Layer Edge, National Aeronautics and Space Administration, Langley Research Center, Hampton, Virginia 23365, NASA CR-112180, (N73-13958), October 1972.

16. Babish III, C.A., Aerothermodynamic Evaluation of a Section of an Enhanced Aircraft Windshield at Simulated Supersonic Flight Speeds Up to Mach 3.5, Air Force Wright Aeronautical Laboratories, Wright-Patterson Air Force Base, Ohio 45433, AFWAL-TR-84-3019, (AD B085 795L), July 1984.

17. Hartman, A.S., and Nutt, K.W., Wind Tunnel Test of Windshield Material for a Mach 3.5 Supersonic Aircraft, Arnold Engineering Development Center, Arnold Air Force Station, Tennessee 37389, AEDC-TSR-82-V17, June 1982.

18. Wilson, V.E., Design Analysis of High Temperature Transparent Windshields for High Performance Aircraft, Air Force Wright Aeronautical Laboratories, Wright-Patterson Air Force Base, Ohio 45433, AFWAL-TR-81-3126, (AD-B063 076L), November 1981.

19. Stallings, D.W., Hartman, A.S., Wind Tunnel Testing of a Windshield Material for Supersonic Aircraft, Arnold Engineering Development Center, Arnold Air Force Station, Tennessee 37389, AEDC-TSR-81-V 18, May 1981.

20. Hoffman, J.B., Evaluation of Aircraft Windshield Materials in a Simulated Supersonic Flight Environment, Air Force Wright Aeronautical Laboratories, Wright-Patterson Air Force Base, Ohio 45433, AFFDL-TR-79-3058, June 1979.

21. Carver, D.B., _Aerothermodynamic Evaluation of Windshield Materials at Simulated Flight Speeds of Mach Number 2.4 to 3.0_, Arnold Engineering Development Center, Arnold Air Force Station, Tennessee 37389, AEDC-TSR-78-V33, (AD B032 421L), October 1978.

22. Hoffman, J.B., _Evaluation of Windshield Materials Subjected to Simulated Supersonic Flight Environments_, Air Force Wright Aeronautical Laboratories, Wright-Patterson Air Force Base, Ohio 45433, AFFDL-TR-77-92, (AD-A049 981), September 1977.

23. Carver, D.B., _Aerothermodynamic Evaluation of Windshield Material in a Simulated Supersonic Flight Environment_, Arnold Engineering Development Center, Arnold Air Force Station, Tennessee 37389, AEDC-TR-77-68, (AD B019 653L), June 1977.

24. Carver, D.B., _Experimental Aerothermodynamic Evaluation of Laminated Plastic Windshield Materials at Supersonic Speeds_, Arnold Engineering Development Center, Arnold Air Force Station, Tennessee 37389, AEDC-TR-74-11, (AD-921 097L), July 1974.

25. Wylie Jr., C.R., _Advanced Engineering Mathematics_, McGraw-Hill Book Company, Inc., New York, New York, 1951.

26. Todd, C., _Computation of the Flow Around the F-16 Forebody with an Inlet Using a Three-Dimensional Euler Code (ARO-1)_, Arnold Engineering Development Center, Arnold Air Force Station, Tennessee 37389, AEDC-TR-81-27, (AD B068 119L), September 1982.

LIST OF SYMBOLS

AA thru HH, OO and PP	Temporary computer code variables
ALPD	Angle of attack, deg
ALPHA	Angle of attack, deg
AR	Amplification Ratio
CPU	Central Processor Unit
c_p	Specific heat of air at constant pressure, $\text{ft}^2/(\text{s}^2 \cdot \text{R})$
C_p	Pressure coefficient
$C_{p_{MIN}}$	Minimum pressure coefficient for supersonic flow
C_{p_S}	Pressure coefficient based on stagnation (total) pressure downstream of a normal shock wave
$C_{p_{SHADOW}}$	Pressure coefficient in the shadow region of a body
D	Thickness of the gage, in.
FLT	STAPAT input variable - indicates flight case
h	Convection heat transfer coefficient
H(.9 TO)	Heat transfer coefficient based on an adiabatic wall temperature equal to 0.9 TO, $\text{Btu}/(\text{ft}^2 \cdot \text{s} \cdot \text{R})$

LIST OF SYMBOLS (Continued)

ISMO	STAPAT input variable - forebody smoothing
k	Thermal conductivity of the gage, Btu/(ft·s·R)
KCF	STAPAT input variable - skin friction law
KODE	STAPAT input variable - atmospheric model indicator
KP	STAPAT input variable - streamline type
ℓ, L	Length of the analytic forebody, in.
M	Free-stream Mach number
MU-INF	Free-stream absolute viscosity, $lbf·s/ft^2$
M_∞	Free-stream Mach number
P	Body surface pressure
P	Local static pressure
PHI	Cross-sectional polar coordinate angle of the STAPAT model of the analytic forebody, deg
PHI	Gage circumferential angle location, deg
PINF	Free-stream static pressure
P-INF	Free-stream static pressure, psia
PO	Tunnel stagnation pressure, psia

LIST OF SYMBOLS (Continued)

P_{t_2} Total (stagnation) pressure downstream of a normal shock wave

P_∞ Free-stream static pressure

QDOT Heat transfer rate, $Btu/(ft^2 \cdot s)$

QINF Free-stream dynamic pressure

$\dot{Q}_{COND}$ Conduction heat transfer rate

$\dot{Q}_{CONV}$ Convection heat transfer rate

R Cross-sectional radial polar coordinate of the STAPAT model of the analytic forebody, in.

r, r_1 Radial distances used in describing the analytic forebody, in.

RE-INF Free-stream unit Reynolds number, ft^{-1}

RHO-INF Free-stream static density, $lbf \cdot s^2/ft^4$

ST Stanton number based on free-stream conditions

T Local static temperature

T-BF Backface (inner wall) temperature, R

TINF Free-stream static temperature

T-INF Free-stream static temperature, R

TO Tunnel stagnation temperature, R

LIST OF SYMBOLS (Concluded)

T-S   Surface (outer wall) temperature, R

T-S/TO   Ratio, T-S and TO

T-WATER   Average value of the inlet and outlet water temperatures, R

T_{AW} Adiabatic wall temperature

V-INF   Free-stream velocity, ft/s

X   Gage axial station location, in.

x, y, z   Coordinates along the X, Y and Z axes of the
X, Y, Z   analytic forebody, in.

γ Ratio of specific heats

δ Body slope angle; the angle between the free-stream
              flow direction and the tangency plane of a point
              on a body, deg

ϕ Cross-sectional polar coordinate angle of the STAPAT
              model of the analytic forebody, deg

θ Polar angle used in describing the analytic forebody, rad

Subscript

AVE   Average value of differences between backface and surface
              temperatures

NOTES: For those data reduction parameters (such as free-stream static temperature) listed in the tabulated output (see the Appendix), the symbols presented in the List of Symbols and in the equations, figures, and text of the report are the same as the nonstandard symbols (such as T-INF) used in the tabulated output. Standard and nonstandard symbols in plots from the STAPAT postprocessor were used unchanged in this report. Symbols for other parameters used in this report are presented in more conve'tional notation.

For those symbols where no units are given, any consistent set of units apply.

APPENDIX

WIND TUNNEL TEST DATA TABULATIONS

Copies of tabulations of the data from all 51 wind tunnel tests of the analytic forebody are presented in this Appendix.

MACH 3 CANOPY TEST   RUN 0654

T-INF	P-INF	RHO-INF	V-INF	ALPHA
178.92	5.63	0.2639E-02	1953.7	-0.08
deg R	psia	slug/ft³	ft/s	deg

TO	PO	MU-INF	RE-INF	T WATER
496.68	200.53	0.14390E-06	0.3582E-08	601.44
deg R	psia	lbf·s/ft²	1/ft	deg R

GAGE	X in.	PHI deg	T-BF deg R	T-S deg R	T-S/TO	QDOT Btu/ (ft²·s)	H(,9-TO) Btu/ (ft²·s·R)	ST
1	2.75	60.0	561.99	538.47	1.084	7.759	0.8484E-01	0.2132E-02
2	3.75	60.0	544.65	544.76	1.097	0.036	0.3685E-03	0.9259E-05
3	4.75	60.0	556.38	541.05	1.095	4.071	0.4196E-01	0.1054E-02
5	6.75	60.0	545.58	534.02	1.075	3.815	0.4385E-01	0.1102E-02
6	7.75	60.0	547.11	538.47	1.084	2.849	0.3115E-01	0.7828E-03
7	2.00	0.0	526.29	508.36	1.024	5.915	0.9642E-01	0.2423E-02
8	3.00	0.0	519.85	505.51	1.018	4.733	0.8092E-01	0.2034E-02
9	4.00	0.0	534.70	512.57	1.032	7.302	0.1114E+00	0.2799E-02
12	7.00	0.0	560.68	555.02	1.117	1.867	0.1728E-01	0.4343E-03
13	8.00	0.0	566.33	562.54	1.133	1.250	0.1082E-01	0.2718E-03
14	9.00	0.0	557.85	553.94	1.115	1.290	0.1206E-01	0.3031E-03
15	2.50	30.0	547.55	527.40	1.062	6.649	0.8271E-01	0.2078E-02
16	3.50	30.0	549.12	529.73	1.067	6.396	0.7732E-01	0.1943E-02
17	4.50	30.0	537.72	528.00	1.063	3.207	0.3959E-01	0.9949E-03
18	5.50	30.0	536.96	528.71	1.064	2.723	0.3333E-01	0.8376E-03
19	6.50	30.0	580.85	580.79	1.169	0.019	0.1422E-03	0.3574E-05

MACH 3 CANOPY TEST   RUN= 0655

T-INF	P-INF	RHO-INF	V-INF	ALPHA
179.29	8.42	0.3940E-02	1955.5	0.03
deg R	psia	slug/ft³	ft/s	deg

TO	PO	MU-INF	RE-INF	T WATER
497.74	300.09	0.14421E-06	0.5344E-08	600.22
deg R	psia	lbf·s/ft²	1/ft	deg R

GAGE	X in.	PHI deg	T-BF deg R	T-S deg R	T-S/TO	QDOT Btu/ (ft²·s)	H(,9-TO) Btu/ (ft²·s·R)	ST
1	2.75	60.0	553.56	524.61	1.054	9.552	0.1246E+00	0.2095E-02
2	3.75	60.0	531.88	532.03	1.069	0.049	0.5890E-03	-0.9900E-05
3	4.75	60.0	545.93	530.49	1.066	5.096	0.6174E-01	0.1038E-02
5	6.75	60.0	532.45	518.07	1.041	4.746	0.6769E-01	0.1138E-02
6	7.75	60.0	533.63	522.91	1.051	3.537	0.4718E-01	0.7931E-03
7	2.00	0.0	515.23	495.36	0.995	6.957	0.1383E+00	0.2325E-02
8	3.00	0.0	508.25	492.65	0.990	5.150	0.1153E+00	0.1938E-02
9	4.00	0.0	523.78	498.86	1.002	8.222	0.1615E+00	0.2715E-02
12	7.00	0.0	544.68	542.16	1.089	0.830	0.8887E-02	0.1494E-03
13	8.00	0.0	557.26	552.06	1.109	1.717	0.1649E-01	0.2772E-03
14	9.00	0.0	546.70	541.46	1.088	1.730	0.1850E-01	0.3109E-03
15	2.50	30.0	537.18	513.29	1.031	7.884	0.1207E+00	0.2029E-02
16	3.50	30.0	538.22	515.16	1.035	7.608	0.1132E+00	0.1903E-02
17	4.50	30.0	524.66	513.00	1.031	3.845	0.5911E-01	0.9937E-03
18	5.50	30.0	522.87	512.99	1.031	3.261	0.5015E-01	0.8430E-03
19	6.50	30.0	575.46	575.19	1.156	0.089	0.6971E-03	0.1172E-04

MACH 3 CANOPY TEST   RUN- 0656

T-INF	P-INF	RHO-INF	V-INF	ALPHA
178.97	11.25	0.5274E-02	1954.0	0.07
deg R	psia	slug/ft^3	ft/s	deg

TO	PO	MU-INF	RE-INF	T WATER
496.83	400.94	0.14394E 06	0.7152E+08	599.87
deg R	psia	lbf·s/ft	1/ft	deg R

GAGE	X in.	PHI deg	T-BF deg R	T-S deg R	T-S/TO	QDOT Btu/ (ft^2·s)	H(9 TO) Btu/ (ft·s·R)	ST
1	2.75	60.0	546.13	512.66	1.032	-11.045	0.1686E+00	0.2120E 02
2	3.75	60.0	521.09	521.24	1.049	0.047	-0.6365E-03	-0.8001E-05
3	4.75	60.0	536.99	518.90	1.044	-5.967	0.8316E-01	0.1045E-02
5	6.75	60.0	520.53	504.12	1.015	-5.413	0.9501E-01	0.1194E-02
6	7.75	60.0	521.96	509.57	1.026	-4.087	0.6548E-01	0.8231E-03
7	2.00	0.0	506.11	484.76	0.976	7.047	0.1874E+00	0.2356E-02
8	3.00	0.0	498.68	482.19	0.971	-5.442	0.1553E+00	0.1952E-02
9	4.00	0.0	514.73	487.81	0.982	8.885	0.2186E+00	0.2747E-02
12	7.00	0.0	540.50	530.97	1.069	-3.145	0.3752E-01	0.4716E-03
13	8.00	0.0	548.87	542.28	1.091	-2.175	0.2286E-01	0.2873E-03
14	9.00	0.0	537.22	530.78	1.068	2.128	0.2544E-01	0.3198E-03
15	2.50	30.0	528.37	501.47	1.009	-8.877	0.1634E+00	0.2054E-02
16	3.50	30.0	528.62	502.85	1.012	-8.506	0.1527E+00	0.1920E-02
17	4.50	30.0	514.19	500.90	1.008	-4.383	0.8154E-01	0.1025E-02
18	5.50	30.0	511.65	500.43	1.007	-3.703	0.6950E-01	0.8736E-03
19	6.50	30.0	571.21	570.67	1.149	-0.177	0.1437E-02	0.1806E-04

MACH 3 CANOPY TEST   RUN- 0657

T-INF	P-INF	RHO-INF	V-INF	ALPHA
170.80	2.80	0.1376E-02	1908.9	-0.07
deg R	psia	slug/ft^3	ft/s	deg

TO	PO	MU-INF	RE-INF	T WATER
474.16	99.83	0.13717E-06	0.1915E+08	600.83
deg R	psia	lbf·s/ft^2	1/ft	deg R

GAGE	X in.	PHI deg	T-BF deg R	T-S deg R	T-S/TO	QDOT Btu/ (ft^2·s)	H(9 TO) Btu/ (ft^2·s·R)	ST
1	2.75	60.0	572.80	555.31	1.171	5.769	0.4487E-01	0.2213E 02
2	3.75	60.0	558.30	548.47	1.157	-3.242	0.2664E-01	0.1314E-02
3	4.75	60.0	563.29	554.29	1.169	-2.969	0.2328E-01	0.1148E-02
5	6.75	60.0	555.14	548.10	1.156	-2.321	0.1913E-01	0.9435E 03
6	7.75	60.0	557.25	550.75	1.162	2.147	0.1731E-01	0.8538E 03
7	2.00	0.0	533.83	517.84	1.092	-5.277	0.5793E-01	0.2857E-02
8	3.00	0.0	528.66	515.00	1.086	-4.509	0.5109E-01	0.2520E-02
9	4.00	0.0	542.42	523.09	1.103	-6.381	0.6624E-01	0.3267E 02
12	7.00	0.0	568.24	564.81	1.191	-1.133	0.8201E-02	0.4045E 03
13	8.00	0.0	572.19	569.83	1.202	-0.779	0.5441E-02	0.2683E-03
14	9.00	0.0	565.44	562.86	1.187	-0.853	0.6267E-02	0.3091E-03
15	2.50	30.0	555.01	538.90	1.137	-5.317	0.4741E-01	0.2338E-02
16	3.50	30.0	556.59	541.31	1.142	-5.044	0.4403E-01	0.2171E-02
17	4.50	30.0	548.57	540.73	1.140	-2.587	0.2270E-01	0.1120E-02
18	5.50	30.0	548.82	542.62	1.144	-2.045	0.1764E 01	0.8702E-03
19	6.50	30.0	552.69	544.44	1.148	-2.721	0.2311E-01	0.1140E-02

MACH 3 CANOPY TEST   RUN 0658

T-INF	P-INF	RHO INF	V INF	ALPHA
170.50	5.59	0.2753E 02	1907.2	0.01
deg R	psia	slug/ft³	ft/s	deg

TO	PO	MU INF	RE INF	T WATER
473.31	199.39	0.13692E 06	0.483.E-08	600.74
deg R	psia	lbf·s/ft²	1/ft	deg R

GAGE	X in.	PHI deg	T BF deg R	T-S deg P	T-S/TO	QDOT Btu/ (ft²·s)	H(9 TO) Btu/ (ft²·s·R)	ST
1	2.75	60.0	563.48	536.51	1.134	8.901	0.8052E 01	0.1987E 02
2	3.75	60.0	541.49	526.18	1.112	-5.053	0.5043E-01	0.1244E 02
3	4.75	60.0	548.67	534.31	1.129	-4.740	0.4375E-01	0.1079E-02
5	6.75	60.0	535.65	524.68	1.109	-3.620	0.3668E 01	0.9049E-03
6	7.75	60.0	537.88	527.73	1.115	-3.349	0.3291E 01	0.8120E 03
7	2.00	0.0	513.16	492.03	1.040	-6.974	0.1056E+00	0.2605E-02
8	3.00	0.0	506.41	488.83	1.033	-5.801	0.9230E-01	0.2277E-02
9	4.00	0.0	523.06	496.96	1.050	-8.614	0.1214E+00	0.2994E 02
12	7.00	0.0	554.14	547.70	1.157	-2.126	0.1747E-01	0.4309E-03
13	8.00	0.0	560.70	556.39	1.176	-1.423	0.1091E-01	0.2692E 03
14	9.00	0.0	550.78	546.08	1.154	-1.549	0.1290E-01	0.3182E-03
15	2.50	30.0	538.53	514.68	1.087	-7.872	0.8875E-01	0.2190E-02
16	3.50	30.0	539.82	517.33	1.093	-7.421	0.8123E-01	0.2004E-02
17	4.50	30.0	527.53	516.02	1.090	-3.797	0.4217E-01	0.1040E-02
18	5.50	30.0	526.92	517.55	1.093	-3.091	0.3375E-01	0.8327E-03
19	6.50	30.0	532.59	519.84	1.098	-4.207	0.4482E-01	0.1106E-02

MACH 3 CANOPY TEST   RUN= 0659

T INF	P-INF	RHO INF	V INF	ALPHA
171.17	8.41	0.4123E 02	1911.0	0.06
deg	psia	slug/ft³	ft/s	deg

TO	PO	MU INF	RE INF	T WATER
475.18	299.76	0.13748E 06	0.5731E+08	600.87
deg R	psia	lbf·s/ft²	1/ft	deg P

GAGE	X in.	PHI deg	T BF deg R	T S deg P	T S/TO	QDOT Btu/ (ft²·s)	H(9 TO) Btu/ (ft²·s·R)	ST
1	2.75	60.0	555.70	522.49	1.100	-10.960	0.1156E+00	0.1901E 02
2	3.75	60.0	531.09	512.10	1.078	-6.266	0.7420E-01	0.1220E 02
3	4.75	60.0	539.30	521.25	1.097	-5.955	0.6363E-01	0.1046E 02
5	6.75	60.0	523.00	509.54	1.072	-4.442	0.5425E-01	0.8919E 03
6	7.75	60.0	524.85	512.42	1.078	-4.103	0.4841E 01	0.7959E-03
7	2.00	0.0	502.89	479.48	1.009	-7.725	0.1491E+00	0.2451E-02
8	3.00	0.0	495.41	476.48	1.003	-6.250	0.1281E+00	0.2106E-02
9	4.00	0.0	512.92	483.74	1.018	-9.629	0.1717E+00	0.2823E 02
12	7.00	0.0	544.38	535.59	1.127	-2.900	0.2687E 01	0.4419E-03
13	8.00	0.0	552.64	546.78	1.151	-1.935	0.1625E-01	0.2672E-03
14	9.00	0.0	540.57	534.39	1.125	-2.040	0.1911E-01	0.3143E-03
15	2.50	30.0	528.97	500.80	1.054	-9.298	0.1271E+00	0.2090E 02
16	3.50	30.0	529.67	502.95	1.058	-8.816	0.1171E+00	0.1925E-02
17	4.50	30.0	514.87	501.09	1.055	-4.549	0.6196E 01	0.1019E-02
18	5.50	30.0	513.23	501.94	1.056	-3.728	0.5019E-01	0.8253E-03
19	6.50	30.0	521.72	504.43	1.062	-5.706	0.7432E-01	0.1222E-02

88

MACH 3 CANOPY TEST   RUN= 0660

T-INF	P-INF	RHO-INF	V-INF	ALPHA
172.00	11.21	0.5471E 02	1915 6	0.08
deg R	psia	slug/ft^3	ft/s	deg

TO	PO	MU-INF	RE INF	T WATER
477.49	399.72	0.13817E 06	0.7585E+08	600.30
deg R	psia	lbf·s/ft^2	1/ft	deg R

GAGE	X in.	PHI deg	T BF deg R	T-S deg R	T-S/TO	QDOT Btu/ (ft^2·s)	H(.9 TO) Btu/ (ft^2·s·R)	ST
1	2.75	60.0	549.28	511.37	1.071	12.510	0.1533E+00	0.1894E-02
2	3.75	60.0	521.89	500.19	1.048	-7.161	0.1017E+00	0.1256E-02
3	4.75	60.0	530.70	510.02	1.068	-6.822	0.8498E-01	0.1050E-02
5	6.75	60.0	512.87	497.48	1.042	5.079	0.7499E-01	0.9269E-03
6	7.75	60.0	514.03	499.80	1.047	4.697	0.6705E-01	0.8288E-03
7	2.00	0.0	494.79	469.99	0.984	-8.186	0.2034E+00	0.2514E-02
8	3.00	0.0	486.98	467.26	0.979	-6.508	0.1735E+00	0.2144E-02
9	4.00	0.0	504.76	473.66	0.992	-10.261	0.2337E+00	0.2888E-02
12	7.00	0.0	534.86	523.86	1.097	-3.631	0.3858E-01	0.4769E-03
13	8.00	0.0	544.42	537.14	1.125	-2.401	0.2235E-01	0.2763E-03
14	9.00	0.0	531.11	523.69	1.097	-2.447	0.2605E-01	0.3219E-03
15	2.50	30.0	520.82	489.49	1.025	-10.340	0.1731E+00	0.2139E-02
16	3.50	30.0	520.71	491.15	1.029	-9.754	0.1589E+00	0.1964E-02
17	4.50	30.0	504.42	489.09	1.024	-5.059	0.8526E-01	0.1054E-02
18	5.50	30.0	501.96	489.41	1.025	4.143	0.6944E-01	0.8583E-03
19	6.50	30.0	509.44	491.72	1.030	5.848	0.9437E-01	0.1166E-02

MACH 3 CANOPY TEST   RUN= 0661

T-INF	P-INF	RHO-INF	V INF	ALPHA
168.71	2.80	0.1394E-02	1897.2	3.08
deg R	psia	slug/ft^3	ft/s	deg

TO	PO	MU-INF	RE INF	T-WATER
468.35	99.91	0.13543E-06	0.1953E+08	600.41
deg R	psia	lbf·s/ft^2	1/ft	deg R

GAGE	X in.	PHI deg	T-BF deg R	T-S deg R	T-S/TO	QDOT Btu/ (ft^2·s)	H(.9 TO) Btu/ (ft^2·s·R)	ST
1	2.75	60.0	566.05	547.55	1.169	-6.106	0.4844E-01	0.2373E 02
2	3.75	60.0	555.69	545.23	1.164	-3.453	0.2791E-01	0.1367E-02
3	4.75	60.0	560.74	551.08	1.177	3.188	0.2461E-01	0.1205E-02
5	6.75	60.0	552.48	544.95	1.164	-2.486	0.2014E-01	0.9864E-03
6	7.75	60.0	554.32	547.30	1.169	-2.318	0.1841E-01	0.9018E-03
7	2.00	0.0	528.82	511.66	1.092	-5.663	0.6282E-01	0.3077E-02
8	3.00	0.0	523.68	509.24	1.087	-4.767	0.5434E-01	0.2661E-02
9	4.00	0.0	537.85	517.07	1.104	-6.857	0.7176E-01	0.3514E-02
12	7.00	0.0	564.13	559.75	1.195	-1.446	0.1046E-01	0.5124E-03
13	8.00	0.0	568.97	566.07	1.209	-0.958	0.6631E-02	0.3248E-03
14	9.00	0.0	563.16	560.34	1.196	-0.930	0.6699E-02	0.3281E-03
15	2.50	30.0	551.81	534.53	1.141	-5.702	0.5045E-01	0.2471E-02
16	3.50	30.0	553.53	537.31	1.147	-5.353	0.4623E-01	0.2264E-02
17	4.50	30.0	545.04	536.82	1.146	2.710	0.2351E-01	0.1151E-02
18	5.50	30.0	544.56	537.87	1.148	-2.208	0.1897E-01	0.9291E-03
19	6.50	30.0	551.50	540.85	1.155	3.516	0.2946E-01	0.1443E-02

MACH 3 CANOPY TEST   RUN   0662

T-INF	P INF	RHO INF	V INF	ALPHA
169.89	5.60	0.2768E-02	1903.8	3.00
deg R	psia	slug/ft³	ft/s	deg

TO	PO	MU INF	RE INF	T WATER
471.63	199.79	0.13641E 06	0.3864E+08	600.34
deg R	psia	lbf·s/ft²	1/ft	deg

GAGE	X in.	PHI deg	T-BF deg R	T S deg R	T S/TO	QDOT Btu/ (ft²·s)	H(9 TO) Btu/ (ft²·s·R)	ST
1	2.75	60.0	556.76	529.32	1.122	9.057	0.8638E 01	0.2123E 02
2	3.75	60.0	539.36	523.54	1.110	5.221	0.5270E 01	0.1295E 02
3	4.75	60.0	546.26	531.40	1.127	4.903	0.4586E-01	0.1127E 02
5	6.75	60.0	533.64	522.39	1.108	3.714	0.3763E 01	0.9323E 03
6	7.75	60.0	535.25	524.71	1.113	3.477	0.3468E 01	0.8524E 03
7	2.00	0.0	509.75	488.06	1.035	7.156	0.1125E+00	0.2765E 02
8	3.00	0.0	503.25	485.50	1.029	5.856	0.9595E-01	0.2358E 02
9	4.00	0.0	519.72	492.99	1.045	-8.821	0.1287E+00	0.3164E 02
12	7.00	0.0	549.25	541.54	1.148	-2.544	0.2173E 01	0.5341E 03
13	8.00	0.0	556.80	551.81	1.170	-1.645	0.1291E 01	0.3174E 03
14	9.00	0.0	548.93	544.13	1.154	1.586	0.1326E-01	0.3258E 03
15	2.50	30.0	535.85	511.27	1.084	8.110	0.9343E-01	0.2296E 02
16	3.50	30.0	536.98	514.01	1.090	7.580	0.8465E-01	0.2081E 02
17	4.50	30.0	524.57	512.77	1.087	-3.894	0.4410E-01	0.1084E 02
18	5.50	30.0	523.13	513.39	1.089	3.214	0.3614E-01	0.8883E 03
19	6.50	30.0	532.32	516.74	1.096	-5.142	0.5573E-01	0.1370E 02

MACH 3 CANOPY TEST   RUN= 0663

T INF	P INF	RHO-INF	V INF	ALPHA
169.12	2.81	0.1393E 02	1899.5	2.91
deg R	psia	slug/ft³	ft/s	deg

TO	PO	MU-INF	RE INF	T WATER
469.50	100.04	0.13577E-06	0.1948E·08	600.96
deg R	psia	lbf·s/ft²	1 ft	deg R

GAGE	X in.	PHI deg	T-BF deg R	T-S deg R	T S/TO	QDOT Btu/ (ft²·s)	H(9 TO) Btu/ (ft²·s·P)	ST
1	2.75	60.0	567.82	550.17	1.172	5.823	0.4562E 01	0.2234E 02
2	3.75	60.0	557.94	548.16	1.168	-3.226	0.2568E 01	0.1258E 02
3	4.75	60.0	563.35	554.54	1.181	2.905	0.2201E-01	0.1078E-02
5	6.75	60.0	555.79	548.97	1.169	2.249	0.1779E-01	0.8715E 03
6	7.75	60.0	558.07	551.77	1.175	2.078	0.1608E-01	0.7876E-03
7	2.00	0.0	533.99	518.09	1.103	-5.246	0.5491E 01	0.2689E-02
8	3.00	0.0	528.51	514.96	1.097	4.474	0.4841E 01	0.2371E-02
9	4.00	0.0	542.20	523.26	1.114	6.251	0.6207E 01	0.3040E 02
12	7.00	0.0	569.91	567.24	1.208	0.881	0.6085E-02	0.2980E-03
13	8.00	0.0	572.74	570.42	1.217	0.766	0.5180E 02	0.2537E-03
14	9.00	0.0	564.72	561.57	1.196	-1.039	0.7473E 02	0.3660E-03
15	2.50	30.0	554.81	538.57	1.147	-5.357	0.4617E-01	0.2261E-02
16	3.50	30.0	556.27	540.82	1.152	-5.097	0.4309E-01	0.2110E-02
17	4.50	30.0	548.33	540.49	1.151	-2.586	0.2192E-01	0.1074E-02
18	5.50	30.0	548.91	542.62	1.156	-2.076	0.1729E-01	0.8468E-03
19	6.50	30.0	552.39	545.50	1.162	-2.275	0.1850E 01	0.9061E-03

MACH 3 CANOPY TEST   RUN= 0664

T-INF	P-INF	RHO INF	V INF	ALPHA
170.75	5.61	0.2757E-02	1908.6	2.95
deg R	psia	slug/ft^3	ft/s	deg

TO	PO	MU INF	RE INF	T WATER
474.00	199.96	0.13712E 06	0.3837E+08	600.79
deg R	psia	lbf·s/ft^2	1/ft	deg R

GAGE	X in.	PHI deg	T BF deg R	T-S deg R	T S/TO	QDOT Btu/ (ft^2·s)	H(.9 TO) Btu/ (ft^2·s·R)	ST
1	2.75	60.0	558.13	531.64	1.122	-8.741	0.8322E-01	0.2049E 02
2	3.75	60.0	542.22	527.29	1.112	4.927	0.4893E-01	0.1205E-02
3	4.75	60.0	549.34	535.53	1.130	-4.560	0.4186E-01	0.1031E-02
5	6.75	60.0	537.48	526.95	1.112	-3.477	0.3465E-01	0.8531E-03
6	7.75	60.0	539.89	530.19	1.119	3.202	0.3091E-01	0.7610E-03
7	2.00	0.0	514.87	494.13	1.042	6.846	0.1014E+00	0.2496E-02
8	3.00	0.0	508.18	490.98	1.036	5.675	0.8814E-01	0.2170E-02
9	4.00	0.0	524.89	499.50	1.054	-8.379	0.1150E+00	0.2830E-02
12	7.00	0.0	557.09	551.74	1.164	-1.766	0.1411E-01	0.3473E-03
13	8.00	0.0	562.35	558.39	1.178	-1.307	0.9918E-02	0.2442E-03
14	9.00	0.0	550.27	544.93	1.150	-1.763	0.1490E-01	0.3668E-03
15	2.50	30.0	539.55	516.21	1.089	7.702	0.8595E-01	0.2116E-02
16	3.50	30.0	540.44	518.30	1.093	-7.305	0.7966E-01	0.1961E-02
17	4.50	30.0	528.64	517.30	1.091	-3.743	0.4127E-01	0.1016E-02
18	5.50	30.0	528.29	519.12	1.095	-3.027	0.3272E-01	0.8055E-03
19	6.50	30.0	534.27	522.21	1.102	3.982	0.4165E-01	0.1025E-02

MACH 3 CANOPY TEST   RUN= 0665

T-INF	P-INF	RHO-INF	V-INF	ALPHA
177.45	2.80	0.1325E 02	1945.7	0.05
deg R	psia	slug/ft^3	ft/s	deg

TO	PO	MU-INF	RE-INF	T-WATER
492.61	99.86	0.14269E-06	0.1807E+08	610.31
deg R	psia	lbf·s/ft^2	1/ft	deg R

GAGE	X in.	PHI deg	T BF deg R	T-S deg R	T S/TO	QDOT Btu/ (ft^2·s)	H(.9 TO) Btu/ (ft^2·s·R)	ST
1	2.75	60.0	586.57	569.39	1.156	-5.667	0.4496E 01	0.2260E-02
2	3.75	60.0	578.75	569.13	1.155	-3.176	0.2525E-01	0.1269E-02
3	4.75	60.0	583.23	574.29	1.166	-2.950	0.2253E-01	0.1132E-02
5	6.75	60.0	576.43	569.76	1.157	-2.200	0.1741E-01	0.8747E-03
6	7.75	60.0	578.10	571.66	1.160	-2.127	0.1658E-01	0.8331E-03
7	2.00	0.0	553.78	537.82	1.092	-5.269	0.5578E-01	0.2803E-02
8	3.00	0.0	548.66	535.00	1.086	-4.509	0.4920E-01	0.2472E-02
9	4.00	0.0	562.36	543.16	1.103	-6.335	0.6347E-01	0.3189E-02
12	7.00	0.0	588.48	585.18	1.188	-1.091	0.7691E-02	0.3865E-03
13	8.00	0.0	592.15	589.89	1.197	0.746	0.5090E-02	0.2558E-03
14	9.00	0.0	585.86	583.17	1.184	-0.891	0.6368E-02	0.3200E-03
15	2.50	30.0	574.89	559.00	1.135	-5.246	0.4536E-01	0.2279E-02
16	3.50	30.0	577.41	562.13	1.141	-5.044	0.4247E-01	0.2134E-02
17	4.50	30.0	569.10	561.38	1.140	-2.549	0.2159E-01	0.1085E-02
18	5.50	30.0	569.49	563.34	1.144	-2.032	0.1694E-01	0.8510E-03
19	6.50	30.0	573.75	565.84	1.149	-2.611	0.2132E-01	0.1071E-02

MACH 3 CANOPY TEST   RUN - 0666

T-INF	P-INF	RHO-INF	V-INF	ALPHA
178.28	5.59	0.2633E-02	1950.2	-0.03
deg R	psia	slug/ft^3	ft/s	deg

TO	PO	MU-INF	RE-INF	T WATER
494.91	199.40	0.14337E-06	0.3582E-08	610.51
deg R	psia	lbf·s/ft^2	1/ft	deg R

GAGE	X in.	PHI deg	T-BF deg R	T-S deg R	T-S/TO	QDOT Btu/(ft^2·s)	H(.9 TO) Btu/(ft^2·s·R)	ST
1	2.75	60.0	579.64	553.52	1.118	8.620	0.7975E-01	0.2012E-02
2	3.75	60.0	563.50	548.58	1.108	-4.924	0.4774E-01	0.1204E-02
3	4.75	60.0	570.00	555.94	1.123	4.641	0.4199E-01	0.1059E-02
5	6.75	60.0	558.82	548.47	1.108	3.416	0.3315E-01	0.8363E-03
6	7.75	60.0	560.49	550.61	1.113	-3.263	0.3102E-01	0.7825E-03
7	2.00	0.0	534.69	513.89	1.038	-6.864	0.1003E+00	0.2529E-02
8	3.00	0.0	528.18	510.87	1.032	-5.710	0.8723E-01	0.2201E-02
9	4.00	0.0	544.85	519.21	1.049	-8.460	0.1146E+00	0.2892E-02
12	7.00	0.0	575.37	569.14	1.150	-2.058	0.1663E-01	0.4196E-03
13	8.00	0.0	581.49	577.39	1.167	-1.354	0.1026E-01	0.2587E-03
14	9.00	0.0	572.34	567.65	1.147	1.549	0.1267E-01	0.3197E-03
15	2.50	30.0	559.65	536.47	1.084	-7.650	0.8402E-01	0.2120E-02
16	3.50	30.0	562.00	539.83	1.091	7.316	0.7749E-01	0.1955E-02
17	4.50	30.0	549.60	538.31	1.088	-3.724	0.4009E-01	0.1011E-02
18	5.50	30.0	549.24	539.98	1.091	-3.058	0.3234E-01	0.8158E-03
19	6.50	30.0	555.14	543.09	1.097	-3.977	0.4072E-01	0.1027E-02

MACH 3 CANOPY TEST   RUN= 0667

T-INF	P-INF	RHO-INF	V-INF	ALPHA
176.97	2.79	0.1322E-02	1943.1	3.97
deg R	psia	slug/ft^3	ft/s	deg

TO	PO	MU-INF	RE-INF	T WATER
491.28	99.40	0.14229E-06	0.1806E+08	610.67
deg R	psia	lbf·s/ft^2	1/ft	deg R

GAGE	X in.	PHI deg	T-BF deg R	T-S deg R	T-S/TO	QDOT Btu/(ft^2·s)	H(.9 TO) Btu/(ft^2·s·R)	ST
1	2.75	60.0	586.87	570.10	1.160	-5.537	0.4328E-01	0.2182E-02
2	3.75	60.0	579.75	570.51	1.161	-3.048	0.2375E-01	0.1197E-02
3	4.75	60.0	584.42	575.81	1.172	-2.841	0.2126E-01	0.1072E-02
5	6.75	60.0	578.00	571.70	1.164	-2.078	0.1604E-01	0.8086E-03
6	7.75	60.0	579.85	573.80	1.168	1.998	0.1518E-01	0.7651E-03
7	2.00	0.0	556.45	541.13	1.101	-5.055	0.5108E-01	0.2575E-02
8	3.00	0.0	551.17	538.02	1.095	-4.338	0.4525E-01	0.2281E-02
9	4.00	0.0	564.78	546.58	1.113	-6.006	0.5752E-01	0.2900E-02
12	7.00	0.0	591.50	589.23	1.199	-0.750	0.5100E-02	0.2571E-03
13	8.00	0.0	593.56	591.42	1.204	-0.706	0.4731E-02	0.2385E-03
14	9.00	0.0	585.89	582.92	1.187	-0.979	0.6958E-02	0.3508E-03
15	2.50	30.0	576.28	560.85	1.142	-5.092	0.4290E-01	0.2163E-02
16	3.50	30.0	578.49	563.40	1.147	-4.980	0.4107E-01	0.2071E-02
17	4.50	30.0	570.38	562.82	1.146	-2.494	0.2067E-01	0.1042E-02
18	5.50	30.0	571.26	565.24	1.151	-1.985	0.1613E-01	0.8131E-03
19	6.50	30.0	575.86	568.60	1.157	-2.395	0.1894E-01	0.9550E-03

MACH 3 CANOPY TEST   RUN= 0668

T-INF	P-INF	RHO-INF	V-INF	ALPHA
177.56	5.59	0.2641E-02	1946.3	3.91
deg R	psia	slug/ft^3	ft/s	deg

TO	PO	MU-INF	RE INF	T WATER
492.93	199.22	0.14278E-06	0.3600E+08	610.70
deg R	psia	lbf·s/ft^2	1/ft	deg R

GAGE	X in.	PHI deg	T-BF deg R	T-S deg R	T-S/TO	QDOT Btu/(ft^2·s)	H(.9 TO) Btu/(ft^2·s·R)	ST
1	2.75	60.0	579.35	553.42	1.123	-8.557	0.7795E-01	0.1964E-02
2	3.75	60.0	564.29	549.60	1.115	-4.847	0.4574E-01	0.1153E-02
3	4.75	60.0	570.58	556.75	1.129	-4.562	0.4033E-01	0.1016E-02
5	6.75	60.0	559.81	549.66	1.115	-3.350	0.3159E-01	0.7961E-03
6	7.75	60.0	562.10	552.58	1.121	-3.143	0.2885E-01	0.7271E-03
7	2.00	0.0	536.32	515.69	1.046	-6.806	0.9446E-01	0.2380E-02
8	3.00	0.0	529.54	512.38	1.039	-5.663	0.8238E-01	0.2076E-02
9	4.00	0.0	546.55	521.53	1.058	-8.255	0.1060E+00	0.2670E-02
12	7.00	0.0	579.30	574.42	1.165	-1.609	0.1230E-01	0.3101E-03
13	8.00	0.0	583.64	579.89	1.176	-1.237	0.9083E-02	0.2289E-03
14	9.00	0.0	571.66	566.44	1.149	-1.722	0.1402E-01	0.3533E-03
15	2.50	30.0	560.68	537.78	1.091	-7.558	0.8028E-01	0.2023E-02
16	3.50	30.0	562.61	540.47	1.096	-7.307	0.7546E-01	0.1901E-02
17	4.50	30.0	550.45	539.23	1.094	-3.701	0.3872E-01	0.9757E-03
18	5.50	30.0	550.88	541.84	1.099	2.982	0.3037E-01	0.7652E-03
19	6.50	30.0	557.18	545.80	1.107	-3.755	0.3676E-01	0.9263E-03

MACH 3 CANOPY TEST   RUN= 0669

T-INF	P-INF	RHO-INF	V-INF	ALPHA
176.35	2.80	0.1331E-02	1939.7	4.05
deg R	psia	slug/ft^3	ft/s	deg

TO	PO	MU-INF	RE INF	T WATER
489.56	99.73	0.14178E-06	0.1821E+08	610.74
deg R	psia	lbf·s/ft^2	1/ft	deg R

GAGE	X in.	PHI deg	T-BF deg R	T-S deg R	T-S/TO	QDOT Btu/(ft^2·s)	H(.9 TO) Btu/(ft^2·s·R)	ST
1	2.75	60.0	587.30	569.29	1.163	-5.945	0.4620E-01	0.2318E-02
2	3.75	60.0	578.61	568.22	1.161	-3.430	0.2688E-01	0.1348E-02
3	4.75	60.0	582.49	572.94	1.170	-3.150	0.2380E-01	0.1194E-02
5	6.75	60.0	575.32	568.18	1.161	-2.357	0.1848E-01	0.9271E-03
6	7.75	60.0	576.87	569.90	1.164	-2.300	0.1779E-01	0.8925E-03
7	2.00	0.0	550.81	533.60	1.090	-5.682	0.6110E-01	0.3065E-02
8	3.00	0.0	545.88	531.43	1.086	-4.769	0.5251E-01	0.2634E-02
9	4.00	0.0	559.93	539.28	1.102	-6.814	0.6905E-01	0.3464E-02
12	7.00	0.0	585.96	581.49	1.188	-1.477	0.1049E-01	0.5260E-03
13	8.00	0.0	590.59	587.71	1.200	-0.949	0.6449E-02	0.3235E-03
14	9.00	0.0	585.32	582.36	1.190	0.977	0.6893E-02	0.3458E-03
15	2.50	30.0	573.70	556.56	1.137	-5.654	0.4876E-01	0.2446E-02
16	3.50	30.0	576.41	560.13	1.144	5.373	0.4496E-01	0.2255E-02
17	4.50	30.0	567.66	559.55	1.143	2.675	0.2249E-01	0.1128E-02
18	5.50	30.0	567.42	560.74	1.145	-2.204	0.1834E-01	0.9201E-03
19	6.50	30.0	572.65	564.22	1.153	-2.780	0.2249E-01	0.1128E-02

93

MACH 3 CANOPY TEST   RUN= 0670

T-INF	P-INF	RHO INF	V INF	ALPHA
176.73	5.60	0.2658E-02	1941.7	-4.00
deg R	psia	slug/ft³	ft/s	deg

TO	PO	MU-INF	RE INF	T WATER
490.61	199.55	0.14209E-06	0.3632E-08	610.50
deg R	psia	lbf·s/ft²	1/ft	deg R

GAGE	X	PHI	T BF	T S	T-S/TO	QDOT	H(θ TO)	ST
	in.	deg	deg R	deg R		Btu/	Btu/	
						(ft²·s)	(ft²·s·R)	
1	2.75	60.0	574.61	547.15	1.115	-9.062	0.8581E-01	0.2154E 02
2	3.75	60.0	561.89	545.99	1.113	-5.247	0.5024E-01	0.1261E 02
3	4.75	60.0	568.00	553.06	1.127	4.933	0.4424E-01	0.1110E 02
5	6.75	60.0	556.06	545.07	1.111	-3.627	0.3504E-01	0.8793E 03
6	7.75	60.0	557.48	546.92	1.115	-3.486	0.3308E-01	0.8303E-03
7	2.00	0.0	530.77	508.71	1.037	-7.278	0.1084E+00	0.2720E 02
8	3.00	0.0	524.47	506.42	1.032	-5.957	0.9184E-01	0.2305E 02
9	4.00	0.0	541.35	514.27	1.048	-8.936	0.1229E-00	0.3084E 02
12	7.00	0.0	570.26	562.28	1.146	-2.635	0.2183E-01	0.5478E-03
13	8.00	0.0	577.61	572.51	1.167	1.686	0.1287E-01	0.3230E 03
14	9.00	0.0	570.24	565.32	1.152	-1.623	0.1311E-01	0.3291E-03
15	2.50	30.0	557.02	532.46	1.085	-8.106	0.8916E-01	0.2238E-02
16	3.50	30.0	559.47	536.06	1.093	-7.725	0.8174E-01	0.2051E-02
17	4.50	30.0	546.46	534.67	1.090	3.891	0.4178E-01	0.1049E-02
18	5.50	30.0	545.14	535.32	1.091	-3.242	0.3457E-01	0.8676E-03
19	6.50	30.0	552.30	539.73	1.100	-4.149	0.4226E-01	0.1061E-02

MACH 3 CANOPY TEST   RUN= 0671

T-INF	P-INF	RHO-INF	V INF	ALPHA
175.68	2.82	0.1348E-02	1936.0	3.03
deg R	psia	slug/ft³	ft/s	deg

TO	PO	MU-INF	RE INF	T WATER
487.71	100.57	0.14123E-06	0.1847E-08	610.71
deg R	psia	lbf·s/ft²	1/ft	deg P

GAGE	X	PHI	T BF	T S	T S/TO	QDOT	H(θ TO)	ST
	in.	deg	deg R	deg R		Btu/	Btu/	
						(ft²·s)	(ft²·s·R)	
1	2.75	60.0	584.46	566.13	1.161	-6.049	0.4756E-01	0.2361E 02
2	3.75	60.0	577.25	566.79	1.162	-3.452	0.2700E-01	0.1341E 02
3	4.75	60.0	581.49	571.85	1.173	-3.181	0.2393E-01	0.1188E-02
5	6.75	60.0	574.12	566.91	1.162	2.378	0.1858E-01	0.9224E 03
6	7.75	60.0	575.73	568.73	1.166	-2.310	0.1780E-01	0.8837E-03
7	2.00	0.0	549.68	532.42	1.092	-5.697	0.6095E-01	0.3026E-02
8	3.00	0.0	544.70	530.19	1.087	-4.789	0.5248E-01	0.2606E-02
9	4.00	0.0	559.00	538.25	1.104	-6.848	0.6897E-01	0.3424E 02
12	7.00	0.0	585.48	581.18	1.192	-1.419	0.9974E-02	0.4952E 03
13	8.00	0.0	589.95	587.17	1.204	-0.919	0.6198E-02	0.3077E 03
14	9.00	0.0	584.17	581.28	1.192	0.951	0.6682E-02	0.3317E-03
15	2.50	30.0	572.64	555.45	1.139	-5.673	0.4869E-01	0.2418E-02
16	3.50	30.0	575.21	558.80	1.146	5.413	0.4516E-01	0.2242E-02
17	4.50	30.0	566.33	558.11	1.144	-2.711	0.2275E-01	0.1130E-02
18	5.50	30.0	566.20	559.54	1.147	2.197	0.1822E-01	0.9046E-03
19	6.50	30.0	571.25	562.68	1.154	2.828	0.2285E-01	0.1135E 02

MACH 3 CANOPY TEST   RUN   0672

T INF	P INF	RHO-INF	V-INF	ALPHA
176.34	5.61	0.2669E 02	1939.6	3.06
deg R	psia	slug/ft³	ft/s	deg

TO	PO	MU INF	RE INF	T WATER
489.54	199.92	0.14177E 06	0.3651E-08	610.35
deg R	psia	lbf·s/ft²	1/ft	deg R

GAGE	X in.	PHI deg	T-BF deg R	T-S deg R	T S/TO	QDOT Btu/ (ft²·s)	H(.9 TO) Btu/ (ft²·s·R)	ST
1	2.75	60.0	573.41	545.96	1.115	9.057	0.8595E-01	0.2151E-02
2	3.75	60.0	560.34	544.54	1.112	-5.213	0.5015E-01	0.1255E-02
3	4.75	60.0	566.54	551.74	1.127	-4.885	0.4395E-01	0.1100E-02
5	6.75	60.0	554.82	543.90	1.111	-3.602	0.3487E-01	0.8725E-03
6	7.75	60.0	556.26	545.81	1.115	-3.449	0.3277E-01	0.8201E-03
7	2.00	0.0	529.70	507.75	1.037	7.246	0.1079E+00	0.2700E-02
8	3.00	0.0	523.30	505.29	1.032	-5.942	0.9184E-01	0.2298E-02
9	4.00	0.0	540.30	513.32	1.049	8.903	0.1224E+00	0.3064E-02
12	7.00	0.0	569.82	562.22	1.148	-2.509	0.2063E-01	0.5163E-03
13	8.00	0.0	576.96	572.15	1.169	-1.585	0.1205E-01	0.3016E-03
14	9.00	0.0	568.76	564.07	1.152	-1.547	0.1253E-01	0.3135E-03
15	2.50	30.0	555.80	531.28	1.085	-8.093	0.8924E-01	0.2233E-02
16	3.50	30.0	558.06	534.63	1.092	-7.731	0.8221E-01	0.2057E-02
17	4.50	30.0	544.76	532.91	1.089	-3.912	0.4238E-01	0.1060E-02
18	5.50	30.0	543.53	533.71	1.090	-3.242	0.3481E-01	0.8710E-03
19	6.50	30.0	550.31	537.39	1.098	4.262	0.4403E-01	0.1102E-02

MACH 3 CANOPY TEST   RUN= 0673

T INF	P-INF	RHO-INF	V INF	ALPHA
175.37	2.77	0.1326E 02	1934.2	3.00
deg R	psia	slug/ft³	ft/s	deg

TO	PO	MU-INF	RE-INF	T WATER
486.83	98.80	0.14097E 06	0.1820E+08	610.59
deg R	psia	lbf·s/ft²	1/ft	deg R

GAGE	X in.	PHI deg	T-BF deg R	T-S deg	T S/TO	QDOT Btu/ (ft²·s)	H(.9 TO) Btu/ (ft²·s·R)	ST
1	2.75	60.0	585.30	567.91	1.167	5.741	0.4424E-01	0.2234E-02
2	3.75	60.0	578.98	569.27	1.169	-3.206	0.2445E-01	0.1235E-02
3	4.75	60.0	583.43	574.42	1.180	2.973	0.2182E-01	0.1102E-02
5	6.75	60.0	576.77	570.23	1.171	-2.157	0.1633E-01	0.8247E-03
6	7.75	60.0	578.79	572.52	1.176	-2.067	0.1539E-01	0.7769E-03
7	2.00	0.0	554.24	538.28	1.106	-5.267	0.5260E-01	0.2656E-02
8	3.00	0.0	548.62	534.95	1.099	-4.509	0.4658E-01	0.2352E-02
9	4.00	0.0	562.70	543.75	1.117	-6.255	0.5923E 01	0.2991E-02
12	7.00	0.0	590.50	587.97	1.208	-0.835	0.5575E-02	0.2815E-03
13	8.00	0.0	592.94	590.75	1.213	-0.722	0.4730E 02	0.2388E-03
14	9.00	0.0	585.22	582.15	1.196	-1.012	0.7029E 02	0.3549E-03
15	2.50	30.0	574.87	558.78	1.148	-5.310	0.4402E-01	0.2223E-02
16	3.50	30.0	577.05	561.62	1.154	-5.091	0.4123E-01	0.2082E-02
17	4.50	30.0	568.96	561.19	1.153	-2.564	0.2084E-01	0.1052E-02
18	5.50	30.0	569.84	563.51	1.158	-2.087	0.1665E-01	0.8406E-03
19	6.50	30.0	574.62	567.02	1.165	-2.509	0.1947E-01	0.9832E-03

MACH 3 CANOPY TEST   RUN   0674

	T INF	P INF	RHO INF	V INF	ALPHA
	176.27	5.60	0.2666E 02	1939.2	2.97
	deg R	psia	slug/ft^3	ft/s	deg

	TO	PO	MU INF	RE INF	T WATER
	489.35	199.64	0.14172E 06	0.3648E 08	610.58
	deg R	psia	lbf·s/ft^2	1/ft	deg R

GAGE	X in.	PHI deg	T BF deg R	T S deg R	T S/TO	QDOT Btu/ (ft^2·s)	H(.9 TO) Btu/ (ft^2·s·R)	ST
1	2.75	60.0	575.76	548.98	1.122	8.836	0.8139E-01	0.2039E 02
2	3.75	60.0	563.48	548.23	1.120	5.034	0.4670E-01	0.1170E 02
3	4.75	60.0	570.06	555.71	1.136	4.736	0.4108E-01	0.1029E 02
5	6.75	60.0	558.66	548.15	1.120	3.467	0.3219E-01	0.8064E 03
6	7.75	60.0	561.01	551.15	1.126	3.254	0.2939E-01	0.7362E-03
7	2.00	0.0	534.41	513.18	1.049	7.007	0.9629E-01	0.2412E 02
8	3.00	0.0	527.39	509.74	1.042	5.827	0.8406E-01	0.2106E-02
9	4.00	0.0	544.61	518.93	1.060	-8.473	0.1079E+00	0.2704E-02
12	7.00	0.0	578.10	572.80	1.171	1.750	0.1322E-01	0.3311E 03
13	8.00	0.0	582.99	579.06	1.183	-1.295	0.9342E-02	0.2341E 03
14	9.00	0.0	571.19	565.93	1.157	-1.73C	0.1383E-01	0.3464E 03
15	2.50	30.0	559.50	535.91	1.095	7.786	0.8153E 01	0.2043E 02
16	3.50	30.0	561.60	538.83	1.101	7.514	0.7636E-01	0.1913E 02
17	4.50	30.0	549.09	537.60	1.099	-3.790	0.3899E-01	0.9769E-03
18	5.50	30.0	549.27	539.89	1.103	3.097	0.3113E-01	0.7800E-03
19	6.50	30.0	555.65	543.82	1.111	-3.903	0.3775E 01	0.9457E 03

MACH 3 CANOPY TEST   RUN   0675

	T INF	P INF	RHO INF	V INF	ALPHA
	168.27	2.84	0.1418E 02	1894.7	0.04
	deg R	psia	slug/ft^3	ft/s	deg

	TO	PO	MU INF	RE INF	T WATER
	467.14	101.39	0.13506E 06	0.1990E 08	567.08
	deg R	psia	lbf·s/ft^2	1/ft	deg R

GAGE	X in.	PHI deg	T BF deg R	T S deg R	T S/TO	QDOT Btu/ (ft^2·s)	H(.9 TO) Btu/ (ft^2·s·R)	ST
1	2.75	60.0	551.44	534.67	1.145	5.535	0.4843E-01	0.2334E-02
2	3.75	60.0	543.31	533.84	1.143	-3.128	0.2758E-01	0.1329E 02
3	4.75	60.0	547.50	538.77	1.153	2.881	0.2434E-01	0.1173E 02
5	6.75	60.0	541.05	534.40	1.144	2.195	0.1925E-01	0.9281E-03
6	7.75	60.0	542.33	536.13	1.148	-2.043	0.1766E-01	0.8512E-03
7	2.00	0.0	519.97	504.79	1.081	-5.011	0.5941E-01	0.2863E-02
8	3.00	0.0	514.75	501.84	1.074	-4.260	0.5233E-01	0.2522E-02
9	4.00	0.0	526.93	508.63	1.089	6.040	0.6848E-01	0.3301E 02
12	7.00	0.0	534.22	533.31	1.142	-0.301	0.2669E-02	0.1286E-03
13	8.00	0.0	549.43	547.34	1.172	-0.690	0.5440E-02	0.2622E-03
14	9.00	0.0	550.10	547.31	1.172	-0.922	0.7264E-02	0.3501E-03
15	2.50	30.0	540.03	524.45	1.123	-5.140	0.4942E-01	0.2382E-02
16	3.50	30.0	540.79	526.22	1.126	-4.805	0.4542E-01	0.2189E-02
17	4.50	30.0	533.53	526.10	1.126	-2.451	0.2319E-01	0.1118E 02
18	5.50	30.0	533.86	527.80	1.130	-2.000	0.1863E-01	0.8978E-03
19	6.50	30.0	539.30	531.61	1.138	-2.540	0.2284E-01	0.1101E 02

MACH 3 CANOPY TEST   RUN= 0676

T-INF	P-INF	RHO-INF	V-INF	ALPHA
166.71	5.59	0.2812E-02	1885.9	-0.01
deg R	psia	slug/ft^3	ft/s	deg

TO	PO	MU-INF	RE-INF	T WATER
162.79	199.15	0.13375E-06	0.3965E+08	592.20
deg R	psia	lbf·s/ft^2	1/ft	deg R

GAGE	X in.	PHI deg	T-BF deg R	T-S deg R	T-S/TO	QDOT Btu/ (ft^2·s)	H(.9 TO) Btu/ (ft^2·s·R)	ST
1	2.75	60.0	539.33	513.17	1.109	8.636	0.8934E-01	0.2182E-02
2	3.75	60.0	526.03	511.15	1.104	4.911	0.5189E-01	0.1267E-02
3	4.75	60.0	531.76	517.92	1.119	-4.566	0.4503E-01	0.1100E-02
5	6.75	60.0	519.58	509.05	1.100	-3.473	0.3753E-01	0.9167E-03
6	7.75	60.0	521.2	511.66	1.106	-3.155	0.3316E-01	0.8100E-03
7	2.00	0.0	499.03	478.81	1.035	-6.673	0.1071E+00	0.2616E-02
8	3.00	0.0	492.06	475.53	1.028	-5.458	0.9249E-01	0.2259E-02
9	4.00	0.0	506.97	482.38	1.042	-8.113	0.1232E+00	0.3008E-02
12	7.00	0.0	537.81	531.50	1.148	-2.082	0.1811E-01	0.4422E-03
13	8.00	0.0	544.11	539.90	1.167	-1.489	0.1207E-01	0.2948E-03
14	9.00	0.0	534.58	529.86	1.145	-1.556	0.1373E-01	0.3353E-03
15	2.50	30.0	523.13	500.19	1.081	-7.569	0.9045E-01	0.2209E-02
16	3.50	30.0	523.06	501.89	1.084	-7.053	0.8281E-01	0.2023E-02
17	4.50	30.0	511.84	500.75	1.082	-3.659	0.4344E-01	0.1061E-02
18	5.50	30.0	510.23	501.40	1.083	-2.917	0.3436E-01	0.8392E-03
19	6.50	30.0	515.47	503.60	1.088	-3.916	0.4496E-01	0.1098E-02

MACH 3 CANOPY TEST   RUN= 0677

T-INF	P-INF	RHO-INF	V-INF	ALPHA
165.42	2.81	0.1426E-02	1878.6	2.96
deg R	psia	slug/ft^3	ft/s	deg

TO	PO	MU-INF	RE-INF	T WATER
459.21	100.22	0.13267E-06	0.2020E+08	591.72
deg R	psia	lbf·s/ft^2	1/ft	deg R

GAGE	X in.	PHI deg	T-BF deg R	T-S deg R	T-S/TO	QDOT Btu/ (ft^2·s)	H(.9 TO) Btu/ (ft^2·s·R)	ST
1	2.75	60.0	548.74	531.64	1.158	-5.643	0.4768E-01	0.2305E-02
2	3.75	60.0	540.50	531.05	1.156	-3.117	0.2646E-01	0.1279E-02
3	4.75	60.0	544.90	536.18	1.168	-2.879	0.2343E-01	0.1133E-02
5	6.75	60.0	537.45	530.85	1.156	-2.178	0.1853E-01	0.8957E-03
6	7.75	60.0	539.37	533.34	1.161	-1.990	0.1657E-01	0.8012E-03
7	2.00	0.0	517.65	502.48	1.094	-5.007	0.5614E-01	0.2714E-02
8	3.00	0.0	512.30	499.27	1.087	-4.300	0.5001E-01	0.2418E-02
9	4.00	0.0	524.80	506.55	1.103	-6.020	0.6455E-01	0.3121E-02
12	7.00	0.0	551.83	549.20	1.196	-0.867	0.6376E-02	0.3083E-03
13	8.00	0.0	554.89	552.42	1.203	-0.814	0.5851E-02	0.2829E-03
14	9.00	0.0	546.79	543.83	1.184	-0.977	0.7483E-02	0.3618E-03
15	2.50	30.0	537.60	521.82	1.136	-5.208	0.4799E-01	0.2320E-02
16	3.50	30.0	538.01	523.22	1.139	-4.880	0.4439E-01	0.2146E-02
17	4.50	30.0	530.65	523.14	1.139	-2.477	0.2255E-01	0.1090E-02
18	5.50	30.0	530.53	524.65	1.143	1.941	0.1743E-01	0.8425E-03
19	6.50	30.0	534.59	527.12	1.148	2.466	0.2166E-01	0.1047E-02

MACH 3 CANOPY TEST   RUN- 0678

	T INF	P INF	RHO-INF	V INF	ALPHA
	165.76	5.59	0.2832E-02	1880.	2.94
	deg R	psia	slug/ft^3	ft/s	deg

	TO	PO	MU INF	RE INF	T WATER
	460.17	199.39	0.13296E-06	0.4005E+08	591.07
	deg R	psia	lbf·s/ft^2	1/ft	deg R

GAGE	X in.	PHI deg	T-BF deg R	T S deg R	T S/TO	QDOT Btu/ (ft²·s)	H(9 TO) Btu/ (ft²·s·R)	ST
1	2.75	60.0	536.49	510.68	1.110	8.515	0.8821E-01	0.2146E-02
2	3.75	60.0	523.16	508.59	1.105	4.807	0.5091E-01	0.1238E-02
3	4.75	60.0	529.17	515.64	1.121	4.464	0.4398E-01	0.1070E-02
5	6.75	60.0	517.27	507.02	1.102	3.383	0.3642E-01	0.8860E-03
6	7.75	60.0	519.28	510.02	1.108	-3.058	0.3190E-01	0.7759E-03
7	2.00	0.0	497.12	477.16	1.037	6.586	0.1045E+00	0.2543E-02
8	3.00	0.0	490.06	473.68	1.029	5.406	0.9083E-01	0.2210E-02
9	4.00	0.0	504.99	481.00	1.045	-7.917	0.1184E+00	0.2881E-02
12	7.00	0.0	537.41	532.10	1.156	-1.754	0.1487E-01	0.3617E-03
13	8.00	0.0	542.89	538.68	1.171	-1.390	0.1116E-01	0.2714E-03
14	9.00	0.0	530.93	525.83	1.143	-1.686	0.1510E-01	0.3672E-03
15	2.50	30.0	520.78	497.99	1.082	-7.522	0.8973E-01	0.2183E-02
16	3.50	30.0	520.22	498.93	1.084	-7.028	0.8291E-01	0.2017E-02
17	4.50	30.0	509.34	498.38	1.083	-3.618	0.4295E-01	0.1045E-02
18	5.50	30.0	508.12	499.38	1.085	2.885	0.3386E-01	0.8236E-03
19	6.50	30.0	513.42	502.01	1.091	3.763	0.4283E-01	0.1042E-02

MACH 3 CANOPY TEST   RUN 0679

	T INF	P INF	RHO INF	V INF	ALPHA
	164.61	2.80	0.1429E-02	1874.0	-3.04
	deg R	psia	slug/ft^3	ft/s	deg

	TO	PO	MU INF	RE INF	T WATER
	456.97	99.89	0.13199E-06	0.2028E+08	590.55
	deg R	psia	lbf·s/ft^2	1/ft	deg R

GAGE	X in.	PHI deg	T-BF deg R	T S deg R	T S/TO	QDOT Btu/ (ft²·s)	H(9 TO) Btu/ (ft²·s·R)	ST
1	2.75	60.0	545.36	527.59	1.155	5.861	0.5039E-01	0.2438E-02
2	3.75	60.0	536.55	526.46	1.152	3.331	0.2892E-01	0.1399E-02
3	4.75	60.0	540.58	531.42	1.163	3.022	0.2515E-01	0.1217E-02
5	6.75	60.0	532.67	525.52	1.150	2.358	0.2063E-01	0.9985E-03
6	7.75	60.0	534.04	527.43	1.154	-2.180	0.1877E-01	0.9084E-03
7	2.00	0.0	511.29	495.08	1.083	-5.348	0.6382E-01	0.3088E-02
8	3.00	0.0	506.18	492.60	1.078	-4.480	0.5509E-01	0.2666E-02
9	4.00	0.0	518.68	499.12	1.092	6.454	0.7348E-01	0.3555E-02
12	7.00	0.0	544.32	540.06	1.182	-1.406	0.1092E-01	0.5283E-03
13	8.00	0.0	549.27	546.20	1.195	1.014	0.7514E-02	0.3636E-03
14	9.00	0.0	543.25	540.46	1.183	-0.923	0.7110E-02	0.3455E-03
15	2.50	30.0	533.02	516.32	1.130	-5.510	0.5245E-01	0.2538E-02
16	3.50	30.0	533.52	518.01	1.134	-5.118	0.4795E-01	0.2320E-02
17	4.50	30.0	525.70	517.85	1.133	-2.590	0.2431E-01	0.1176E-02
18	5.50	30.0	524.45	518.11	1.134	-2.091	0.1957E-01	0.9472E-03
19	6.50	30.0	528.81	520.53	1.139	-2.732	0.2501E-01	0.1210E-02

MACH 3 CANOPY TEST   RUN= 0680

	T-INF	P-INF	RHO-INF	V-INF	ALPHA
	165.92	5.60	0.2832E-02	1881.4	3.03
	deg R	psia	slug/ft^3	ft/s	deg

	TO	PO	MU-INF	RE-INF	T WATER
	460.60	199.63	0.13309E-06	0.4004E+08	589.72
	deg R	psia	lbf·s/ft^2	1/ft	deg R

GAGE	X	PHI	T BF	T S	T-S/TO	QDOT	H(.9 TO)	ST
	in.	deg	deg R	deg R		Btu/ (ft^2·s)	Btu/ (ft^2·s·R)	
1	2.75	60.0	533.05	506.89	1.101	-8.633	0.9348E-01	0.2272E-02
2	3.75	60.0	519.78	504.81	1.096	-4.941	0.5474E-01	0.1331E-02
3	4.75	60.0	525.20	511.38	1.110	-4.561	0.4710E-01	0.1145E-02
5	6.75	60.0	512.96	502.37	1.091	-3.495	0.3979E-01	0.9672E-03
6	7.75	60.0	514.17	504.46	1.095	-3.204	0.3563E-01	0.8662E-03
7	2.00	0.0	492.62	472.46	1.026	-6.652	0.1148E+00	0.2792E-02
8	3.00	0.0	486.05	469.70	1.020	-5.398	0.9788E-01	0.2379E-02
9	4.00	0.0	500.25	475.68	1.033	-8.105	0.1326E+00	0.3222E-02
12	7.00	0.0	528.51	521.02	1.131	-2.469	0.2319E-01	0.5637E-03
13	8.00	0.0	536.12	530.92	1.153	-1.716	0.1474E-01	0.3584E-03
14	9.00	0.0	528.16	523.54	1.137	-1.526	0.1400E-01	0.3403E-03
15	2.50	30.0	516.68	493.46	1.071	-7.664	0.9712E-01	0.2361E-02
16	3.50	30.0	516.03	494.76	1.074	-7.020	0.8752E-01	0.2127E-02
17	4.50	30.0	505.05	493.94	1.072	-3.668	0.4619E-01	0.1123E-02
18	5.50	30.0	502.44	493.60	1.072	2.915	0.3686E-01	0.8960E-03
19	6.50	30.0	508.26	496.35	1.078	-3.933	0.4807E-01	0.1168E-02

MACH 3 CANOPY TEST   RUN= 0681

	T-INF	P-INF	RHO-INF	V-INF	ALPHA
	164.92	2.81	0.1430E-02	1875.8	4.05
	deg R	psia	slug/ft^3	ft/s	deg

	TO	PO	MU-INF	RE-INF	T WATER
	457.84	100.19	0.13226E-06	0.2028E+08	589.48
	deg R	psia	lbf·s/ft^2	1/ft	deg R

GAGE	X	PHI	T BF	T S	T-S/TO	QDOT	H(.9 TO)	ST
	in.	deg	deg R	deg R		Btu/ (ft^2·s)	Btu/ (ft^2·s·R)	
1	2.75	60.0	543.07	525.74	1.148	-5.718	0.5029E-01	0.2428E-02
2	3.75	60.0	534.88	524.93	1.147	3.286	0.2911E-01	0.1406E-02
3	4.75	60.0	538.66	529.65	1.157	-2.975	0.2530E-01	0.1222E-02
5	6.75	60.0	530.93	523.92	1.144	-2.314	0.2068E-01	0.9988E-03
6	7.75	60.0	532.31	525.80	1.148	-2.149	0.1889E-01	0.9123E-03
7	2.00	0.0	509.37	493.37	1.078	-5.283	0.6497E-01	0.3137E-02
8	3.00	0.0	504.29	490.90	1.072	-4.419	0.5604E-01	0.2706E-02
9	4.00	0.0	516.21	496.94	1.085	-6.359	0.7491E-01	0.3617E-02
12	7.00	0.0	541.78	537.36	1.174	-1.458	0.1163E-01	0.5617E-03
13	8.00	0.0	546.92	543.75	1.188	-1.047	0.7949E-02	0.3838E-03
14	9.00	0.0	541.55	538.78	1.177	-0.914	0.7210E-02	0.3482E-03
15	2.50	30.0	530.82	514.29	1.123	-5.455	0.5336E-01	0.2577E-02
16	3.50	30.0	531.33	516.05	1.127	-5.042	0.4848E-01	0.2341E-02
17	4.50	30.0	523.95	516.26	1.128	-2.537	0.2434E-01	0.1176E-02
18	5.50	30.0	522.62	516.48	1.128	-2.027	0.1941E-01	0.9375E-03
19	6.50	30.0	527.26	519.11	1.134	-2.690	0.2513E-01	0.1213E-02

MACH 3 CANOPY TEST   RUN= 0682

	T-INF	P-INF	RHO-INF	V-INF	ALPHA
	166.45	5.60	0.2822E-02	1884.4	-4.09
	deg R	psia	slug/ft^3	ft/s	deg

	TO	PO	MU-INF	RE-INF	T WATER
	462.07	199.54	0.13353E-06	0.3983E-08	588.48
	deg R	psia	lbf·s/ft^2	1/ft	deg R

GAGE	X	PHI	T BF	T S	T S/TO	QDOT	H(9 TO)	ST
	in.	deg	deg R	deg R		Btu/ (ft^2·s)	Btu/ (ft^2·s·R)	
1	2.75	60.0	531.24	505.78	1.095	8.404	0.9347E-01	0.2277E-02
2	3.75	60.0	518.32	503.73	1.090	4.814	0.5478E-01	0.1334E-02
3	4.75	60.0	523.45	509.96	1.104	-4.451	0.4730E-01	0.1152E-02
5	6.75	60.0	511.52	501.18	1.085	-3.411	0.3998E-01	0.9738E-03
6	7.75	60.0	512.62	503.08	1.089	3.146	0.3607E-01	0.8785E-03
7	2.00	0.0	491.80	472.22	1.022	6.461	0.1146E+00	0.2792E-02
8	3.00	0.0	485.36	469.56	1.016	-5.215	0.9713E-01	0.2366E-02
9	4.00	0.0	498.94	475.07	1.028	7.875	0.1330E+00	0.3240E-02
12	7.00	0.0	525.67	518.02	1.121	-2.523	0.2470E-01	0.6016E-03
13	8.00	0.0	533.47	528.10	1.143	1.772	0.1578E-01	0.3845E-03
14	9.00	0.0	526.16	521.59	1.129	-1.511	0.1429E-01	0.3481E-03
15	2.50	30.0	515.15	492.39	1.066	7.509	0.9812E-01	0.2390E-02
16	3.50	30.0	514.45	493.60	1.068	6.880	0.8851E-01	0.2156E-02
17	4.50	30.0	503.70	492.92	1.067	-3.557	0.4616E-01	0.1124E-02
18	5.50	30.0	500.85	492.17	1.065	2.865	0.3754E-01	0.9145E-03
19	6.50	30.0	506.61	494.95	1.071	3.847	0.4864E-01	0.1185E-02

MACH 3 CANOPY TEST   RUN= 0683

	T-INF	P-INF	RHO-INF	V-INF	ALPHA
	165.53	2.80	0.1422E-02	1879.2	3.97
	deg R	psia	slug/ft^3	ft/s	deg

	TO	PO	MU-INF	RE-INF	T WATER
	459.53	99.98	0.13277E-06	0.2013E+08	588.14
	deg R	psia	lbf·s/ft^2	1/ft	deg R

GAGE	X	PHI	T-BF	T-S	T S/TO	QDOT	H(9 TO)	ST
	in.	deg	deg R	deg R		Btu/ (ft^2·s)	Btu/ (ft^2·s·R)	
1	2.75	60.0	542.03	526.05	1.145	-5.272	0.4687E-01	0.2272E-02
2	3.75	60.0	534.25	525.34	1.143	2.940	0.2630E-01	0.1275E-02
3	4.75	60.0	538.16	530.11	1.154	-2.656	0.2279E-01	0.1105E-02
5	6.75	60.0	531.45	525.21	1.143	-2.058	0.1844E-01	0.8939E-03
6	7.75	60.0	533.27	527.62	1.148	-1.866	0.1636E-01	0.7932E-03
7	2.00	0.0	513.16	499.02	1.086	4.667	0.5462E-01	0.2648E-02
8	3.00	0.0	507.84	495.84	1.079	-3.962	0.4816E-01	0.2335E-02
9	4.00	0.0	519.24	502.51	1.094	5.521	0.6208E-01	0.3009E-02
12	7.00	0.0	545.41	543.07	1.182	-0.771	0.5958E-02	0.2889E-03
13	8.00	0.0	548.07	545.62	1.187	-0.806	0.6105E-02	0.2960E-03
14	9.00	0.0	539.86	537.08	1.169	-0.915	0.7409E-02	0.3592E-03
15	2.50	30.0	531.72	516.81	1.125	4.922	0.4768E-01	0.2312E-02
16	3.50	30.0	531.48	517.40	1.126	-4.646	0.4474E-01	0.2169E-02
17	4.50	30.0	524.57	517.47	1.126	-2.345	0.2257E-01	0.1094E-02
18	5.50	30.0	524.39	518.81	1.129	1.841	0.1750E-01	0.8482E-03
19	6.50	30.0	528.37	521.32	1.134	2.327	0.2159E-01	0.1047E-02

MACH 3 CANOPY TEST   RUN   0684

T INF	P INF	RHO INF	V INF	ALPHA
166.45	5.61	0.2826E-02	1884.4	4.04
deg R	psia	slug/ft^3	ft/s	deg

TO	PO	MU-INF	RE INF	T WATER
462.08	199.81	0.13354E-06	0.3988E+08	587.30
deg R	psia	lbf·s/ft^2	1/ft	deg R

GAGE	X in.	PHI deg	T BF deg R	T S deg R	T-S/TO	QDOT Btu/ (ft^2·s)	H(θ TO) Btu/ (ft^2·s·R)	ST
1	2.75	60.0	530.53	506.51	1.096	7.927	0.8747E-01	0.2128E-02
2	3.75	60.0	518.22	504.66	1.092	4.474	0.5039E-01	0.1226E-02
3	4.75	60.0	523.55	511.10	1.106	-4.111	0.4317E-01	0.1050E-02
5	6.75	60.0	512.48	502.85	1.088	-3.176	0.3652E-01	0.8883E-03
6	7.75	60.0	514.43	505.76	1.095	2.861	0.3183E-01	0.7742E-03
7	2.00	0.0	494.26	475.87	1.030	6.067	0.1011E+00	0.2460E-02
8	3.00	0.0	487.45	472.40	1.022	4.969	0.8792E-01	0.2139E-02
9	4.00	0.0	501.30	479.21	1.037	7.292	0.1151E+00	0.2801E-02
12	7.00	0.0	532.13	527.36	1.141	1.577	0.1415E-01	0.3441E-03
13	8.00	0.0	537.01	532.95	1.153	1.339	0.1143E-01	0.2781E-03
14	9.00	0.0	524.96	520.07	1.125	1.615	0.1550E-01	0.3771E-03
15	2.50	30.0	516.11	494.90	1.071	6.997	0.8854E-01	0.2154E-02
16	3.50	30.0	515.05	495.11	1.071	6.581	0.8306E-01	0.2020E-02
17	4.50	30.0	504.89	494.69	1.071	-3.366	0.4270E-01	0.1039E-02
18	5.50	30.0	503.57	495.51	1.072	2.659	0.3339E-01	0.8122E-03
19	6.50	30.0	508.66	498.14	1.078	3.470	0.4219E-01	0.1026E-02

MACH 3 CANOPY TEST   RUN 0685

T INF	P INF	RHO INF	V INF	ALPHA
167.70	2.80	0.1399E-02	1891.5	0.01
deg R	psia	slug/ft^2	ft/s	deg

TO	PO	MU-INF	RE INF	T WATER
465.55	99.65	0.13458E-06	0.1966E+08	582.99
deg R	psia	lbf·s/ft^2	1/ft	deg R

GAGE	X in.	PHI deg	T BF deg R	T S deg R	T S/TO	QDOT Btu/ (ft^2·s)	H(θ TO) Btu/ (ft^2·s·R)	ST
1	2.75	60.0	533.13	518.33	1.113	4.881	0.4913E-01	0.2406E-02
2	3.75	60.0	525.83	517.50	1.112	2.748	0.2790E-01	0.1366E-02
3	4.75	60.0	529.17	521.77	1.121	2.443	0.2377E-01	0.1164E-02
5	6.75	60.0	522.57	516.63	1.110	1.961	0.2008E-01	0.9832E-03
6	7.75	60.0	524.01	518.55	1.114	1.804	0.1812E-01	0.8870E-03
7	2.00	0.0	505.88	492.72	1.058	4.343	0.5891E-01	0.2884E-02
8	3.00	0.0	501.01	489.89	1.052	3.669	0.5176E-01	0.2534E-02
9	4.00	0.0	511.01	495.31	1.064	5.183	0.6792E-01	0.3325E-02
12	7.00	0.0	534.01	531.04	1.141	0.980	0.8745E-02	0.4281E-03
13	8.00	0.0	538.21	535.74	1.151	0.815	0.6985E-02	0.3420E-03
14	9.00	0.0	532.00	529.76	1.138	0.739	0.6668E-02	0.3265E-03
15	2.50	30.0	523.30	509.53	1.094	4.544	0.5019E-01	0.2457E-02
16	3.50	30.0	523.07	510.25	1.096	4.233	0.4639E-01	0.2271E-02
17	4.50	30.0	516.85	510.30	1.096	2.162	0.2368E-01	0.1160E-02
18	5.50	30.0	515.97	510.81	1.097	1.703	0.1855E-01	0.9081E-03
19	6.50	30.0	518.99	512.07	1.100	2.284	0.2453E-01	0.1201E-02

MACH 3 CANOPY TEST   RUN   0686

	T-INF	P INF	RHO INF	V INF	ALPHA
	166.17	5.61	0 2835E 02	1882.8	0 02
	deg R	psia	slug/ft^3	ft/s	deg

	TO	PO	MU INF	RE INF	T WATER
	481.30	200.00	0 13330E 06	0 4004E 08	582.40
	deg R	psia	lbf·s/ft^2	1/ft	deg R

GAGE	X in.	PHI deg	T BF deg R	T S deg R	T S/TO	QDOT Btu/ (ft^2·s)	HC 9 TO Btu/ (ft^2·s·R)	ST
1	2.75	60.0	521 58	498.43	1.080	-7.640	0.9177E 01	0 2227E 02
2	3.75	60.0	509 72	496.59	1.077	4.331	0.5319E 01	0 1291E 02
3	4.75	60.0	514.45	502.60	1.090	3.912	0.4475E 01	0 1086E 02
5	6.75	60.0	503.48	494.11	1.071	-3.093	0.3918E 01	0 9509E 03
6	7.75	60.0	504 82	496.33	1 076	2.800	0.3450E 01	0.8374E 03
7	2.00	0.0	487 13	469.56	1 018	5.797	0.1066E+00	0 2587E 02
8	3.00	0.0	480.56	466.41	1.011	4.671	0.9117E-01	0.2213E 02
9	4.00	0.0	492.84	471 71	1.023	6.975	0.1234E+00	0.2994E 02
12	7.00	0.0	519.77	513.90	1.114	1.937	0 1963E 01	0.4763E-03
13	8.00	0.0	526.41	522.06	1 132	1 438	0 1345E-01	0.3265E 03
14	9.00	0.0	517.09	512.97	1 112	1.363	0 1393E 01	0.3382E 03
15	2.50	30 0	507.83	487.52	1.057	6 704	0 9266E 01	0 2249E 02
16	3.50	30.0	506 61	487.78	1.057	6 214	0 8559E 01	0 2077E 02
17	4.50	30.0	496.74	486.96	1.056	-3 226	0 4493E 01	0 1091E 02
18	5.50	30.0	494.31	486.74	1.055	2 499	0.3491E 01	0 8473E-03
19	6.50	30.0	498.68	488.09	1.058	3 497	0 4796E 01	0.1164E 02

MACH 3 CANOPY TEST   RUN 0687

	T INF	P INF	RHO INF	V INF	ALPHA
	164.95	2.81	0.1431E 02	1875 9	2 98
	deg R	psia	slug/ft^3	ft/s	deg

	TO	PO	MU INF	RE INF	T WATER
	457.92	100.30	0.13228E 06	0 2030E 08	581 96
	deg R	psia	lbf·s/ft^2	1/ft	deg R

GAGE	X in.	PHI deg	T BF deg R	T S deg R	T S/TO	QDOT Btu/ (ft^2·s)	HC 9 TO Btu/ (ft^2·s·R)	ST
1	2 75	60.0	530 79	515.53	1 126	5 038	0 4823E 01	0 2351E 02
2	3.75	60.0	522.92	514 50	1 124	2 777	0 2713E 01	0 1309E 02
3	4.75	60 0	526.59	519.08	1 134	2 480	0.2319E 01	0.1118E 02
5	6.75	60.0	519.97	514.00	1.122	1 972	0.1936E 01	0 9341E-03
6	7.75	60.0	521.60	516.20	1.127	1 781	0.1711E-01	0.8256E-03
7	2.00	0.0	503.38	490.05	1.070	-4 401	0.5648E-01	0 2724E 02
8	3.00	0.0	498.15	486.92	1.063	3 706	0.4955E-01	0.2390E-02
9	4.00	0.0	508.65	492.83	1.076	5 220	0.6468E-01	0.3120E-02
12	7.00	0.0	533.11	530.64	1.159	-0.814	0.6872E-02	0.3315E-03
13	8.00	0.0	536.40	534.00	1.166	-0.792	0.6493E-02	0.3132E-03
14	9.00	0 0	528.52	525.95	1.149	-0.846	0.7428E-02	0.3583E-03
15	2.50	30.0	520.80	506.72	1.107	-4.646	0.4911E-01	0.2369E-02
16	3.50	30.0	520.24	507.04	1.107	-4.359	0.4592E-01	0 2215E-02
17	4.50	30.0	513.77	507.02	1.107	2.227	0.2346E-01	0.1132E-02
18	5.50	30.0	512.99	507.79	1.109	1 717	0 1795E-01	0.8658E 03
19	6.50	30.0	516.37	509.58	1.113	2.239	0 2298E 01	0.1108E 02

MACH 3 CANOPY TEST   RUN= 0688

T-INF	P-INF	RHO-INF	V-INF	ALPHA
165.39	5.60	0.2843E-02	1878.4	2.99
deg R	psia	slug/ft^3	ft/s	deg

TO	PO	MU-INF	RE-INF	T WATER
459.13	199.76	0.13265E-06	0.4027E+08	581.82
deg R	psia	lbf·s/ft^2	1/ft	deg R

GAGE	X	PHI	T BF	T S	T S/TO	QDOT	H(.9 TO)	ST
	in.	deg	deg R	deg R		Btu/ (ft^2·s)	Btu/ (ft^2·s·R)	
1	2.75	60.0	519.90	497.00	1.082	7.559	0.9023E-01	0.2188E-02
2	3.75	60.0	507.88	495.01	1.078	4.246	0.5191E-01	0.1259E-02
3	4.75	60.0	512.74	501.10	1.091	3.839	0.4368E-01	0.1059E-02
5	6.75	60.0	502.03	492.83	1.073	3.036	0.3813E-01	0.9248E-03
6	7.75	60.0	503.60	495.35	1.079	2.724	0.3317E-01	0.8045E-03
7	2.00	0.0	486.22	468.90	1.021	-5.718	0.1027E+00	0.2491E-02
8	3.00	0.0	479.44	465.43	1.014	-4.624	0.8858E-01	0.2148E-02
9	4.00	0.0	492.06	471.26	1.026	-6.862	0.1182E+00	0.2867E-02
12	7.00	0.0	520.28	515.37	1.122	-1.622	0.1588E-01	0.3851E-03
13	8.00	0.0	525.80	521.71	1.136	-1.349	0.1243E-01	0.3016E-03
14	9.00	0.0	514.31	509.83	1.110	-1.480	0.1532E-01	0.3716E-03
15	2.50	30.0	506.51	486.48	1.060	6.609	0.9021E-01	0.2188E-02
16	3.50	30.0	504.82	486.19	1.059	-6.146	0.8421E-01	0.2042E-02
17	4.50	30.0	495.35	485.67	1.058	-3.196	0.4411E-01	0.1070E-02
18	5.50	30.0	493.22	485.71	1.058	-2.478	0.3418E-01	0.8291E-03
19	6.50	30.0	497.60	487.48	1.062	-3.341	0.4499E-01	0.1091E-02

MACH 3 CANOPY TEST   RUN- 0689

T-INF	P-INF	RHO-INF	V-INF	ALPHA
164.53	2.80	0.1427E-02	1873.5	3.07
deg R	psia	slug/ft^3	ft/s	deg

TO	PO	MU-INF	RE-INF	T WATER
456.75	99.70	0.13193E-06	0.2026E+08	582.12
deg R	psia	lbf·s/ft^2	1/ft	deg R

GAGE	X	PHI	T BF	T S	T S/TO	QDOT	H(.9 TO)	ST
	in.	deg	deg R	deg R		Btu/ (ft^2·s)	Btu/ (ft^2·s·R)	
1	2.75	60.0	529.46	513.45	1.124	-5.283	0.5161E-01	0.2502E-02
2	3.75	60.0	521.15	512.10	1.121	-2.987	0.2956E-01	0.1433E-02
3	4.75	60.0	524.57	516.53	1.131	-2.654	0.2517E-01	0.1220E-02
5	6.75	60.0	517.35	510.85	1.118	-2.144	0.2150E-01	0.1042E-02
6	7.75	60.0	518.49	512.49	1.122	-1.978	0.1951E-01	0.9456E-03
7	2.00	0.0	499.50	485.17	1.062	-4.728	0.6381E-01	0.3093E-02
8	3.00	0.0	494.53	482.64	1.057	-3.923	0.5483E-01	0.2657E-02
9	4.00	0.0	505.00	487.83	1.068	-5.666	0.7382E-01	0.3578E-02
12	7.00	0.0	528.05	524.12	1.147	-1.299	0.1149E-01	0.5570E-03
13	8.00	0.0	533.12	530.08	1.161	-1.001	0.8415E-02	0.4079E-03
14	9.00	0.0	527.13	524.66	1.149	-0.815	0.7174E-02	0.3477E-03
15	2.50	30.0	518.53	503.58	1.103	-4.933	0.5334E-01	0.2585E-02
16	3.50	30.0	518.15	504.25	1.104	4.588	0.4925E-01	0.2387E-02
17	4.50	30.0	511.18	504.10	1.104	-2.338	0.2513E-01	0.1218E-02
18	5.50	30.0	509.39	503.78	1.103	-1.852	0.1998E-01	0.9683E-03
19	6.50	30.0	513.06	505.53	1.107	2.486	0.2632E-01	0.1276E-02

MACH 3 CANOPY TEST   RUN   0690

T-INF	P INF	RHO INF	V INF	ALPHA
165 22	5 61	0 2851E 02	1877 4	3 03
deg R	psia	slug/ft^3	ft/s	deg

TO	PO	MU INF	RE INF	T WATER
458 66	200.05	0 13250E 06	0 4039E-08	582 15
deg R	psia	lbf·s/ft^2	1/ft	deg R

GAGE	X in.	PHI deg	T BF deg R	T S deg R	T S/TO	QDOT Btu/ (ft^2·s)	RE 9 TO Btu/ (ft^2·s·R)	ST
1	2.75	60.0	518 62	494.86	1.079	7 839	0 9552E 01	0 2312E 02
2	3.75	60.0	506 17	492 60	1 074	1 480	0 5615E 01	0 1359E 02
3	4.75	60.0	510.64	498.39	1.087	4 042	0 4723E 01	0 1143E 02
5	6.75	60.0	499.31	489.62	1 067	3.197	0 4162E 01	0.1007E 02
6	7.75	60.0	500.26	491.43	1 071	2 913	0 3703E-01	0.8968E-03
7	2.00	0.0	483.29	465 25	1 014	5.950	0.1137E+00	0.2746E 02
8	3.00	0.0	476.57	462.19	1.008	4.746	0 9608E 01	0.2326E 02
9	4.00	0.0	488.77	467.04	1.018	7 171	0 1322E+00	0.3201E 02
12	7.00	0.0	513.89	506.88	1.105	2 314	0 2459E 01	0.5953E 03
13	8 00	0 0	521.37	516.28	1 126	1 680	0 1624E-01	0 3931E 03
14	9 00	0 0	513 28	509.07	1.110	1 392	0 1445E-01	0.3498E 03
15	2.50	30.0	504.26	483.29	1 051	6.918	0.9813E 01	0.2375E-02
16	3 50	30.0	502.70	483 45	1.054	6 353	0 8992E 01	0.2177E 02
17	4 50	30.0	492 55	482.46	1.052	3.332	0 4783E-01	0.1158E 02
18	5.50	30.0	489.29	481 38	1.050	2.612	0 3808E-01	0.9218E 03
19	6.50	30.0	494.22	483.39	1.054	3.573	0.5061E-01	0.1225E-02

MACH 3 CANOPY TEST   RUN=   0691

T-INF	P INF	RHO INF	V INF	ALPHA
164.28	2.80	0.1432E 02	1872 1	4 00
deg R	psia	slug/ft^3	ft/s	deg

TO	PO	MU INF	RE INF	T WATER
456.06	99 92	0.13172E 06	0 2035E-08	581 57
deg R	psia	lbf·s/ft^2	1/ft	deg R

GAGE	X in.	PHI deg	T BF deg R	T S deg R	T S/TO	QDOT Btu/ (ft^2·s)	RE 9 TO Btu/ (ft^2·s·R)	ST
1	2.75	60.0	527.42	511.50	1.122	5.255	0 5200E 01	0 2513E 02
2	3.75	60.0	519 24	510.18	1.119	-2 990	0 2998E 01	0.1449E-02
3	4.75	60.0	522.58	514.48	1.128	2.672	0 2568E 01	0.1241E 02
5	6.75	60.0	515.31	508.86	1.116	2 131	0 2166E 01	0.1047E 02
6	7 75	60.0	516 44	510.46	1.119	1.975	0.1975E 01	0.9544E 03
7	2.00	0.0	497.49	483 09	1.059	-4 754	0 6546E-01	0.3163E 02
8	3.00	0.0	492.50	480.65	1.054	3 913	0.5574E-01	0.2694E-02
9	4.00	0.0	502.87	485.60	1.065	5.700	0.7586E-01	0.3666E-02
12	7.00	0.0	525.60	521.44	1.143	1.374	0.1238E 01	0.5981E 03
13	8.00	0.0	530.86	527.65	1.157	-1.058	0.9028E-02	0.4363E 03
14	9.00	0.0	525.04	522.54	1.146	-0.827	0.7377E-02	0.3565E 03
15	2.50	30.0	516.56	501.53	1.100	4.961	0.5447E-01	0.2632E-02
16	3.50	30.0	516.11	502.20	1.101	-4.590	0.5003E-01	0 2418E 02
17	4.50	30.0	509.18	502.12	1.101	-2 330	0.2542E-01	0 1228E-02
18	5.50	30.0	507 24	501 55	1.100	1.876	0.2060E-01	0 9953E-03
19	6.50	30.0	511.08	503.57	1.104	-2 477	0.2659E-01	0.1285E-02

MACH 3 CANOPY TEST   RUN   0692

	T-INF	P-INF	RHO INF	V-INF	ALPHA
	165.32	5.61	0.2847E 02	1878.0	4.03
	deg R	psia	slug/ft^3	ft/s	deg

	TO	PO	MU INF	RE INF	T-WATER
	458.95	199.95	0.13259E-06	0.4033E+08	580.98
	deg R	psia	lbf·s/ft^2	1/ft	deg R

GAGE	X in.	PHI deg	T BF deg R	T S deg R	T S/TO	QDOT Btu/ (ft^2·s)	H(.9 TO) Btu/ (ft^2·s·R)	ST
1	2.75	60.0	517.39	494.00	1.076	7.717	0.9535E-01	0.2310E-02
2	3.75	60.0	505.34	491.92	1.072	-4.427	0.5614E-01	0.1360E-02
3	4.75	60.0	509.73	497.64	1.084	-3.991	0.4719E-01	0.1143E-02
5	6.75	60.0	498.58	489.01	1.065	3.157	0.4157E-01	0.1007E-02
6	7.75	60.0	499.40	490.65	1.069	2.885	0.3719E-01	0.9009E-03
7	2.00	0.0	482.63	464.96	1.013	5.830	0.1123E+00	0.2721E-02
8	3.00	0.0	476.05	461.98	1.007	-4.644	0.9493E-01	0.2300E-02
9	4.00	0.0	487.91	466.54	1.017	-7.051	0.1419E+00	0.3194E-02
12	7.00	0.0	511.90	504.68	1.100	2.382	0.2600E-01	0.6298E-03
13	8.00	0.0	519.66	514.40	1.121	1.737	0.1714E-01	0.4152E-03
14	9.00	0.0	512.35	508.09	1.107	-1.405	0.1478E-01	0.3581E-03
15	2.50	30.0	503.12	482.50	1.051	-6.804	0.9798E-01	0.2374E-02
16	3.50	30.0	501.50	482.57	1.051	-6.246	0.8986E-01	0.2177E-02
17	4.50	30.0	491.80	481.91	1.050	-3.263	0.4740E-01	0.1148E-02
18	5.50	30.0	488.33	480.55	1.047	-2.569	0.3807E-01	0.9223E-03
19	6.50	30.0	493.39	482.76	1.052	-3.506	0.5029E-01	0.1218E-02

MACH 3 CANOPY TEST   RUN-   0693

	T-INF	P-INF	RHO-INF	V-INF	ALPHA
	165.07	2.80	0.1422E 02	1876.6	4.02
	deg R	psia	slug/ft^3	ft/s	deg

	TO	PO	MU-INF	RE INF	T WATER
	458.24	99.73	0.13238E-06	0.2016E+08	580.63
	deg R	psia	lbf·s/ft^2	1/ft	deg R

GAGE	X in.	PHI deg	T BF deg R	T S deg R	T S/TO	QDOT Btu/ (ft^2·s)	H(.9 TO) Btu/ (ft^2·s·R)	ST
1	2.75	60.0	528.50	513.77	1.121	-4.862	0.4797E-01	0.2328E-02
2	3.75	60.0	521.02	512.88	1.119	-2.687	0.2675E-01	0.1298E-02
3	4.75	60.0	524.54	517.27	1.129	2.400	0.2289E-01	0.1111E-02
5	6.75	60.0	518.22	512.40	1.118	-1.922	0.1922E-01	0.9327E-03
6	7.75	60.0	519.80	514.53	1.123	-1.739	0.1703E-01	0.8267E-03
7	2.00	0.0	502.33	489.50	1.068	-4.235	0.5494E-01	0.2667E-02
8	3.00	0.0	497.06	486.30	1.061	3.553	0.4809E-01	0.2334E-02
9	4.00	0.0	506.93	491.80	1.073	4.993	0.6290E-01	0.3053E-02
12	7.00	0.0	531.45	529.30	1.155	-0.710	0.6073E-02	0.2947E-03
13	8.00	0.0	534.28	531.84	1.161	-0.805	0.6743E-02	0.3272E-03
14	9.00	0.0	526.42	523.77	1.143	0.876	0.7867E-02	0.3818E-03
15	2.50	30.0	519.00	505.44	1.103	4.477	0.4812E-01	0.2336E-02
16	3.50	30.0	518.26	505.44	1.103	4.231	0.4549E-01	0.2208E-02
17	4.50	30.0	512.10	505.59	1.103	-2.149	0.2306E-01	0.1119E-02
18	5.50	30.0	511.43	506.36	1.105	-1.673	0.1781E-01	0.8643E-03
19	6.50	30.0	514.92	508.46	1.110	-2.133	0.2221E-01	0.1078E-02

MACH 3 CANOPY TEST   RUN: 0694

	T INF 166.02 deg R	P INF 5.60 psia	RHO INF 0.2830E-02 slug/ft^3	V INF 1882.0 ft/s	ALPHA 3.97 deg
	TO 460.89 deg R	PO 199.56 psia	MU INF 0.13318E-06 lbf·s/ft^2	RE INF 0.3999E+08 1/ft	T WATER 580.31 deg R

GAGE	X in.	PHI deg	T-BF deg R	T S deg R	T S/TO	QDOT Btu/ (ft^2·s)	H(·,0·TO) Btu/ (ft^2·s·R)	ST
1	2.75	60.0	517.93	496.05	1.076	7.220	0.8886E-01	0.2161E-02
2	3.75	60.0	506.48	494.16	1.072	4.066	0.5125E-01	0.1247E-02
3	4.75	60.0	511.00	499.87	1.085	3.671	0.4315E-01	0.1050E-02
5	6.75	60.0	500.82	491.94	1.067	2.933	0.3803E-01	0.9251E-03
6	7.75	60.0	502.37	494.40	1.073	2.630	0.3305E-01	0.8038E-03
7	2.00	0.0	485.85	469.25	1.018	5.478	0.1006E+00	0.2447E-02
8	3.00	0.0	479.08	465.65	1.010	4.432	0.8717E-01	0.2120E-02
9	4.00	0.0	490.94	471.16	1.022	6.528	0.1158E+00	0.2817E-02
12	7.00	0.0	519.24	514.72	1.117	1.492	0.1493E-01	0.3631E-03
13	8.00	0.0	524.12	520.15	1.129	1.309	0.1243E-01	0.3024E-03
14	9.00	0.0	512.52	508.03	1.102	1.480	0.1588E-01	0.3862E-03
15	2.50	30.0	505.16	485.96	1.054	6.335	0.8904E-01	0.2166E-02
16	3.50	30.0	503.26	485.36	1.053	5.908	0.8373E-01	0.2037E-02
17	4.50	30.0	494.29	485.02	1.052	3.060	0.4358E-01	0.1060E-02
18	5.50	30.0	492.34	485.13	1.053	2.379	0.3383E-01	0.8227E-03
19	6.50	30.0	496.75	487.12	1.057	3.177	0.4394E-01	0.1069E-02

MACH 3 CANOPY TEST   RUN: 0695

	T INF 166.82 deg R	P INF 2.81 psia	RHO INF 0.1413E-02 slug/ft^3	V INF 1886.5 ft/s	ALPHA 3.79 deg
	TO 463.11 deg R	PO 100.16 psia	MU INF 0.13385E-06 lbf·s/ft^2	RE INF 0.1992E+08 1/ft	T WATER 611.39 deg R

GAGE	X in.	PHI deg	T BF deg R	T S deg R	T S/TO	QDOT Btu/ (ft^2·s)	H(·,0·TO) Btu/ (ft^2·s·R)	ST
1	2.75	60.0	584.45	564.37	1.219	6.628	0.4492E-01	0.2182E-02
2	3.75	60.0	575.29	564.10	1.218	3.692	0.2507E-01	0.1218E-02
3	4.75	60.0	581.12	570.58	1.232	3.478	0.2262E-01	0.1099E-02
5	6.75	60.0	575.03	567.52	1.225	2.479	0.1645E-01	0.7990E-03
6	7.75	60.0	575.58	568.53	1.228	2.326	0.1533E-01	0.7448E-03
7	2.00	0.0	547.30	528.64	1.142	6.156	0.5504E-01	0.2674E-02
8	3.00	0.0	541.03	525.03	1.134	5.278	0.4876E-01	0.2369E-02
9	4.00	0.0	556.94	535.06	1.155	7.219	0.6104E-01	0.2965E-02
12	7.00	0.0	571.35	570.52	1.232	0.274	0.1780E-02	0.8645E-04
13	8.00	0.0	584.02	583.39	1.260	0.208	0.1248E-02	0.6063E-04
14	9.00	0.0	583.10	579.45	1.251	1.207	0.7424E-02	0.3606E-03
15	2.50	30.0	570.82	552.05	1.192	6.194	0.4580E-01	0.2225E-02
16	3.50	30.0	573.91	555.63	1.200	6.033	0.4346E-01	0.2111E-02
17	4.50	30.0	564.10	555.00	1.198	3.003	0.2173E-01	0.1056E-02
18	5.50	30.0	566.37	558.82	1.207	2.493	0.1756E-01	0.8529E-03
19	6.50	30.0	573.84	565.39	1.221	2.789	0.1877E-01	0.9118E-03

MACH 3 CANOPY TEST   RUN= 0696

	T-INF	P-INF	RHO-INF	V-INF	ALPHA
	164.31	5.60	0.2861E-02	1872.3	4.04
	deg R	psia	slug/ft^3	ft/s	deg

	TO	PO	MU-INF	RE-INF	T WATER
	456.12	199.60	0.13174E-06	0.4006E-08	610.20
	deg R	psia	lbf·s/ft^2	1/ft	deg R

GAGE	X in.	PHI deg	T-BF deg R	T-S deg R	T-S/TO	QDOT Btu/(ft^2·s)	H(.9 TO) Btu/(ft^2·s·R)	ST
1	2.75	60.0	569.66	537.72	1.179	-10.540	0.8285E-01	0.2004E-02
2	3.75	60.0	552.04	533.88	1.170	-5.992	0.4857E-01	0.1175E-02
3	4.75	60.0	560.20	542.89	1.190	-5.713	0.4315E-01	0.1044E-02
5	6.75	60.0	547.19	534.73	1.172	-4.114	0.3312E-01	0.8011E-03
6	7.75	60.0	548.35	536.87	1.177	-3.787	0.2997E-01	0.7248E-03
7	2.00	0.0	518.35	492.64	1.080	-8.485	0.1033E+00	0.2499E-02
8	3.00	0.0	510.01	488.52	1.071	-7.090	0.9089E-01	0.2198E-02
9	4.00	0.0	530.21	499.34	1.095	-10.185	0.1147E+00	0.2773E-02
12	7.00	0.0	572.18	566.29	1.242	-1.943	0.1247E-01	0.3016E-03
13	8.00	0.0	576.49	573.42	1.257	1.012	0.6215E-02	0.1503E-03
14	9.00	0.0	562.00	555.48	1.218	-2.153	0.1485E-01	0.3591E-03
15	2.50	30.0	547.87	519.53	1.139	-9.355	0.8581E-01	0.2075E-02
16	3.50	30.0	550.49	522.98	1.147	-9.079	0.8073E-01	0.1952E-02
17	4.50	30.0	535.46	521.64	1.144	4.560	0.4104E-01	0.9925E-03
18	5.50	30.0	536.53	525.22	1.151	3.732	0.3253E-01	0.7868E-03
19	6.50	30.0	544.10	530.32	1.163	4.548	0.3796E-01	0.9182E-03

MACH 3 CANOPY TEST   RUN 0697

	T-INF	P-INF	RHO-INF	V-INF	ALPHA
	163.64	5.60	0.2872E-02	1868.4	2.94
	deg R	psia	slug/ft^3	ft/s	deg

	TO	PO	MU-INF	RE-INF	T WATER
	454.26	199.63	0.13117E-06	0.4091E-08	609.55
	deg R	psia	lbf·s/ft^2	1/ft	deg R

GAGE	X in.	PHI deg	T-BF deg R	T-S deg R	T-S/TO	QDOT Btu/(ft^2·s)	H(.9 TO) Btu/(ft^2·s·R)	ST
1	2.75	60.0	570.56	538.29	1.185	-10.650	0.8227E-01	0.1986E-02
2	3.75	60.0	551.01	532.49	1.172	-6.111	0.4942E-01	0.1193E-02
3	4.75	60.0	559.31	541.68	1.192	-5.819	0.4381E-01	0.1057E-02
5	6.75	60.0	546.16	533.55	1.175	4.162	0.3338E-01	0.8057E-03
6	7.75	60.0	547.19	535.61	1.179	-3.822	0.3015E-01	0.7279E-03
7	2.00	0.0	516.20	490.10	1.079	-8.612	0.1060E+00	0.2559E-02
8	3.00	0.0	507.85	486.11	1.070	-7.172	0.9282E-01	0.2241E-02
9	4.00	0.0	528.09	496.81	1.094	10.321	0.1173E+00	0.2832E-02
12	7.00	0.0	570.20	563.93	1.241	-2.068	0.1333E-01	0.3219E-03
13	8.00	0.0	575.30	572.14	1.259	-1.043	0.6384E-02	0.1541E-03
14	9.00	0.0	561.55	555.14	1.222	-2.115	0.1446E-01	0.3491E-03
15	2.50	30.0	546.19	517.48	1.139	9.474	0.8721E-01	0.2105E-02
16	3.50	30.0	549.09	521.38	1.148	9.145	0.8126E-01	0.1962E-02
17	4.50	30.0	534.17	520.24	1.145	-4.597	0.4126E-01	0.9961E-03
18	5.50	30.0	534.98	523.45	1.152	-3.806	0.3321E-01	0.8017E-03
19	6.50	30.0	542.45	528.39	1.163	-4.643	0.3883E-01	0.9374E-03

MACH 3 CANOPY TEST   RUN= 0698

T-INF	P-INF	RHO-INF	V-INF	ALPHA
162.49	2.81	0.1452E-02	1861.9	3.01
deg R	psia	slug/ft^3	ft/s	deg

TO	PO	MU-INF	RE-INF	T-WATER
451.07	100.24	0.13021E-06	0.2077E-08	609.18
deg R	psia	lbf·s/ft^2	1/ft	deg R

GAGE	X in.	PHI deg	T-BF deg R	T-S deg R	T-S/TO	QDOT Btu/ (ft^2·s)	H(.9 TO) Btu/ (ft^2·s·R)	ST
1	2.75	60.0	579.21	557.87	1.237	7.043	0.4637E-01	0.2221E-02
2	3.75	60.0	568.79	556.87	1.235	3.934	0.2607E-01	0.1249E-02
3	4.75	60.0	574.64	563.42	1.249	-3.704	0.2352E-01	0.1127E-02
5	6.75	60.0	566.70	558.65	1.238	-2.654	0.1739E-01	0.8329E-03
6	7.75	60.0	567.91	560.42	1.242	-2.470	0.1599E-01	0.7660E-03
7	2.00	0.0	539.20	519.55	1.152	6.486	0.5711E-01	0.2736E-02
8	3.00	0.0	532.86	515.96	1.144	5.578	0.5071E-01	0.2429E-02
9	4.00	0.0	549.24	526.09	1.166	7.640	0.6360E-01	0.3047E-02
12	7.00	0.0	583.95	580.84	1.288	1.025	0.5858E-02	0.2807E-03
13	8.00	0.0	586.14	584.87	1.297	0.420	0.2348E-02	0.1125E-03
14	9.00	0.0	576.75	572.97	1.270	1.246	0.7458E-02	0.3573E-03
15	2.50	30.0	564.34	544.45	1.207	-6.564	0.4740E-01	0.2271E-02
16	3.50	30.0	567.24	548.11	1.215	-6.311	0.4440E-01	0.2127E-02
17	4.50	30.0	556.88	547.33	1.213	-3.151	0.2229E-01	0.1068E-02
18	5.50	30.0	558.30	550.51	1.220	-2.570	0.1778E-01	0.8520E-03
19	6.50	30.0	563.85	554.76	1.230	-2.998	0.2015E-01	0.9653E-03

MACH 3 CANOPY TEST   RUN= 0699

T-INF	P-INF	RHO-INF	V-INF	ALPHA
162.55	2.80	0.1447E-02	1862.2	0.13
deg R	psia	slug/ft^3	ft/s	deg

TO	PO	MU-INF	RE-INF	T-WATER
451.24	99.88	0.13026E-06	0.2068E-08	609.23
deg R	psia	lbf·s/ft^2	1/ft	deg R

GAGE	X in.	PHI deg	T-BF deg R	T-S deg R	T-S/TO	QDOT Btu/ (ft^2·s)	H(.9 TO) Btu/ (ft^2·s·R)	ST
1	2.75	60.0	577.31	555.51	1.231	7.193	0.4815E-01	0.2315E-02
2	3.75	60.0	567.96	555.61	1.231	4.075	0.2726E-01	0.1311E-02
3	4.75	60.0	573.69	562.22	1.246	3.785	0.2425E-01	0.1166E-02
5	6.75	60.0	565.26	556.86	1.234	-2.771	0.1838E-01	0.8840E-03
6	7.75	60.0	566.23	558.28	1.237	-2.624	0.1725E-01	0.8293E-03
7	2.00	0.0	536.15	515.73	1.143	-6.736	0.6145E-01	0.2955E-02
8	3.00	0.0	529.83	512.31	1.135	-5.781	0.5444E-01	0.2618E-02
9	4.00	0.0	546.73	522.28	1.157	-8.070	0.6947E-01	0.3340E-02
12	7.00	0.0	580.90	576.78	1.278	-1.359	0.7965E-02	0.3830E-03
13	8.00	0.0	584.58	583.18	1.292	-0.461	0.2604E-02	0.1252E-03
14	9.00	0.0	576.76	573.35	1.271	1.124	0.6720E-02	0.3231E-03
15	2.50	30.0	562.66	542.09	1.201	-6.785	0.4990E-01	0.2400E-02
16	3.50	30.0	565.88	546.38	1.211	-6.436	0.4589E-01	0.2207E-02
17	4.50	30.0	555.33	545.55	1.209	-3.229	0.2316E-01	0.1114E-02
18	5.50	30.0	556.08	548.16	1.215	-2.614	0.1840E-01	0.8847E-03
19	6.50	30.0	561.57	551.83	1.223	-3.214	0.2206E-01	0.1061E-02

MACH 3 CANOPY TEST   RUN 0700

	T-INF	P-INF	RHO-INF	V-INF	ALPHA
	163.13	5.61	0.2885E-02	1865.5	0.01
	deg R	psia	slug/ft^3	ft/s	deg

	TO	PO	MU-INF	RE-INF	T-WATER
	452.85	199.90	0.13075E-06	0.4116E+08	608.80
	deg R	psia	lbf·s/ft^2	1/ft	deg R

GAGE	X in.	PHI deg	T-BF deg R	T-S deg R	T-S/TO	QDOT Btu/ (ft^2·s)	H(.9 TO) Btu/ (ft^2·s·R)	ST
1	2.75	60.0	564.42	531.46	1.174	-10.877	0.8779E-01	0.2113E-02
2	3.75	60.0	548.09	529.11	1.168	-6.263	0.5153E-01	0.1240E-02
3	4.75	60.0	556.07	538.07	1.188	5.939	0.4551E-01	0.1095E-02
5	6.75	60.0	541.99	529.00	1.168	4.285	0.3529E-01	0.8494E-03
6	7.75	60.0	542.74	530.61	1.172	-4.001	0.3252E-01	0.7827E-03
7	2.00	0.0	511.88	485.25	1.072	-8.787	0.1131E+00	0.2723E-02
8	3.00	0.0	503.52	481.43	1.063	-7.288	0.9868E-01	0.2375E-02
9	4.00	0.0	523.63	491.47	1.085	10.611	0.1265E+00	0.3044E-02
12	7.00	0.0	564.29	556.68	1.229	-2.510	0.1683E-01	0.4051E-03
13	8.00	0.0	570.98	567.41	1.253	-1.180	0.7381E-02	0.1777E-03
14	9.00	0.0	559.53	553.64	1.223	-1.943	0.1330E-01	0.3202E-03
15	2.50	30.0	542.74	513.28	1.133	-9.721	0.9195E-01	0.2213E-02
16	3.50	30.0	545.70	517.69	1.143	9.246	0.8396E-01	0.2021E-02
17	4.50	30.0	530.26	516.07	1.140	-4.681	0.4314E-01	0.1038E-02
18	5.50	30.0	530.17	518.33	1.145	3.906	0.3526E-01	0.8487E-03
19	6.50	30.0	537.65	522.80	1.154	-4.901	0.4253E-01	0.1024E-02

MACH 3 CANOPY TEST   RUN= 0701

	T-INF	P-INF	RHO-INF	V-INF	ALPHA
	162.98	5.61	0.2888E-02	1864.7	3.10
	deg R	psia	slug/ft^3	ft/s	deg

	TO	PO	MU-INF	RE-INF	T-WATER
	452.44	199.94	0.13062E-06	0.4123E+08	608.44
	deg R	psia	lbf·s/ft^2	1/ft	deg R

GAGE	X in.	PHI deg	T-BF deg R	T-S deg R	T-S/TO	QDOT Btu/ (ft^2·s)	H(.9 TO) Btu/ (ft^2·s·R)	ST
1	2.75	60.0	563.37	529.91	1.171	-11.041	0.8998E-01	0.2164E-02
2	3.75	60.0	546.36	526.92	1.165	-6.416	0.5359E-01	0.1289E-02
3	4.75	60.0	554.17	535.84	1.184	-6.048	0.4702E-01	0.1131E-02
5	6.75	60.0	539.49	526.15	1.163	4.403	0.3702E-01	0.8904E-03
6	7.75	60.0	539.91	527.35	1.166	-4.143	0.3448E-01	0.8294E-03
7	2.00	0.0	509.09	481.93	1.065	-8.963	0.1199E+00	0.2885E-02
8	3.00	0.0	501.26	478.92	1.059	-7.372	0.1028E+00	0.2473E-02
9	4.00	0.0	520.88	487.96	1.078	-10.863	0.1345E+00	0.3236E-02
12	7.00	0.0	559.23	550.08	1.216	-3.022	0.2115E-01	0.5087E-03
13	8.00	0.0	567.13	562.68	1.244	-1.471	0.9459E-02	0.2275E-03
14	9.00	0.0	557.60	551.76	1.220	-1.927	0.1333E-01	0.3207E-03
15	2.50	30.0	540.70	510.66	1.129	-9.914	0.9583E-01	0.2305E-02
16	3.50	30.0	543.87	515.20	1.139	-9.464	0.8763E-01	0.2108E-02
17	4.50	30.0	527.94	513.50	1.135	-4.766	0.4484E-01	0.1079E-02
18	5.50	30.0	527.01	515.03	1.138	-3.952	0.3665E-01	0.8817E-03
19	6.50	30.0	535.42	520.34	1.150	-4.977	0.4399E-01	0.1058E-02

MACH 3 CANOPY TEST   RUN= 0702

	T-INF	P-INF	RHO-INF	V-INF	ALPHA
	162.13	2.82	0.1458E 02	1859.8	3.08
	deg R	psia	slug/ft^3	ft/s	deg

	TO	PO	MU-INF	RE-INF	T WATER
	450.09	100.40	0.12991E-06	0.2087E+08	608.33
	deg R	psia	lbf·s/ft^2	1/ft	deg R

GAGE	X	PHI	T-BF	T-S	T-S/TO	QDOT	H(.9 TO)	ST
	in.	deg	deg R	deg R		$\frac{Btu}{(ft^2 \cdot s)}$	$\frac{Btu}{(ft^2 \cdot s \cdot R)}$	
1	2.75	60.0	574.90	552.67	1.228	7.335	0.4970E-01	0.2374E-02
2	3.75	60.0	564.76	552.04	1.226	4.197	0.2856E-01	0.1364E-02
3	4.75	60.0	570.41	558.60	1.241	3.898	0.2539E-01	0.1213E-02
5	6.75	60.0	561.01	552.36	1.227	-2.853	0.1937E-01	0.9254E-03
6	7.75	60.0	562.27	553.94	1.231	2.750	0.1847E-01	0.8826E-03
7	2.00	0.0	531.56	510.29	1.134	7.017	0.6670E-01	0.3187E-02
8	3.00	0.0	525.52	507.60	1.128	-5.913	0.5768E-01	0.2756E-02
9	4.00	0.0	542.23	516.96	1.149	8.340	0.7455E-01	0.3562E-02
12	7.00	0.0	575.69	570.60	1.268	-1.679	0.1014E-01	0.4846E-03
13	8.00	0.0	580.30	578.41	1.285	0.624	0.3600E-02	0.1720E-03
14	9.00	0.0	573.58	570.06	1.267	-1.161	0.7035E-02	0.3361E-03
15	2.50	30.0	559.18	538.07	1.195	6.967	0.5239E-01	0.2503E-02
16	3.50	30.0	562.27	542.42	1.205	6.552	0.4771E-01	0.2279E-02
17	4.50	30.0	551.71	541.77	1.204	3.280	0.2400E-01	0.1146E-02
18	5.50	30.0	551.76	543.57	1.208	2.705	0.1953E-01	0.9332E-03
19	6.50	30.0	557.92	547.90	1.217	3.304	0.2314E-01	0.1105E-02

MACH 3 CANOPY TEST   RUN 0703

	T-INF	P-INF	RHO-INF	V-INF	ALPHA
	162.59	2.80	0.1448E 02	1862.4	4.13
	deg R	psia	slug/ft^3	ft/s	deg

	TO	PO	MU-INF	RE-INF	T WATER
	451.35	99.98	0.13029E-06	0.2069E+08	608.42
	deg R	psia	lbf·s/ft^2	1/ft	deg R

GAGE	X	PHI	T-BF	T-S	T-S/TO	QDOT	H(.9 TO)	ST
	in.	deg	deg R	deg R		$\frac{Btu}{(ft^2 \cdot s)}$	$\frac{Btu}{(ft^2 \cdot s \cdot R)}$	
1	2.75	60.0	574.90	552.84	1.225	7.281	0.4965E-01	0.2386E-02
2	3.75	60.0	565.48	552.79	1.225	4.189	0.2858E-01	0.1373E-02
3	4.75	60.0	571.05	559.26	1.239	3.889	0.2541E-01	0.1221E-02
5	6.75	60.0	561.71	553.11	1.225	2.836	0.1931E-01	0.9277E-03
6	7.75	60.0	562.93	554.59	1.229	2.753	0.1855E-01	0.8914E-03
7	2.00	0.0	531.60	510.25	1.130	7.048	0.6775E-01	0.3255E-02
8	3.00	0.0	525.73	507.74	1.125	5.938	0.5848E-01	0.2810E-02
9	4.00	0.0	542.23	516.78	1.145	8.398	0.7595E-01	0.3649E-02
12	7.00	0.0	575.30	569.84	1.263	1.799	0.1100E-01	0.5284E-03
13	8.00	0.0	580.18	578.10	1.281	0.686	0.3989E-02	0.1917E-03
14	9.00	0.0	573.91	570.38	1.264	1.163	0.7082E-02	0.3403E-03
15	2.50	30.0	559.40	538.21	1.192	6.994	0.5299E-01	0.2546E-02
16	3.50	30.0	562.85	542.77	1.203	6.626	0.4852E-01	0.2331E-02
17	4.50	30.0	552.12	542.19	1.201	3.276	0.2409E-01	0.1157E-02
18	5.50	30.0	551.89	543.72	1.205	2.698	0.1962E-01	0.9426E-03
19	6.50	30.0	558.28	548.23	1.215	3.316	0.2335E-01	0.1122E-02

MACH 3 CANOPY TEST   RUN= 0704

T-INF	P-INF	RHO-INF	V-INF	ALPHA
163.51	5.60	$0.2875E-02$	1867.7	-3.97
deg R	psia	slug/ft^3	ft/s	deg

TO	PO	MU-INF	RE-INF	T-WATER
453.93	199.68	$0.13107E-06$	$0.4097E+08$	608.02
deg R	psia	lbf·s/ft^2	1/ft	deg R

GAGE	X in.	PHI deg	T-BF deg R	T-S deg R	T-S/TO	QDOT Btu/ (ft^2·s)	H(.9 TO) Btu/ (ft^2·s·R)	ST
1	2.75	60.0	561.04	527.89	1.163	-10.941	$0.9167E-01$	$0.2212E-02$
2	3.75	60.0	544.75	525.54	1.158	-6.342	$0.5420E-01$	$0.1308E-02$
3	4.75	60.0	552.40	534.15	1.177	-6.022	$0.4794E-01$	$0.1157E-02$
5	6.75	60.0	537.59	524.54	1.156	-4.307	$0.3713E-01$	$0.8957E-03$
6	7.75	60.0	538.26	525.74	1.158	-4.129	$0.3523E-01$	$0.8499E-03$
7	2.00	0.0	507.77	480.81	1.059	-8.897	$0.1231E+00$	$0.2970E-02$
8	3.00	0.0	500.07	477.99	1.053	-7.289	$0.1050E+00$	$0.2532E-02$
9	4.00	0.0	519.58	486.72	1.072	-10.845	$0.1387E+00$	$0.3347E-02$
12	7.00	0.0	556.38	546.91	1.205	-3.126	$0.2260E-01$	$0.5451E-03$
13	8.00	0.0	564.49	559.81	1.233	-1.544	$0.1021E-01$	$0.2463E-03$
14	9.00	0.0	555.38	549.55	1.211	-1.923	$0.1364E-01$	$0.3290E-03$
15	2.50	30.0	539.08	509.20	1.122	-9.863	$0.9798E-01$	$0.2364E-02$
16	3.50	30.0	541.77	513.47	1.131	-9.339	$0.8900E-01$	$0.2147E-02$
17	4.50	30.0	526.13	511.83	1.128	-4.719	$0.4569E-01$	$0.1102E-02$
18	5.50	30.0	524.84	512.93	1.130	-3.930	$0.3765E-01$	$0.9083E-03$
19	6.50	30.0	533.03	518.05	1.141	-4.943	$0.4514E-01$	$0.1089E-02$